

The Pennsylvania State University
The Graduate School
College of Earth and Mineral Sciences

**SOIL FORMATION AND TERRESTRIAL BIOSIGNATURES IN
THE MIDDLE CAMBRIAN**

A Dissertation in
Geosciences and Astrobiology

by

Lev B. Horodyskyj

© 2009 Lev B. Horodyskyj

Submitted in Partial Fulfillment
of the Requirements
for the Degree of

Doctor of Philosophy

May 2009

The dissertation of Lev B. Horodyskyj was reviewed and approved* by the following:

Lee R. Kump
Professor of Geosciences
Dissertation Co-Adviser
Co-Chair of Committee

Timothy S. White
Senior Research Associate of the Earth and Environmental Systems Institute
Dissertation Co-Adviser
Co-Chair of Committee

Michael A. Arthur
Professor of Geosciences

Jennifer Macalady
Assistant Professor of Geosciences

Edward J. Ciolkosz
Emeritus Professor of Soil Genesis and Morphology

Katherine H. Freeman
Professor of Geosciences
Associate Head for Graduate Programs and Research

*Signatures are on file in the Graduate School.

ABSTRACT

The composition and importance of terrestrial ecosystems during the Cambrian is the subject of frequent speculation due to poor preservation and a paucity of comprehensive studies. In this thesis, a geographically extensive and geologically heterogeneous Middle Cambrian weathered surface was investigated to better understand both abiotic and biotic weathering effects and site-to-site heterogeneities. The development of Alfisols and Ultisols in the study area is consistent with weathering in a subtropical climate. Western sites tended to be slightly drier as compared to eastern sites. Further heterogeneities in weathering were caused by differences in topography, with higher and better-drained sites developing drier paleosols and lower and more poorly drained sites developing wetter paleosols, and parent material, with sandy *grus* and paleosaprolites developing on granites and clayey paleosols and paleosaprolites developing on mafic material. As a result of these heterogeneities, no one site proved to be representative of the entire study region. Caution must be used when interpreting paleoweathering data to avoid mistaking local conditions for regional or global conditions.

A thorough geochemical analysis of the Middle Cambrian paleoweathered horizons revealed several geochemical trends that could not be explained by abiotic weathering alone. Chief among these was the peculiar depletion in phosphorus from surface horizons, especially at the Elk Point site, which was enriched in apatite content. Enrichments in organic carbon, carbon isotope composition, and apatite dissolution patterns indicate the possible presence of a deeply weathering terrestrial ecosystem. Argillan development in the zone of apatite dissolution, likely a result of calcium enrichment in soil fluids as a consequence of biological apatite dissolution and phosphorus uptake, is consistent with the behavior of modern-day mycorrhizal fungi. The presence of mycorrhizal fungi at Elk Point would extend their geologic record from 460 Ma to >503 Ma. The presence of a more deeply weathering Cambrian terrestrial ecosystem may have had important consequences for biogeochemical cycles, such as increased nutrient flow to the ocean and increased uptake of atmospheric carbon dioxide, previously not considered by other researchers due to the presumed absence of a significant terrestrial biota at this time.

TABLE OF CONTENTS

LIST OF FIGURES	vii
LIST OF TABLES.....	ix
ACKNOWLEDGEMENTS	x
CHAPTER 1: Introduction.....	1
1.1 Overview	1
1.2 Weathering and Surface Alteration.....	2
1.3 Terminology	3
1.4 Soil Formation	4
1.5 Paleosols.....	5
1.6 Previous and New Work Involving Pre-Ordovician Paleosols	6
1.7 References	7
CHAPTER 2: Geologic and Climate History of the Midcontinental Rift System, USA: Paleoproterozoic to Middle Cambrian.....	10
2.1 Abstract	10
2.2 Geologic Setting	10
2.2.1 Rodinia Assembly and Laurentian Paleolatitude.....	10
2.2.2 Assembly of Laurentia	11
2.2.3 Mesoproterozoic and Neoproterozoic Rifting on Laurentia.....	12
2.2.4 Snowball Earth and the Cambrian Transgression	14
2.3 Summary	16
2.4 References	17
CHAPTER 3: Soil Formation in the Pre-Vegetated World: Middle Cambrian Paleosols and Paleosaprolites from the US Midwest.....	23
3.1 Abstract	23
3.2 Introduction	24
3.3 Geologic and Paleoclimatic Setting.....	25
3.4 Sample Locations and Descriptions.....	27
3.4.1 IGS-USGS D-13; Harris (Harris).....	28

3.4.2 R-20-2002-1 Elk Point Core (Elk Point)	28
3.4.3 Lemars School District D-21; Camp Quest (Camp Quest)	28
3.4.4 Sioux Valley 1 LaFleur #1 (LaFleur)	29
3.4.5 Sharp #1 (Sharp)	29
3.4.6 Hummell, Henry #1 and Nelson #1 (Hummell/Nelson)	30
3.4.7 Other Cores	30
3.5 Methodology	31
3.6 Results	33
3.6.1 Harris	33
3.6.2 Elk Point	34
3.6.3 Camp Quest	37
3.6.4 LaFleur	38
3.6.5 Sharp	39
3.6.6 Hummell/Nelson	41
3.7 Discussion	43
3.7.1 Age Constraints	43
3.7.2 Pedogenic Features	44
3.7.2.1 Sodium Mobilization	44
3.7.2.2 Calcium Mobilization and Carbonate Precipitation	45
3.7.2.3 Iron Mobility	46
3.7.2.4 Clay Mineralogy and Mobility	48
3.7.3 Post-Burial Alteration	49
3.7.4 Paleosol Classifications	51
3.7.4.1 Weathering on Granitic Parent Materials	52
3.7.4.2 Weathering on Mafic Parent Materials	53
3.7.5 Soil-Forming Factors	55
3.7.6 Terrestrial Biota?	57
3.7.6.1 Silicon and Aluminum	57
3.7.6.2 Phosphorus	58
3.7.6.3 Organic Carbon	59
3.8 Conclusions	59
3.9 Acknowledgements	61
3.10 References	62
CHAPTER 4: Biosignatures in Middle Cambrian Paleosols: Fungal Weathering at Elk Point?	91
4.1 Abstract	91
4.2 Introduction	92
4.3 Geological Setting	93
4.4 Sample Locations and Descriptions	94
4.4.1 IGS-USGS D-13; Harris (Harris)	94
4.4.2 R-20-2002-1 Elk Point Core (Elk Point)	95

4.4.3 Lemars School District D-21; Camp Quest (Camp Quest)	95
4.4.4 Sharp #1 (Sharp)	95
4.4.5 Hummell, Henry #1 and Nelson #1 (Hummell/Nelson).....	96
4.5 Methodology.....	96
4.6 Results	98
4.6.1 Organic Carbon.....	98
4.6.2 Organic $\delta^{13}\text{C}$	99
4.6.3 Extracted Organic Matter	100
4.6.4 Phosphorus Content and Depletion Patterns.....	100
4.6.5 Apatite Dissolution.....	100
4.7 Discussion.....	102
4.7.1 Organic Matter Sources.....	102
4.7.2 Organic C Patterns	102
4.7.3 Carbon Isotopes.....	103
4.7.4 Phosphorus and Apatite Dissolution at Elk Point	104
4.7.5 Cambrian Terrestrial Ecosystems and Consequences.....	106
4.8 Conclusions	107
4.9 Acknowledgements.....	109
4.10 References	109
CHAPTER 5: Concluding Remarks.....	125
5.1 Current Work.....	125
5.2 Future Work.....	126
5.3 References	128

LIST OF FIGURES

CHAPTER 2: Geologic and Climate History of the Midcontinental Rift System, USA: Paleoproterozoic to Middle Cambrian

2-1 The Midcontinent Rift System	21
2-2 Bedrock Geology of the Study Region	21
2-3 The Cambrian Transgression	22

CHAPTER 3: Soil Formation in the Pre-Vegetated World: Middle Cambrian Paleosols and Paleosaprolites from the US Midwest

3-1a Bedrock Geology of the Study Region	67
3-1b Cross-Section of the Study Region	67
3-2 Harris Core Mineral Distributions	68
3-3a Harris Core Major Oxides	69
3-3b Harris Core Carbon Contents	70
3-4 Elk Point Core Mineral Distributions	70
3-5a Thin Section Image of Nodular Pyrite in the Elk Point Core	71
3-5b Thin Section Image of Argillans in the Elk Point Core	71
3-5c Thin Section Image of Clay-Infilled Cracks in the Elk Point Core	72
3-5d Thin Section Image of Dolomite Rhomb in the Elk Point Core	72
3-5e Thin Section Image of Unweathered Metagabbro in the Elk Point Core	73
3-6a Elk Point Core Major Oxides	74
3-6b Elk Point Core Sulfur and Carbon Contents	75
3-7 Camp Quest Core Mineral Distributions	76
3-8a Camp Quest Core Major Oxides	77
3-8b Camp Quest Core Sulfur and Carbon Contents	78
3-9 LaFleur Cuttings Mineral Distributions	79
3-10 LaFleur Cuttings Major Oxides	80
3-11 Sharp Core Mineral Distributions	81
3-12a Sharp Core Major Oxides	82
3-12b Sharp Core Carbon Contents	83
3-13 Hummell Core Mineral Distributions	84
3-14 Nelson Core Mineral Distributions	84
3-15a Image of Hydrothermally Altered Section of the Hummell Core	85

3-15b Thin Section Image of Altered Chlorite in the Hummell Core	85
3-15c Thin Section Images of Paleosol and Paleosol-like Rip-up Clasts in Overlying Sandstone in the Hummell Core.....	86
3-16a Hummell Core Major Oxides	87
3-16b Hummell Core Sulfur and Carbon Contents	88
3-17a Nelson Core Major Oxides.....	89
3-17b Nelson Core Carbon Contents.....	90
3-18 Elk Point XGT Maps of Ca and P Abundances	90
 CHAPTER 4: Biosignatures in Middle Cambrian Paleosols: Fungal Weathering at Elk Point?	
4-1 Bedrock Geology of the Study Region.....	115
4-2a Harris Core P, C, and $\delta^{13}\text{C}$ Results.....	116
4-2b Elk Point Core P, C, and $\delta^{13}\text{C}$ Results.....	116
4-2c Camp Quest Core P, C, and $\delta^{13}\text{C}$ Results	117
4-2d Sharp Core P, C, and $\delta^{13}\text{C}$ Results	118
4-2e Hummell Core P, C, and $\delta^{13}\text{C}$ Results	119
4-2f Nelson Core P, C, and $\delta^{13}\text{C}$ Results	119
4-3a Image of Extracted Sandstone Organic Matter (Elk Point).....	120
4-3b Image of Extracted Paleosol Organic Matter (Elk Point).....	120
4-4a Thin Section Image of Unweathered Apatite in the Elk Point Core.....	121
4-4b Thin Section Image of Apatite at the Base of the Elk Point Paleosol	121
4-4c Thin Section Images of Apatite Tunnel 140 cm Below Paleosol Surface	122
4-4d Thin Section Images of Apatite Tunnel 50 cm Below Paleosol Surface.....	122
4-4e Thin Section Image of Degraded Apatite Grain in the Elk Point Paleosol.....	123
4-4f Thin Section Image of Fractured Apatite Grain in the Zone of Dissolution	123
4-4g Thin Section Image of Dissolving Apatite Grain in the Zone of Dissolution.....	124

LIST OF TABLES

CHAPTER 4: Biosignatures in Middle Cambrian Paleosols: Fungal Weathering at Elk Point?

4-1 Organic Carbon Content and $\delta^{13}\text{C}$ Results for the Study Area.....	113
4-2 Normative Mineral Analysis of the Elk Point Weathered Horizons	114

ACKNOWLEDGEMENTS

I would like to thank the many people who have supported me during the course of my graduate studies. First and foremost, I would like to thank my immediate and extended family . . . my mother (Luba), father (Ivan), brother (Vsevolod), and sister (Ulyana) for being a constant source of strength and support, especially through the difficult times. I would also like to thank my college friends, Ben, Rosalyn, Ngoc, Dave, Michael, Eric, and John, who have stuck with me even as our lives and career paths have begun to diverge and the time we get to spend together grows ever shorter and less frequent.

I would like to thank my rats Namtar, Rygel, Stark, and my chinchilla Kalen, who although they couldn't talk (mostly), provided (and Kalen still provides) boundless love and affection and a familiar furry face to see every day when I came home. They always brightened my darker days, especially as those days became more frequent towards the end.

I will be forever thankful to the many new people I met during my years at Penn State. First, Sabrina, Pushker, and Tony who befriended me when I first arrived. I am deeply indebted to the Sci-Fi (and associated) crowd . . . Aubreya, Dan, Mouse, Dave, Melissa, Matt, Sam, Daniel, Andrea, Sarah, Arhan, Winchelle, and the many others who have come and gone through the years. They are also deeply indebted to me for a large amount of food. I'm thankful to Carolyn for listening. I'm also thankful for all the other people I have met through the years, whether at EuroClub, salsa, rock-climbing, knitting, or Team Trivia. I am incredibly thankful for the deep and lasting friendships of Ymene, Swathi, Matt, and most especially Fabia, who is forever the calm at the center of the storm that is my mind. Thank you for helping me make it to the end. I wouldn't have done it without you.

CHAPTER 1

Introduction

1.1 Overview

The definitive macroscopic story of terrestrial ecosystems begins during the Silurian with disarticulated arthropod cuticles and tiny primitive vascular plants such as *Cooksonia* (Edwards and Feehan, 1980; Kenrick and Crane, 1997). After the successful colonization of land by macroscopic flora and fauna, terrestrial ecosystems diversified immensely and by the Pennsylvanian, were forming such complex and widespread communities that they were affecting global climate through changes in weathering and the burial of large amounts of carbon in the form of plant matter (Mora et al., 1996; Berner, 2003).

The macroscopic and fossil story of terrestrial life, however, is incomplete. Terrestrial ecosystems can be traced back to as early as the mid-Ordovician through observation of trace fossils (Retallack, 2001a) and microscopic spores (Strother et al., 1996; Wellman et al., 2003). Palynological studies show a diverse suite of spore tetrads and dyads that appear in the rock record as much as 50 million years before the first macroscopic fossil evidence for plants. Changes in spore morphology and diversity reveal a story that is not recorded through plant fossils, perhaps because the first plants lacked the recalcitrant structures and compounds, such as lignin and cellulose, that allowed future generations of plants to leave their mark in the rock record.

The definitive terrestrial spore story can only be pushed back to the mid-Ordovician. However, studies in molecular genomics (Heckman et al., 2001; Battistuzzi et al., 2004; Battistuzzi and Hedges, 2008), cryptospores (Strother et al., 2004), carbon isotope geochemistry (Horodyski and Knauth, 1994; Gutzmer and Beukes, 1998), and biotic enhancement of element mobility during weathering (Neaman et al., 2005a) suggest that terrestrial life and ecosystems have a more distant origin than the fossil evidence suggests. If terrestrial life does indeed have a more ancient origin than originally

into solution. Through the weathering process, bedrock is eventually transformed into clays, such as kaolinite in the hydrolysis example. The resultant clay type is dependent on the time and intensity of weathering. As weathering continues, more recalcitrant ions can be removed as well. In general aluminum, iron (in oxidizing environments), and titanium are the least mobile of the more abundant elements (Neaman et al., 2005b). The cations removed by weathering are eventually flushed into the ocean, where calcium ions (Ca^{2+}) can combine with carbonate (CO_3^{2-}) to form carbonates, some of which are preserved on the ocean floor until subducted and metamorphosed to release the stored carbon dioxide back into the atmosphere via volcanism, thus completing the carbonate-silicate cycle.

1.3 Terminology

A variety of terminology is used in geological and pedological literature to describe surface weathering products, not all of which are consistent with each other. In this thesis, the following terms will be used to describe the surfaces that are exposed to weathering processes:

- 1) Soil – An active weathering zone characterized by loss of cations, little to no relict parent material textures, soil structure, and the presence of pedogenic features such as clay translocation and enrichment
- 2) Saprolite – A weathered zone of rock characterized by loss of cations, but typically preserving parent material textures
- 3) Paleosol – The buried and non-active equivalent of a soil
- 4) Paleosaprolite – The buried and non-active equivalent of a saprolite
- 5) Parent Material – Unaltered basement rock or consolidated material present below the saprolite or paleosaprolite that has not been affected by any weathering processes

Another term frequently used when describing these systems is "regolith". This term is generally used to describe any type of loose, rubbly cover on a landscape and can include

soil zones, saprolites, and rock debris (both transported and residual material). Because of its broad definition, this term will not be used in this study.

1.4 Soil Formation

Rocks and minerals exposed on Earth's surface will eventually weather to form soils. Soil formation can include the development of layers or "horizons" that have features (eg., chemical composition, color, pH, clay content) that separate them from other horizons in the soil. The main horizons typically present in soils are as follows (Staff, 1993):

- 1) O-horizon – Typically the top surface of a soil that is rich in undecomposed or partially decomposed organic matter
- 2) A-horizon – Either the top horizon in a soil in the absence of an O-horizon or present just below the O-horizon, and characterized by accumulation of organic matter and loss of oxides and clays
- 3) E-horizon – A zone of eluviation, where clays, organic matter, and sesquioxides are lost to deeper layers
- 4) B-horizon – A subsurface accumulation horizon that may be rich in clay, carbonates, sesquioxides, or organic matter
- 5) C-horizon – A zone of altered bedrock lacking the degree of development of the B-horizon (saprolite)
- 6) R-horizon – Unaltered basement material (parent material)

Soil horizon descriptions may include subordinate modifiers that provide more information about the horizon, such as the presence of concretions (c), gleying (loss of iron) due to reducing conditions (g), accumulation of carbonates (k), sodium enrichment (n), clay accumulation (t), and sesquioxide enrichment (o, s). In soil science, the degree of soil development is dependent on five "soil-forming factors", which include parent material, climate, organisms, topography, and time (Jenny, 1941).

The United States Department of Agriculture's Soil Survey has developed a classification scheme for soils that divides them into twelve soil orders based primarily on subsurface horizons, although a few are defined by other features, such as organic-rich surface horizons or unusual structures caused by shrink-swell and freezing processes (Staff, 1999). Of these twelve orders, seven develop under special conditions and the other five can be arranged by degree of development (Schaetzl and Anderson, 2005):

- 1) Entisols – New soils that show little sign of development
- 2) Inceptisols – Weakly developed soils showing some horizon development
- 3) Alfisols – Moderately developed soils showing clay-rich lower horizons and a base saturation of cations of >35%
- 4) Ultisols – Well-developed, strongly leached soils with subsurface clay accumulation and a base saturation of cations of <35%
- 5) Oxisols – Intensely weathered soils that have lost almost all cations (including laterites)

The entisol-to-oxisol sequence will be of primary interest in this study when determining the conditions that led to soil development in the past.

1.5 Paleosols

Once a soil is no longer subject to the weathering reactions that formed it due to environmental changes or burial, the relict soil can become a paleosol. Buried paleosols can be exposed to different conditions depending on depth of burial and the types of post-burial fluids that move through the system. Some typical burial alterations that paleosols experience include decomposition of soil organic matter; burial gleization resulting in iron-depleted haloes around decomposed organic matter, such as roots; burial reddening of oxides; cementation; compaction; illitization of clays via K addition; and lithification and metamorphism (Retallack, 2001b). Some of these processes change the chemical composition of the weathered section, and so care must be taken when interpreting chemical profiles so as to not mistake post-burial alteration for weathering effects. In

addition, because soil is usually unconsolidated and quite friable, erosion prior to burial can easily strip away surface horizons, leaving only lower horizons for investigation. In outcrop, evidence of this process may be present in the form of stonelines or an erosive upper surface and rip-up clasts of the underlying paleosol in overlying sediments (Zbinden et al., 1988; Beukes et al., 2002).

Several classification schemes have been devised for paleosols, as some paleosols contain features that are not present in any soil formed today (Retallack, 2001b) and many features useful in classifying active soil horizons (such as base saturation) are not preserved after burial and alteration (Mack et al., 1993). The Retallack (Retallack et al., 1993) paleosol classification scheme, which is based on the twelve soil orders utilized by the United States Department of Agriculture's Soil Survey, is used in this study, with modifications made and discussed as required.

1.6 Previous and New Work Involving Pre-Ordovician Paleosols

Historically, ancient paleosols have been primarily studied to determine the oxidation state of the ancient atmosphere (Holland, 1984, 1992; Ohmoto, 1996; Holland et al., 1997; Beukes et al., 2002). However, organic acids from biological activity have a distinct effect on soil development and tend to increase element mobility (Neaman et al., 2005b) and recently, these effects have been detected in Precambrian paleosols (Neaman et al., 2005a). Several lines of evidence, including paleosol geochemistry (Gutzmer and Beukes, 1998; Watanabe et al., 2000; Neaman et al., 2005a), carbon isotope geochemistry (Horodyski and Knauth, 1994; Gutzmer and Beukes, 1998), and molecular clocks (Heckman et al., 2001; Battistuzzi et al., 2004) suggest that a significant terrestrial biota was present well before the advent of vascular plants and that it was an important component of Precambrian soils (Driese et al., 1995). The presence of extensive microbotic life in terrestrial environments prior to the advent of plants is expected to have stabilized land surfaces and increased soil development rates (Dott, 2003). However, the extent and impact of early terrestrial ecosystems, as well as their nature and

composition, on a spatially extensive and geologically heterogeneous weathering surface has not previously been studied, providing impetus for the current study.

The "Great Unconformity" (detailed in Chapter 2), which is present in outcrop all across North America, formed as a result of the drowning of the Laurentian paleocontinent during the Neoproterozoic and Cambrian. Paleosols are frequently preserved below unconformities on terrain that was exposed to the atmosphere prior to burial. As a result of Cambrian transgressions, a series of Precambrian and Cambrian surfaces that have not been extensively studied for evidence of early terrestrial ecosystems is present all across the North American continent. The Midcontinent region was selected for this study due to the fortuitous discovery of a thick paleosol overlain by Cambrian sediments in core material from near Elk Point, South Dakota. Additional cores with paleoweathered horizons present below Cambrian sediments from the Iowa subsurface were utilized to provide context for the Elk Point core and to determine whether abiological and biological weathering effects were unique to the Elk Point site or widespread in the Midcontinent region during the Cambrian.

1.7 References

- Battistuzzi, F.U., Feijao, A., and Hedges, S.B., 2004, A genomic timescale of prokaryote evolution: insights into the origin of methanogenesis, phototrophy, and the colonization of land: *BMC Evolutionary Biology*, v. 4, p. 44.
- Battistuzzi, F.U., and Hedges, S.B., 2008, A major clade of prokaryotes with ancient adaptations to life on land: *Molecular Biology and Evolution*.
- Berner, R.A., 2003, The rise of trees and their effects on Paleozoic atmospheric CO₂ and O₂: *Comptes Rendus Geosciences*, v. 335, p. 1173-1177.
- Berner, R.A., Lasaga, A.C., and Garrels, R.M., 1983, The carbonate-silicate geochemical cycle and its effect on atmospheric carbon dioxide over the past 100 million years: *American Journal of Science*, v. 283, p. 641-683.
- Beukes, N.J., Dorland, H., Gutzmer, J., Nedachi, M., and Ohmoto, H., 2002, Tropical laterites, life on land, and the history of atmospheric oxygen in the Paleoproterozoic: *Geology*, v. 30, p. 491-494.
- Dott, R.H., 2003, The Importance of Eolian Abrasion in Supermature Quartz Sandstones and the Paradox of Weathering on Vegetation-Free Landscapes: *Journal of Geology*, v. 111, p. 387-405.
- Driese, S.G., Simpson, E.L., and Eriksson, K.A., 1995, Redoximorphic Paleosols in Alluvial and Lacustrine Deposits, 1.8 Ga Lochness Formation, Mount Isa,

- Australia: Pedogenic Processes and Implications for Paleoclimate: *Journal of Sedimentary Research*, v. A65, p. 675-689.
- Edwards, D., and Feehan, J., 1980, Records of *Cooksonia*-type sporangia from late Wenlock strata in Ireland: *Nature*, v. 287, p. 41-42.
- Gutzmer, J., and Beukes, N.J., 1998, Earliest laterites and possible evidence for terrestrial vegetation in the Early Proterozoic: *Geology*, v. 26, p. 263-266.
- Heckman, D.S., Geiser, D.M., Eidell, B.R., Stauffer, R.L., Kardos, N.L., and Hedges, S.B., 2001, Molecular Evidence for the Early Colonization of Land by Fungi and Plants: *Science*, v. 293, p. 1129-1133.
- Holland, H.D., 1984, Oxygen in the Precambrian Atmosphere: Evidence from Terrestrial Environments, *in* Holland, H.D., ed., *The Chemical Evolution of the Atmosphere and Oceans*: Princeton, NJ, Princeton University Press, p. 277-336.
- , 1992, Distribution and Paleoenvironmental Interpretation of Proterozoic Paleosols, *in* Schopf, J.W., and Klein, C., eds., *The Proterozoic Biosphere*: Cambridge, Cambridge University Press, p. 153-155.
- Holland, H.D., Rye, R., and Ohmoto, H., 1997, Evidence in pre-2.2 Ga paleosols for the early evolution of atmospheric oxygen and terrestrial biota: Comment and Reply: *Geology*, v. 25, p. 857-859.
- Horodyski, R.J., and Knauth, L.P., 1994, Life on Land in the Precambrian: *Science*, v. 263, p. 494-498.
- Jenny, H., 1941, *Factors of Soil Formation: A System of Quantitative Pedology*: New York, McGraw-Hill.
- Kenrick, P., and Crane, P.R., 1997, The origin and early evolution of plants on land: *Nature*, v. 389, p. 33-39.
- Mack, G.H., James, W.C., and Monger, H.C., 1993, Classification of paleosols: *GSA Bulletin*, v. 105, p. 129-136.
- Mora, C.I., Driese, S.G., and Colarusso, L.A., 1996, Middle to Late Paleozoic Atmospheric CO₂ Levels from Soil Carbonate and Organic Matter: *Science*, v. 271, p. 1105-1107.
- Neaman, A., Chorover, J., and Brantley, S.L., 2005a, Element mobility patterns record organic ligands in soils on early Earth: *Geology*, v. 33, p. 117-120.
- , 2005b, Implications of the Evolution of Organic Acid Moieties for Basalt Weathering over Geological Time: *American Journal of Science*, v. 305, p. 147-185.
- Ohmoto, H., 1996, Evidence in pre-2.2 Ga paleosols for the early evolution of atmospheric oxygen and terrestrial biota: *Geology*, v. 24, p. 1135-1138.
- Retallack, G.J., 2001a, *Scoyenia* Burrows from Ordovician Palaeosols of the Juniata Formation in Pennsylvania: *Palaeontology*, v. 44, p. 209-235.
- , 2001b, *Soils of the Past: An Introduction to Paleopedology*: Oxford, Blackwell Science, 404 p.
- Retallack, G.J., James, W.C., Mack, G.H., and Monger, H.C., 1993, Classification of paleosols: Discussion and reply: *GSA Bulletin*, v. 105, p. 1635-1637.
- Schaetzl, R.J., and Anderson, S., 2005, *Soils: Genesis and Geomorphology*, Cambridge University Press.
- Staff, S.S., 1999, *Soil Taxonomy: A Basic System of Soil Classification for Making and Interpreting Soil Surveys*, Natural Resources Conservation Service.
- Staff, S.S.D., 1993, *Soil Survey Manual*, Soil Conservation Service.

- Strother, P.K., Al-Hajri, S., and Traverse, A., 1996, New evidence for land plants from the lower Middle Ordovician of Saudi Arabia: *Geology*, v. 24, p. 55-58.
- Strother, P.K., Wood, G., Taylor, W., and Beck, J., 2004, Middle Cambrian cryptospores and the origin of land plants: *Memoirs of the Association of Australasian Palaeontologists*, v. 29, p. 99-113.
- Watanabe, Y., Martini, J.E.J., and Ohmoto, H., 2000, Geochemical evidence for terrestrial ecosystems 2.6 billion years ago: *Nature*, v. 408, p. 574-578.
- Wellman, C.H., Osterloff, P.L., and Mohiuddin, U., 2003, Fragments of the earliest land plants: *Nature*, v. 425, p. 282-285.
- Zbinden, E.A., Holland, H.D., and Feakes, C.R., 1988, The Sturgeon Falls Paleosol and the Composition of the Atmosphere 1.1 Ga BP: *Precambrian Research*, v. 42, p. 141-163.

CHAPTER 2

Geologic and Climate History of the Midcontinental Rift System, USA: Paleoproterozoic to Middle Cambrian

2.1 Abstract

In the modern world, soils develop on sediments and bedrock exposed to the atmosphere and record the effects of various environmental factors, including moisture content, temperature, and biological activity that act upon the soil as it is forming. In addition to environmental conditions, the types of soils that develop in any given region also depend on local geography and geology. The same holds true for paleoweathering horizons that developed on a variety of Laurentian basement materials in the Midwestern US (specifically, western Iowa and southeast South Dakota) during the Middle Cambrian, which are the subject of this study. In order to better constrain environmental conditions under which these paleoweathering features developed, a thorough understanding of the geologic and climate history of the study region is required.

2.2 Geologic Setting

2.2.1 Rodinia Assembly and Laurentian Paleolatitude

During the Neoproterozoic, Laurentia was the central craton around which the supercontinent of Rodinia assembled and eventually broke apart (Weil et al., 1998; Li et al., 2008). There is much uncertainty about the paleolocation of Laurentia due to difficulty in dating strata used for constraining continental paleolatitudes. Recent literature reviews and synthesis studies suggest that Rodinia was assembled between 1300 Ma and 900 Ma and rifted apart between 825 Ma and 740 Ma (Li et al., 2008), shortly after which the Neoproterozoic Snowball Earth episodes occurred (Trindade and Macouin, 2007). Permissible paleolatitudes for Laurentia during the end of the Mesoproterozoic suggest that Laurentia moved from mid-northern latitudes to high southern latitudes between 1.1 Ga and 1.0 Ga (Li et al., 2008). During the subsequent

Neoproterozoic, Laurentia, as part of Rodinia, moved towards a more equatorial location where it remained as Rodinia rifted apart. Laurentia may have again moved towards high southern latitudes between 600 Ma and 580 Ma (Symons and Chiasson, 1991; Park, 1994), although ambiguous results for Laurentian poles have resulted in much debate over the paleocontinent's paleolatitude at this time, with some studies disputing the evidence for a polar Laurentia (Hodych et al., 2004). Paleogeographic reconstructions for this period of time usually show both possible scenarios (Trindade and Macouin, 2007; Li et al., 2008). During the end of the Neoproterozoic, Gondwanaland had assembled from many of the rifted remnants of Rodinia, but did not include Laurentia, which continued to move northwards across the equator as an independent craton during the Neoproterozoic-Cambrian transition (McKerrow et al., 1992; Dalziel, 1997; Hodych et al., 2004).

2.2.2 Assembly of Laurentia

The assembly of Laurentia took place during the Paleoproterozoic and continued through the Mesoproterozoic (Whitmeyer and Karlstrom, 2007). In the study region, Archean basement material from the Superior Province is present in the northwestern-most portion of the region and extends down to the Spirit Lake Trend, which separates this province from younger terranes accreted during subsequent orogenies (Figure 2-1).

The first event of interest in the assembly of Laurentia in the study area is the 1.880-1.835 Ga Penokeyan Orogeny, which has been extensively studied in the Lake Superior region (Schulz and Cannon, 2007; Whitmeyer and Karlstrom, 2007). During this time a volcanic arc (the Pembine-Wausau Terrane) was sandwiched between two Archean terranes (the Superior Craton and the Marshfield Terrane). Post-tectonic plutons intruded newly accreted terranes and propagated southeast into the study region towards the end of the orogeny (Holm et al., 2005; Whitmeyer and Karlstrom, 2007).

The second event of interest, the 1.71-1.68 Ga Yavapai Orogeny, which has been most extensively studied in the southwestern United States and projected to encompass terrane

in the study region, lies adjacent to the Superior Province (Van Schmus, 1992). The terranes involved in this collision included a variety of 1.80-1.70 Ga volcanic island arcs that accreted onto the Superior Craton (Whitmeyer and Karlstrom, 2007).

Emplacement of 1.70 Ga quartzites occurred during the 1.7-1.5 Ga Baraboo Interval (Van Schmus et al., 2007; Whitmeyer and Karlstrom, 2007) and included the Sioux Quartzite, present in the northwestern-most extent of the study area. The Sioux Quartzite is extremely resistant to erosion and existed as a local highland well into the Cambrian (Runkel et al., 1998).

Several further terrane accretions followed the Yavapai Orogeny. The 1.69-1.65 Ga Mazatzal Province accreted to the east of the Yavapai Province, which was then followed by the 1.55-1.35 Ga Granite-Rhyolite Province. Granitoid intrusions throughout the Yavapai and Mazatzal provinces sutured the terranes together (Whitmeyer and Karlstrom, 2007). Amalgamation of Laurentia concluded 1.3-0.95 Ga with the Grenville Orogeny (Whitmeyer and Karlstrom, 2007).

2.2.3 Mesoproterozoic and Neoproterozoic Rifting on Laurentia

Several episodes of rifting during the Mesoproterozoic and Neoproterozoic are recorded on the Laurentian craton. One such episode occurred in the Midcontinental Rift System (MRS) region, the area of focus for this study. Rifting took place within terrane involved in the Penokean and Yavapai Orogenies (Whitmeyer and Karlstrom, 2007). U-Pb dating of the subaerial Keweenaw flood basalts indicates that a majority were extruded synchronously across the MRS's entire extent between 1.109 and 1.087 Ga (Davis and Paces, 1990; Anderson and McKay, 1997; Ojakangas et al., 2001; Ojakangas and Dickas, 2002), during which time Rodinia was being assembled. Early studies had suggested that mantle plume activity may have caused rifting in this region (Van Schmus, 1992), but more recent studies suggest that collisions between terranes at oblique angles during the assembly of Laurentia may have resulted in crustal extension in the MRS region (Dalziel et al., 2000; Whitmeyer and Karlstrom, 2007).

Both during and after Keweenaw flood basalt deposition, the entire region was subject to erosion, which resulted in deposition of rift-associated "Red Clastics" and texturally similar units that are interbedded with Keweenaw basalts in the northern extent of the MRS in Minnesota and the Upper Peninsula of Michigan (Mitchell and Sheldon, 2009), but are not interbedded in the Iowa subsurface. The Red Clastics series can be subdivided into the Lower Red Clastics and the Upper Red Clastics, with tentative correlations to similar deposits in the northern portion of the MRS.

The most in-depth analysis of the Red Clastics and how to differentiate them from the overlying Cambrian Mt. Simon Sandstone was conducted by Anderson and McKay (1997) in an investigation of the Eischeid core from Carroll County, Iowa. The basement gabbro (Unit A) in the Eischeid core has a U-Pb age of 1.281 ± 0.050 Ga and is associated with the Granite-Rhyolite Province (Van Schmus and Shearer, 1990; Whitmeyer and Karlstrom, 2007). The gabbro is overlain by the rift-associated Lower Red Clastics, which have been divided into three units (B-D). These units have been interpreted as fluvial (Units B and D) and lacustrine deposits (Unit C). The Upper Red Clastics overlie the Lower Red Clastics. They are closely associated with uplift of the Iowa Horst, which may have been a result of regional compression during the Grenville Orogeny (Van Schmus, 1992; Soofi and King, 2002). The Upper Red Clastics have been subdivided into four units (E-H) and appear to be fluvial deposits. Uplift of the Iowa Horst resulted in erosion, which supplied the sediments of the Upper Red Clastics deposited in basins on either side of the Iowa Horst (Figure 2-2). The increase in volcanic fragments up-section in the Upper Red Clastics has been interpreted to be a consequence of the removal of Lower Red Clastics on the Iowa Horst, exposing the underlying basalts to weathering and erosion. The Ames Block is present on the eastern flank of the Iowa Horst and is an elongated feature that was uplifted with respect to the surrounding terrain, but is down-dropped with respect to the main body of the Iowa Horst. Downward displacement of the block increases to the north (Figure 2-2).

Compression of the MRS region during the Grenville Orogeny resulted in uplift along reverse normal faults of the central portion of the MRS, forming the Iowa Horst and ultimately resulting in a failed rift zone (Figure 2-1). Successful rifting during the break-up of Rodinia and the opening of the Iapetus Ocean is recorded in the Mount Rogers region in southwestern Virginia, northwestern North Carolina, and northeastern Tennessee. Mount Rogers flood basalts in this rift zone have U-Pb ages of 758 ± 12 Ma (Aleinikoff et al., 1995), and a similar sequence of rift-associated clastics as in the MRS is present above the Mount Rogers basalts. The Mount Rogers region has been subject to previous scrutiny due to the presence of possible glacial deposits (diamictites and dropstones) in the rift-associated clastics (Miller, 1994; Bailey and Peters, 1998), whereas no such features have yet been described from clastics in the MRS region, most likely because the sediments predate Snowball Earth events.

2.2.4 Snowball Earth and the Cambrian Transgression

The most significant paleoclimatic events during the Neoproterozoic were Snowball Earth glaciations, during which time the entire planet may have been covered in ice (Hoffman et al., 1998). There is considerable debate as to the number of Snowball Earth events and their geographic extent and duration (Hoffman et al., 1998; Condon and Prave, 2000; Trindade and Macouin, 2007). Glacial deposits at low latitudes suggest that at least two glaciations, the Sturtian (~750-680 Ma) and Marinoan (~635 Ma), were global, while the Gaskiers glaciation (~580 Ma) may have been regional in extent (Trindade and Macouin, 2007). Neoproterozoic Snowball Earth events have been associated with the break-up of Rodinia and the low paleolatitudes of most major cratons, resulting in increased carbon dioxide removal from the atmosphere due to higher weathering rates at tropical latitudes and the presence of high albedo cratons at low latitudes, which both acted in concert to cool the planet (Godderis et al., 2007).

After a relatively frigid Neoproterozoic, warmer temperatures prevailed during the early Paleozoic (Bernier, 2006; Came et al., 2007). Laurentia was progressively inundated by the Cambrian ocean and this transgression overlies the "Great Unconformity", which can

be found at a variety of sites around North America, including: Newfoundland and the Strait of Belle Isle region, where the Early Cambrian (?) Bradore Sandstone overlies 600 Ma Lighthouse Cove volcanics and older Precambrian basement (Bostock, 1983; Hiscott et al., 1984; Knight, 1987); Massachusetts, New Jersey, and eastern Pennsylvania, where the Early Cambrian (?) Hardyston Quartzite overlies 1.18 Ga Grenville Gneiss (Markewicz and Dalton, 1977); southwest Virginia, where Early Cambrian Chilhowee Sandstone overlies Precambrian Mount Rogers rift-associated flood basalts and sediments (Rankin, 1967); the Grand Canyon, where the Cambrian Tapeats Sandstone overlies the 1.1 Ga Cardenas Lavas (Elston and Scott, 1976); the Llano Uplift region in Texas, where Late Middle Cambrian Hickory Sandstone overlies paleosols developed on Town Mountain granite (Capo, 1984, 1994); the MRS region, where the Late Middle Cambrian Mt. Simon Sandstone overlies the Precambrian basement and rift-associated deposits (Driese et al., 2007); and Missouri, where the Upper Cambrian Lamotte Sandstone overlies Precambrian basement (Meert and Stuckey, 2002). The ages of the overlying sandstones in these various regions demonstrate time-transgressive sandstone deposition across Laurentia, from the Early Cambrian on the paleocontinent's margins through the Upper Cambrian in the paleocontinental interior (Figure 2-3).

The Mt. Simon Sandstone is the dominant sandstone that overlies most of the MRS region, although the younger Reagan Sandstone and Munising Sandstone are present in the southwest and northeast extents of the MRS, respectively (Anderson and McKay, 1997; Ojakangas and Dickas, 2002). The transgressive sandstones are very mature, with most yielding 90-100% silica, leading some researchers to suggest that intense vegetation-free weathering, assisted by stabilization of the landscape by microbial mats, produced mature sediments that were redistributed by transgressing shorelines (Dott et al., 1986; Dott, 2003; Driese et al., 2007).

Historically, Red Clastic sediments have been difficult to distinguish from the Mt. Simon Sandstone due to the lack of any diagnostic fossils and similarities in composition and color. Anderson and McKay (1997) have proposed a series of criteria (cement mineralogy and lithology) to distinguish between the two types of rock, as the difference

in time of deposition between the two may be as much as 500 million years. The Mt. Simon Sandstone is dominated by quartz and potassium feldspar cements, with minor carbonate, hematite, kaolinite, and illite cements. Detrital rock fragments are very rare in the Mt. Simon Sandstone, except in the basal conglomerate present at some locations. The Red Clastics, on the other hand, are dominantly cemented by quartz, calcite, hematite, and clay, with only minor feldspar cement. The Red Clastics can consist of up to 20% lithic fragments, which are mostly volcanic and metamorphic in origin, in addition to quartz grains. Mineralogical and major oxide data from this study, discussed subsequently, suggest that no Red Clastics are present above weathered basement material in the cores used in this study, indicating that all are overlain by the Mt. Simon Sandstone.

2.3 Summary

Paleoweathering features present in cores from the study region could have developed anytime between 1800 Ma (Harris Granite) and the late Middle Cambrian (Mt. Simon Sandstone), a time that encompasses all of the Snowball Earth events. As paleosols and paleosaprolites are typically unconsolidated and can be easily scoured off of a land surface by glaciation, it is highly unlikely that any paleosols and paleosaprolites in these cores would have survived Snowball Earth glaciations, unless buried and subsequently exhumed during the Middle Cambrian. However, unless such paleosols were buried very shortly after exhumation, any Neoproterozoic weathering signatures would have been quickly overprinted by Middle Cambrian weathering, as the vast majority of paleolatitudinal studies indicate that the study area was located at or near the equator during the Middle Cambrian. As long as a weathering surface is exposed to the atmosphere, it will undergo weathering reactions and the presence of Middle Cambrian Mt. Simon Sandstone directly above the weathered zones indicates that the paleosols and paleosaprolites were likely active weathering zones during the Middle Cambrian, an interpretation consistent with nearby penecontemporaneous samples investigated by Driese et al. (2007).

2.4 References

- Aleinikoff, J.N., Zartman, R.E., Walter, M., Rankin, D.W., Lyttle, P.T., and Burton, W.C., 1995, U-Pb Ages of Metarhyolites of the Catoctin and Mount Rogers Formations, Central and Southern Appalachians: Evidence for two pulses of Iapetan Rifting: *American Journal of Science*, v. 295, p. 428-454.
- Anderson, R.R., 2006, *Geology of the Precambrian Surface of Iowa and surrounding area*, Iowa Geological Survey.
- Anderson, R.R., and McKay, R.M., 1997, Clastic Rocks Associated with the Midcontinent Rift System in Iowa, *in* Interior, U.D.o.t., ed., US Geological Survey, p. I1-I44.
- Bailey, C.M., and Peters, S.E., 1998, Glacially influenced sedimentation in the late Neoproterozoic Mechum River Formation, Blue Ridge province, Virginia: *Geology*, v. 26, p. 623-626.
- Beebee, R.A., 1996, Depositional environments of the Cambrian Flathead Sandstone: Park County, Wyoming: Tenth Keck Research Symposium in Geology Proceedings, p. 126-129.
- Berner, R.A., 2006, GEOCARBSULF: A combined model for Phanerozoic atmospheric O₂ and CO₂: *Geochimica et Cosmochimica Acta*, v. 70, p. 5653-5664.
- Bjornerud, M., 1990, An Upper Proterozoic unconformity in northern Wedel Jarlsberg Land, southwest Spitsbergen: Lithostratigraphy and tectonic implications: *Polar Research*, v. 8, p. 127-139.
- Bostock, H.H., 1983, Precambrian rocks of the Strait of Belle Isle area: *Memoir - Geological Survey of Canada*, v. 400, p. 1-73.
- Came, R.E., Eiler, J.M., Veizer, J., Azmy, K., Brand, U., and Weidman, C.R., 2007, Coupling of surface temperatures and atmospheric CO₂ concentrations during the Palaeozoic era: *Nature*, v. 449, p. 198-201.
- Capo, R.C., 1984, Petrology and geochemistry of a Cambrian paleosol developed on Precambrian granite, Llano Uplift, Texas: Austin, University of Texas at Austin.
- , 1994, Micromorphology of a Cambrian paleosol developed on granite: Llano Uplift region, Central Texas, USA, *in* Ringrose-Voase, A.J., and Humphreys, G.S., eds., *Soil Micromorphology: Studies in Management and Genesis*, Volume Developments in Soil Science 22: Amsterdam, Elsevier, p. 257-264.
- Condon, D.J., and Prave, A.R., 2000, Two from Donegal: Neoproterozoic glacial episodes on the northeast margin of Laurentia: *Geology*, v. 28, p. 951-954.
- Dalziel, I.W.D., 1997, Neoproterozoic-Paleozoic geography and tectonics: Review, hypothesis, environmental speculation: *GSA Bulletin*, v. 109, p. 16-42.
- Dalziel, I.W.D., Mosher, S., and Gahagan, L.M., 2000, Laurentia-Kalahari Collision and the Assembly of Rodinia: *Journal of Geology*, v. 108, p. 499-513.
- Davis, D.W., and Paces, J.B., 1990, Time resolution of geologic events on the Keweenaw Peninsula and implications for development of the Midcontinent Rift system: *Earth and Planetary Science Letters*, v. 97, p. 54-64.
- Dott, R.H., 2003, The Importance of Eolian Abrasion in Supermature Quartz Sandstones and the Paradox of Weathering on Vegetation-Free Landscapes: *Journal of Geology*, v. 111, p. 387-405.

- Dott, R.H., Byers, C.W., Fielder, G.W., Stenzel, S.R., and Winfree, K.E., 1986, Aeolian to marine transition in Cambro—Ordovician cratonic sheet sandstones of the northern Mississippi valley, USA: *Sedimentology*, v. 33, p. 345-367.
- Driese, S.G., Medaris, L.G., Ren, M., Runkel, A.C., and Langford, R.P., 2007, Differentiating Pedogenesis from Diagenesis in Early Terrestrial Paleoweathering Surfaces Formed on Granitic Composition Parent Materials: *Journal of Geology*, v. 115, p. 387-406.
- Elston, D.P., and Scott, G.R., 1976, Unconformity at the Cardenas-Nankowep contact (Precambrian), Grand Canyon Supergroup, northern Arizona: *GSA Bulletin*, v. 87, p. 1763-1772.
- Fairchild, I.J., and Herrington, P.M., 1989, A Tempestite-Stromatolite-Evaporite Association (Late Vendian, East Greenland): a Shoreface-Lagoon Model: *Precambrian Research*, v. 43, p. 101-127.
- Godderis, Y., Donnadieu, Y., Dessert, C., Dupre, B., Fluteau, F., Francois, L.M., Meert, J., Nedelec, A., and Ramstein, G., 2007, Coupled modeling of global carbon cycle and climate in the Neoproterozoic; links between Rodinia breakup and major glaciations: *Comptes Rendus Geosciences*, v. 339, p. 212-222.
- Hiscott, R.N., James, N.P., and Pemberton, S.G., 1984, Sedimentology and ichnology of the Lower Cambrian Bradore Formation, coastal Labrador; fluvial to shallow-marine transgressive sequence: *Bulletin of Canadian Petroleum Geology*, v. 32, p. 11-26.
- Hodych, J.P., Cox, R.A., and Kosler, J., 2004, An equatorial Laurentia at 550 Ma confirmed by Grenvillian inherited zircons dated by LAM ICP-MS in the Skinner Cove volcanics of western Newfoundland: implications for inertial interchange true polar wander: *Precambrian Research*, v. 129, p. 93-113.
- Hoffman, P.F., Kaufman, A.J., Halverson, G.P., and Schrag, D.P., 1998, A Neoproterozoic Snowball Earth: *Science*, v. 281, p. 1342-1346.
- Holm, D.K., Van Schmus, W.R., MacNeill, L.C., Boerboom, T.J., Schweitzer, D., and Schneider, D., 2005, U-Pb zircon geochronology of Paleoproterozoic plutons from the northern midcontinent, USA: Evidence for subduction flip and continued convergence after geon 18 Penokean orogenesis: *GSA Bulletin*, v. 117, p. 259-275.
- Knight, I., 1987, Geology of the Roddickton (12I/16) map area, Current Research - Mineral Development Division (St. John's), Volume 87-1, p. 343-357.
- Li, Z.X., Bogdanova, S.V., Collins, A.S., Davidson, A., De Waele, B., Ernst, R.E., Fitzsimons, I.C.W., Fuck, R.A., Gladkochub, D.P., Jacobs, J., Karlstrom, K.E., Lu, S., Natapov, L.M., Pease, V., Pisarevsky, S.A., Thrane, K., and Vernikovskiy, V., 2008, Assembly, configuration, and break-up history of Rodinia: A synthesis: *Precambrian Research*, v. 160, p. 179-210.
- Markewicz, F.J., and Dalton, R., 1977, Stratigraphy and Applied Geology of the Lower Paleozoic Carbonates in Northwestern New Jersey, Guidebook for the 42nd Annual Field Conference of Pennsylvania Geologists, p. 6-7.
- McKerrow, W.S., Scotese, C.R., and Brasier, M.D., 1992, Early Cambrian continental reconstructions: *Journal of the Geological Society, London*, v. 149, p. 599-606.
- Meert, J., and Stuckey, W., 2002, Revisiting the paleomagnetism of the 1.476 Ga St. Francois Mountains igneous province, Missouri: *Tectonics*, v. 21, p. X1-X19.

- Mensing, T.M., and Faure, G., 1983, Identification and Age of Neofomed Paleozoic Feldspar (Adularia) in a Precambrian Basement Core from Scioto County, Ohio, USA: *Contributions to Mineralogy and Petrology*, v. 82, p. 327-333.
- Miller, J.M.G., 1994, The Neoproterozoic Konnarock Formation, southwestern Virginia, USA: glaciolacustrine facies in a continental rift, *in* Deynoux, M., Miller, J.M.G., Domack, E.W., Eyles, N., Fairchild, I.J., and Young, G.M., eds., *Earth's Glacial Record*: Cambridge, Cambridge University Press, p. 47-59.
- Mitchell, R.L., and Sheldon, N.D., 2009, Weathering and paleosol formation in the 1.1 Ga Keweenaw Rift Precambrian Research, v. 168, p. 271-283.
- Myrow, P.M., Taylor, J.F., Miller, J.F., Ethington, R.L., Ripperdan, R.L., and Brachle, C.M., 1999, Stratigraphy, sedimentology, and paleontology of the Cambrian-Ordovician of Colorado, *in* Lageson, D.R., Lester, A.P., and Trudgill, B.D., eds., *Colorado and Adjacent Areas, Volume Field Guide 1: Boulder, Colorado*, Geological Society of America.
- Ojakangas, R.W., and Dickas, A.B., 2002, The 1.1-Ga Midcontinent Rift System, central North America: sedimentology of two deep boreholes, Lake Superior region: *Sedimentary Geology*, v. 147, p. 13-36.
- Ojakangas, R.W., Morey, G.B., and Green, J.C., 2001, The Mesoproterozoic Midcontinent Rift System, Lake Superior Region, USA: *Sedimentary Geology*, v. 141-142, p. 421-442.
- Park, J.K., 1994, Palaeomagnetic constraints on the position of Laurentia from middle Neoproterozoic to Early Cambrian times: *Precambrian Research*, v. 69, p. 95-112.
- Patel, I.M., 1977, Late Precambrian Fossil Soil Horizon in Southern New Brunswick, and its Stratigraphic Significance: *GSA Abstracts with Programs*, v. 9, p. 308.
- Rankin, D.W., 1967, *Stops, Guide to the Geology of the Mt. Rogers Area, Virginia, North Carolina and Tennessee*, p. 27.
- Runkel, A.C., McKay, R.M., and Palmer, A.R., 1998, Origin of a classic cratonic sheet sandstone: Stratigraphy across the Sauk II-Sauk III boundary in the Upper Mississippi Valley: *GSA Bulletin*, v. 110, p. 188-210.
- Runkel, A.C., Miller, J.F., McKay, R.M., Palmer, A.R., and Taylor, J.F., 2007, High-resolution sequence stratigraphy of lower Paleozoic sheet sandstones in central North America: The role of special conditions of cratonic interiors in development of stratal architecture: *GSA Bulletin*, v. 119, p. 860-881.
- Schulz, K.J., and Cannon, W.F., 2007, The Penokean orogeny in the Lake Superior region: *Precambrian Research*, v. 157, p. 4-25.
- Skehan, J.W., 2001, US 7: Sheffield--Williamstown, *in* Skehan, J.W., ed., *Roadside Geology of Massachusetts*, p. 289-311.
- Soofi, M.A., and King, S.D., 2002, Post-rift deformation of the Midcontinent rift under Grenville tectonism: *Tectonophysics*, v. 359, p. 209-223.
- Swett, K., 1981, Cambro-Ordovician strata in Ny Friesland, Spitsbergen and their palaeotectonic significance: *Geological Magazine*, v. 118, p. 225-250.
- Symons, D.T.A., and Chiasson, A.D., 1991, Paleomagnetism of the Callander Complex and the Cambrian apparent polar wander path for North America: *Canadian Journal of Earth Sciences*, v. 28, p. 355-363.

- Trindade, R.I.F., and Macouin, M., 2007, Palaeolatitude of glacial deposits and palaeogeography of Neoproterozoic ice ages: *Comptes Rendus Geosciences*, v. 339, p. 200-211.
- van Diver, B.B., 1985, NY 37, NY 12, NY 12E: Ogdensburg--Cape Vincent--Watertown, *Roadside Geology of New York*, p. 294-295.
- Van Schmus, W.R., 1992, Tectonic setting of the Midcontinent Rift system: *Tectonophysics*, v. 213, p. 1-15.
- Van Schmus, W.R., Schneider, D.A., Holm, D.K., Dodson, S., and Nelson, B.K., 2007, New insights into the southern margin of the Archean-Proterozoic boundary in the north-central United States based on U-Pb, Sm-Nd, and Ar-Ar geochronology: *Precambrian Research*, v. 157, p. 80-105.
- Van Schmus, W.R., and Shearer, C.K., 1990, Age Relationships for Gabbro from the Amoco M. G. Eischeid #1 Well, *in* Anderson, R.R., ed., *The Amoco M. G. Eischeid #1 Deep Petroleum Test, Carroll County, Iowa; Preliminary Investigations*, Iowa Department of Natural Resources, p. 67-76.
- Weil, A.B., Van der Voo, R., Niocaill, C.M., and Meert, J.G., 1998, The Proterozoic supercontinent Rodinia: paleomagnetically derived reconstructions for 1100 to 800 Ma: *Earth and Planetary Science Letters*, v. 154, p. 13-24.
- Whitmeyer, S.J., and Karlstrom, K.E., 2007, Tectonic model for the Proterozoic growth of North America: *Geosphere*, v. 3, p. 220-259.

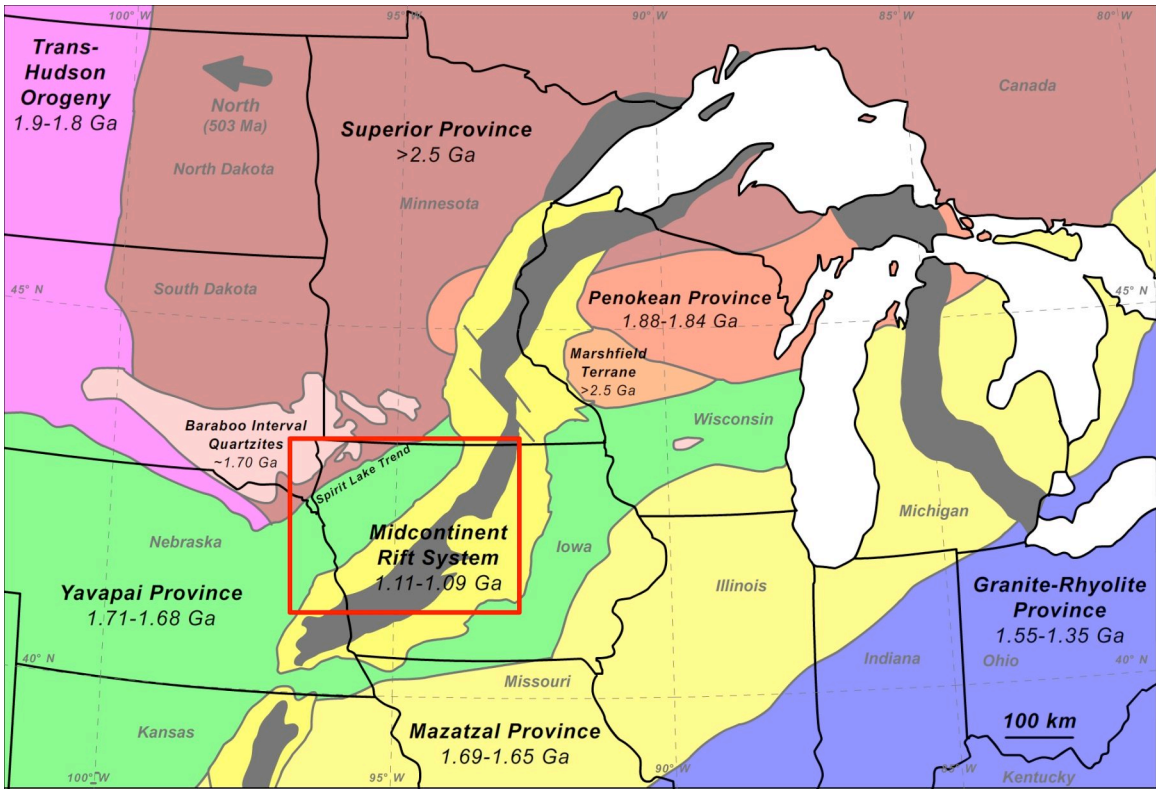


Figure 2-1: Precambrian terranes in the Midcontinent Region in the US Midwest, modified from Anderson (2006), Van Schmus (2007), and Whitmeyer (2007).

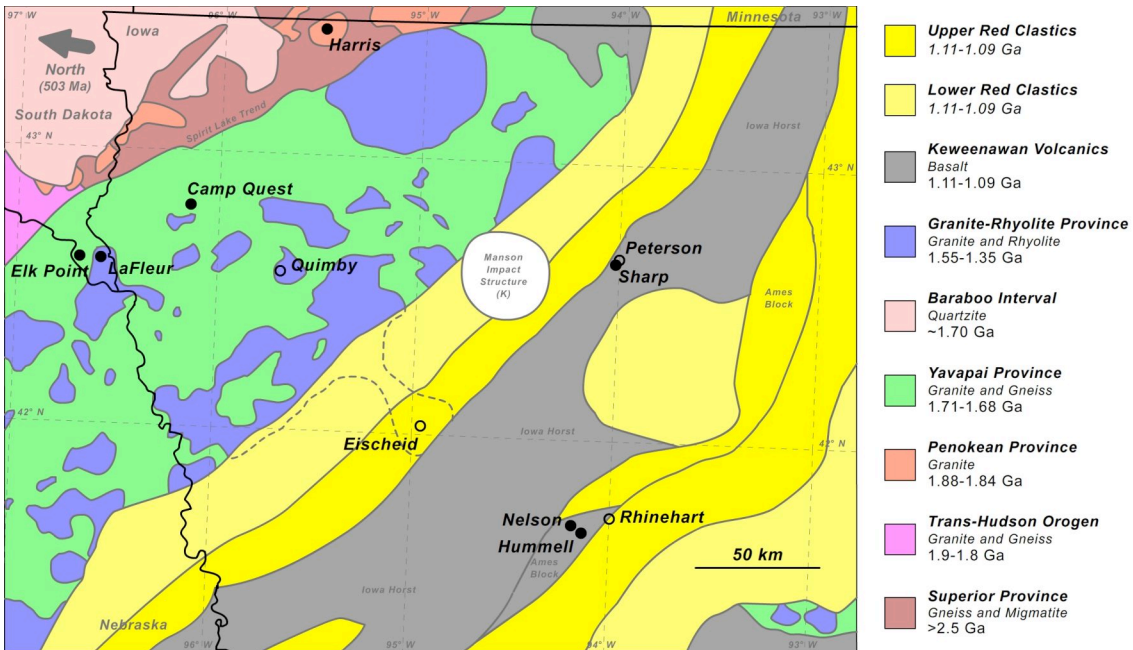


Figure 2-2: Detailed bedrock map of the study region, showing the variety of terranes upon which paleoweathering features developed (solid circles). Open circles indicate additional cores that were used to constrain the age of the overlying Middle Cambrian Mt. Simon Sandstone and differentiate older Red Clastics from the Mt. Simon Sandstone. Modified from Anderson (2006).

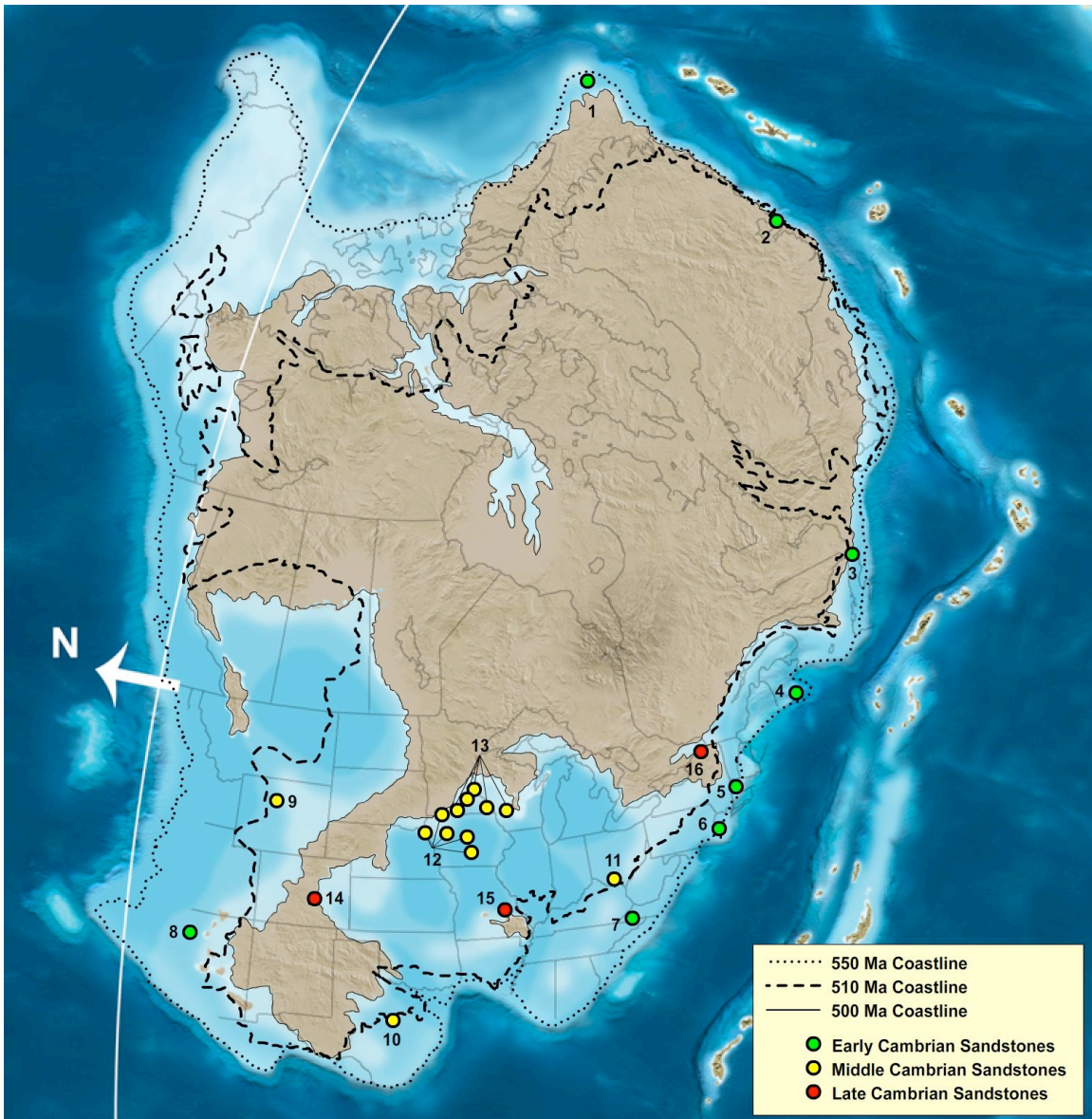


Figure 2-3: Map and coastlines modified from original paleogeographic reconstructions by Ron Blakey. Early Cambrian sandstones: 1 (Swett, 1981; Bjornerud, 1990), 2 (Fairchild and Herrington, 1989), 3 (Bostock, 1983; Hiscott et al., 1984; Knight, 1987), 4 (Patel, 1977), 5 (Skehan, 2001), 6 (Markewicz and Dalton, 1977), 7 (Rankin, 1967), and 8 (Elston and Scott, 1976); Middle Cambrian sandstones: 9 (Beebee, 1996), 10 (Capo, 1984, 1994), 11 (Mensing and Faure, 1983), 12 (this study), and 13 (Runkel et al., 2007); Late Cambrian sandstones: 14 (Myrow et al., 1999), 15 (Meert and Stuckey, 2002), and 16 (van Diver, 1985).

CHAPTER 3

Soil Formation in the Pre-Vegetated World:

Middle Cambrian Paleosols and Paleosaprolites from the US Midwest

3.1 Abstract

Although paleosols have been the subject of much scrutiny, few studies have investigated variability in paleosol development across a geographically limited, geologically heterogeneous, pre-vegetation land surface. To address this deficiency, seven paleosols and paleosaprolites from southeast South Dakota and northwest and central Iowa, United States, have been analyzed to assess the extent of weathering and possible presence of terrestrial life during the Middle Cambrian. Evidence for weathering exists on a variety of basement materials, from the 1800 Ma Harris granite to the 1100 Ma Keweenawan basalts. All of the weathered profiles are overlain by the Middle Cambrian Mt. Simon Sandstone, placing their most likely time of development shortly before the advent of vascular plants. All weathered horizons show high chemical indices of alteration (typically >85) and considerable leaching of mobile cations, such as Na, Ca, Mg, and Mn. The presence of smectites (later illitized) throughout the study area indicate incomplete weathering, likely a result of development in a subtropical climate. Western sites tend to be drier than eastern sites, with one example of weathering in an aquic moisture regime. Heterogeneity in paleosol and paleosaprolite formation is enhanced by variability in topography and parent material. Within both the western and eastern halves of the study area, sites at higher elevations tend to be drier than sites at lower elevations, likely a result of different drainage conditions. Granitic parent materials tend to yield paleosaprolites capped by thin, sandy paleosols, while mafic parent materials tend to yield paleosaprolites and clay-rich paleosols, a contrast that is consistent with modern weathering patterns. Si, Al, and P mobilization at some of the sites may be best explained by the presence of organic ligands from a terrestrial ecosystem. Despite slight alteration by later metasomatism, useful information about paleoclimate can be recovered from the paleosols and paleosaprolites. A thorough investigation of a geographically restricted area demonstrates the great variability in weathered profiles that can develop as

a result of local variability in topography, bedrock, and biological activity. Care must be taken when interpreting limited paleosol data so as not to misconstrue local weathering signatures for global ones.

3.2 Introduction

Soils form on sediments and bedrock exposed to the atmosphere, and, if deposited in a non-erosive setting, can record the effects of various factors, including changes in moisture content, temperature, and biological activity that acted upon the soil prior to burial. Although paleosols can be subjected to post-burial alteration, careful analysis that distinguishes pedogenesis from diagenesis can yield information about ancient conditions of soil formation (Retallack, 1991; Driese et al., 2007). In this study, the mineralogy and geochemical profiles of major oxides, carbon, and sulfur of seven Middle Cambrian paleosols and paleosaprolites were investigated to determine the environmental conditions that led to the formation of these weathered horizons and the major abiotic factors that contributed to differences in profiles from site to site.

Several lines of evidence, including paleosol geochemistry (Gutzmer and Beukes, 1998; Watanabe et al., 2000; Neaman et al., 2005a), carbon isotope geochemistry (Horodyski and Knauth, 1994; Gutzmer and Beukes, 1998), and molecular clocks (Heckman et al., 2001; Battistuzzi et al., 2004) suggest that a significant terrestrial biota was present well before the advent of terrestrial plants and that it was an important component of Precambrian soils (Driese et al., 1995; Dott, 2003), serving to stabilize land surfaces and increase soil development rates (Dott, 2003). Organic acids from biological activity have a distinct effect on soil development and element mobility (Neaman et al., 2005b, 2006) and recently, these effects have been detected in Precambrian paleosols (Neaman et al., 2005a). The extent and impact of such an early terrestrial ecosystem on a spatially extensive and geologically heterogeneous weathering surface has not previously been studied. In addition to understanding the abiotic factors that contributed to weathering across the study region, the seven Middle Cambrian paleosols were investigated for

evidence of biotic influence on element mobilization, mineral dissolution, and soil formation.

3.3 Geologic and Paleoclimatic Setting

Paleosols and paleosaprolites in the study region (the subsurface of western Iowa and southeast South Dakota) developed on a variety of basement material in the central region of Laurentia. Therefore, it is important to understand the paleogeographic and depositional history of the region in order to place proper constraints on paleosol and paleosaprolite ages as well as environmental conditions during their development.

The assembly of Laurentia took place during the Paleoproterozoic and continued through the Mesoproterozoic (Whitmeyer and Karlstrom, 2007). In the study region (the Midwestern US), Archean basement material from the Superior Province is present in the northwestern-most portion of the region and extends down to the Spirit Lake Trend, which separates this province from younger terranes accreted during subsequent orogenies (Figure 3-1a). The events of interest that contributed to the underlying geology in the study area prior to Middle Cambrian weathering include: the 1.880-1.835 Ga Penokean Orogeny, which resulted in post-tectonic pluton intrusions north of the Spirit Lake Trend towards the end of the orogeny (Holm et al., 2005; Whitmeyer and Karlstrom, 2007); the 1.71-1.68 Ga Yavapai Orogeny (Whitmeyer and Karlstrom, 2007); the emplacement of 1.70 Ga quartzites during the 1.7-1.5 Ga Baraboo Interval (Van Schmus et al., 2007; Whitmeyer and Karlstrom, 2007), including the erosion-resistant Sioux Quartzite, present as a local highland well into the Cambrian in the northwestern-most extent of the study area (Runkel et al., 1998); the 1.69-1.65 Ga Mazatzal Province, accreted to the east of the Yavapai Province; the 1.55-1.35 Ga Granite-Rhyolite Province, followed by granitoid intrusions throughout the Yavapai and Mazatzal provinces, which sutured the terranes together (Whitmeyer and Karlstrom, 2007); the development of the 1.109-1.087 Ga Midcontinental Rift System (MRS), which included subaerial extrusion of Keweenawan basalts followed by "Lower Red Clastics" deposition (Davis and Paces, 1990; Anderson and McKay, 1997; Ojakangas et al., 2001; Ojakangas and Dickas, 2002)

on terrane involved in the Penokean and Yavapai orogenies (Whitmeyer and Karlstrom, 2007); and the 1.3-0.95 Ga Grenville orogeny (Whitmeyer and Karlstrom, 2007), which resulted in compression of the MRS (Van Schmus, 1992; Soofi and King, 2002), uplift and unroofing of the Iowa Horst, and deposition of the "Upper Red Clastics" within the MRS (Davis and Paces, 1990; Anderson and McKay, 1997; Ojakangas et al., 2001; Ojakangas and Dickas, 2002).

After a relatively frigid Neoproterozoic, characterized by at least two purported Snowball Earth events (Hoffman et al., 1998; Condon and Prave, 2000; Trindade and Macouin, 2007), warmer temperatures prevailed during the early Paleozoic (Berner, 2006; Came et al., 2007). During the late Neoproterozoic, Laurentia (rotated 90° clockwise relative to today) was moving northwards across the equator as an independent craton (McKerrow et al., 1992; Dalziel, 1997; Hodych et al., 2004). Laurentia was progressively inundated during this time and this transgression can be traced across North America today above the "Great Unconformity", which is sometimes associated with paleosols and paleoweathering features. The ages of the sandstones overlying Precambrian basement material demonstrate time-transgressive sandstone deposition across Laurentia, from the Early Cambrian on the paleocontinent's margins through the Upper Cambrian in the paleocontinental interior. The Mt. Simon Sandstone overlies most of the MRS region, although the younger Reagan Sandstone and Munising Sandstone are present in the southwest and northeast extents of the MRS, respectively (Anderson and McKay, 1997; Ojakangas and Dickas, 2002). The transgressive sandstones are very mature, with most yielding 90-100% silica, leading some researchers to suggest that intense vegetation-free weathering, assisted by stabilization of the landscape by microbial mats, produced mature sediments that were redistributed by transgressing shorelines (Dott et al., 1986; Dott, 2003; Driese et al., 2007).

Historically, Proterozoic Red Clastic sediments found in the MRS have been difficult to distinguish from the Cambrian Mt. Simon Sandstone due to lack of any diagnostic fossils and similarities in composition and color. It is critical to the interpretation of the age of paleoweathered features to be able to distinguish between the two overlying deposits, as

the difference in time of deposition may be as much as 500 million years. Anderson and McKay (1997) have proposed a series of criteria (cement mineralogy and lithology) to distinguish between the two types of sediments. The Mt. Simon Sandstone is primarily cemented by quartz and potassium feldspar with minor carbonate, hematite, kaolinite, and illite cement. Detrital rock fragments are very rare in the Mt. Simon Sandstone, except in the basal conglomerate that is present at some locations. The "Red Clastics", on the other hand, are dominantly cemented by quartz, calcite, hematite, and clay, with only minor feldspar cement. The "Red Clastics" can consist of up to 20% lithic fragments, which are mostly volcanic and metamorphic in origin. Mineralogical and major oxide data suggest that no "Red Clastics" are present above weathered basement material in the cores used in this study, indicating that all study sites are overlain by the Mt. Simon Sandstone.

3.4 Sample Locations and Descriptions

The cores of interest were drilled by a variety of agencies, including the United States Geological Survey (USGS), the Iowa Geological Survey (IGS), Northern Natural Gas Company (NNGC), and Kirby Drilling, between 1954 and 1979 in northwestern and central Iowa and extreme southeast South Dakota and are stored at the Iowa Geological Survey (IGS) core repository in Coralville, Iowa, and the South Dakota Geological Survey (SDGS) core repository in Vermillion, South Dakota, respectively. MRS-associated rift sediments and the surrounding terrane in the Iowa-South Dakota region are present in the subsurface and are accessible only via drill cores. For this study, seven cores were sampled and analyzed (Figures 1a and 1b). Existing biostratigraphic data from four additional cores were applied to constrain the ages of the Mt. Simon Sandstone present above weathered basement in the cores. The analyzed cores can be grouped into two regions and arranged northwest to southeast based on the age of Precambrian basement material. The Harris, Elk Point, LaFleur, and Camp Quest cores are located on pre-MRS terrane in northwest Iowa and extreme southeast South Dakota. The Sharp, Hummell, and Nelson cores are located on the Iowa Horst. These cores were selected for analysis because all display visible evidence of parent material alteration beneath the Mt. Simon Sandstone. The degree of alteration decreases with depth.

3.4.1 IGS-USGS D-13; Harris (Harris)

The Harris core was drilled in Osceola County, northwest Iowa (T100N R39W Sec. 17 SE SW SW SW), in 1963. The basement material in this core is the Harris granite (zircon date of 1.804 ± 0.017 Ga), which intruded Archean basement in the northwestern portion of the study area after the end of the Penokean Orogeny (Van Schmus et al., 2007). A 1.5 m-thick paleosaprolite is developed on this granite. Visually, the paleosaprolite displays textures similar to the underlying granite, and it is extremely friable. Unconsolidated and poorly recovered sandstone is present above the paleosaprolite, which may or may not be Mt. Simon Sandstone. Cemented Mt. Simon Sandstone is present above this unconsolidated zone. The Mt. Simon Sandstone thickness in this core is 28.0 m.

3.4.2 R-20-2002-1 Elk Point Core (Elk Point)

The Elk Point core was drilled south of Elk Point, South Dakota (T90N R50W Sec. 13 NW NW NW NE), by the SDGS. The basement material in this core is a strongly foliated metagabbro associated with the Yavapai Province, with a zircon date of 1.733 ± 0.002 Ga (McCormick, 2004; McCormick, 2005; Van Schmus et al., 2007). The weathered section can be divided into two distinct zones: a paleosaprolite (1.6 m) and an overlying red paleosol (2.9 m). The paleosaprolite is less friable than the paleosol but breaks apart more readily than the unweathered metagabbro. The paleosol is indurated, but disaggregates in water or under slight pressure, making it somewhat friable. The overlying Mt. Simon Sandstone contains a basal conglomerate rich in diagenetic pyrite. Mt. Simon Sandstone thickness in this core is 2.7 m.

3.4.3 Lemars School District D-21; Camp Quest (Camp Quest)

The Camp Quest core was drilled in Plymouth County, northwest Iowa (T92N R45W Sec. 2 SW NW SW NW), by the IGS/USGS in 1979, and is located approximately 40 km

northeast of Elk Point and approximately 90 km southwest of Harris. The basement material in this core is granitic gneiss associated with the Yavapai Province, although an anomalously old age of 2.065 ± 0.010 Ga (Van Schmus, 1987) may be a result of contamination from Archean zircons (Anderson, personal communication). No paleosol is present in this core, but a thick paleosaprolite zone (14.8 m) is developed on the parent material. The paleosaprolite zone is poorly developed and strongly resembles the underlying granitic gneiss, except that it is more brittle. The Mt. Simon Sandstone (13 m thick) overlies the paleosaprolite in this core.

3.4.4 Sioux Valley 1 LaFleur #1 (LaFleur)

The LaFleur well was drilled approximately 13 km to the east of the Elk Point core (T90N R48W Sec. 18 SW NE NW SW). Samples are present only as well cuttings collected at 1-3 meter intervals, so detailed stratigraphic descriptions are taken from field descriptions. The basement granite has a Rb-Sr minimum age of 1.46 Ga (McCormick, 2005), indicating that it is most closely associated with suturing following orogeny of the Granite-Rhyolite Province. McCormick (2004; 2005) hypothesized that the "white sand" present in this section between the Mt. Simon Sandstone and the granitic basement may be a weathering product of the granite. Mineralogical results from this study support this hypothesis. The white sandy paleosaprolite present in this section is ~2 m in thickness. Approximately 3-5 m of Mt. Simon Sandstone is present above the purported paleosaprolite.

3.4.5 Sharp #1 (Sharp)

The Sharp core was drilled in Webster County, central Iowa (T90N R27W Sec. 10 NW W NW NW), in 1963 on the western edge of the Iowa Horst. The weathered section is developed on MRS-associated Keweenawan flood basalts. A red paleosol (1.5 m) is located above a paleosaprolite zone (8.2 m). In the original log for this core, Mesoproterozoic "Red Clastics" were proposed to have been present above the weathered basalt due to the darker coloration of the sandstone, as opposed to the colorless sandstone

seen in other cores in the region. However, geochemical and mineralogical data from this study indicate that the overlying sandstone is composed of quartz almost exclusively, suggesting that the sandstone is Mt. Simon Sandstone, not "Red Clastics", based on the criteria of Anderson and McKay (1997). 7.6 m of Mt. Simon Sandstone are present above the paleosol.

3.4.6 Hummell, Henry #1 and Nelson #1 (Hummell/Nelson)

The Hummell and Nelson cores were drilled in Dallas County, central Iowa (T79N R28W Sec. 18 NW NE NW and T79N R29W Sec. 12 SW SE NW, respectively), in 1954. Both cores are similar to the Sharp core, with darker sandstone present above the Keweenawan basalt basement. In the Hummell core, a brown paleosol (0.6 m) is present above a paleosaprolite. No unweathered basalt appears to be present, although alteration is incomplete at the base of this core. The Nelson core, which is located near the Hummell core, may have a very thin alteration zone near the top of the basalt, but most of the basalt is poorly weathered. Similar questions as to the nature of the overlying clastics have been raised for these two cores, but data from this study indicate that Mt. Simon Sandstone is present above the weathered sections in these cores as well. 37.5 m of Mt. Simon Sandstone is present in the Hummell core, and 34.4 m is present in the Nelson core.

3.4.7 Other Cores

Previous studies of the M. G. Eischeid #1 core (Anderson and McKay, 1997) were utilized to understand the nature of "Red Clastic" sediments present in this region, which in the past have been confused with overlying Cambrian sediments (especially in the original core logs for Sharp, Hummell, and Nelson). The Eischeid core penetrates 4.5 kilometers of MRS-associated clastics and intersects pre-Keweenawan gabbro.

Biostratigraphic data from additional cores (Runkel et al., 1998; Runkel et al., 2007) have been utilized to constrain ages on the Mt. Simon Sandstone in the study area. These

include the Quimby core, located southeast of Camp Quest; Peterson #1 core, located near Sharp; and Rhinehart A-1, located near Hummell and Nelson (Figures 1a and 1b).

3.5 Methodology

All work subsequent to core description, which was completed at the core repositories, was undertaken at the Pennsylvania State University. Cores were sampled from the overlying sandstone down through unweathered parent material (or the deepest available sample if unweathered material was not available) at regular intervals that varied from site to site depending on the thickness of weathered zones. Paleosols were typically sampled at finer intervals (<30 cm). Retrieved samples were cut with a water-lubricated rock saw to remove exterior surfaces on lithified sandstones and parent material. Exterior surfaces were removed manually on poorly lithified paleosol and paleosaprolite samples, which would have otherwise disaggregated under the water-lubricated rock saw. Samples were sonicated in deionized (DI) water for 2-3 minutes 3 times to remove surface contaminants, unless the sample began to disaggregate. Samples were dried, then ground to -100 mesh (149 μm). Powders were split into two aliquots. One aliquot was retained for bulk analysis while the other was reacted with 2 N hydrochloric acid for 48 hours to remove carbonate, then rinsed three times in DI water, dried in an oven, homogenized to create uniform powder for analysis, and weighed to determine mass loss during decarbonation.

C and S contents were determined using a CE Instruments NA 2500 elemental analyzer (EA). The detection limit was 0.01 wt% for all elements and precision on replicate analysis was better than ± 0.06 wt% for C and S for bulk analyses and ± 0.01 wt% for C and ± 0.02 wt% for S for decarbonated analyses. Results for the decarbonated powders were corrected to account for mass loss during decarbonation.

Major oxides were determined for bulk samples using a Perkin-Elmer Optima 5300 inductively-coupled plasma atomic emission spectroscope (ICP-AES). Samples were prepared following a technique modified from Suhr and Ingamells (1966), where 0.1 gm

of sample were mixed with 1 gm of lithium metaborate, fused in a graphite crucible at 1000° C for 15 minutes, and reacted in 100 ml of 5% nitric acid for 30 minutes to produce a solution that was analyzed in the ICP-AES.

Samples were sent to National Petrographic Service, Inc. for thin section preparation. Cut surfaces and thin sections were used for quantitative x-ray mapping of elemental distributions on a Horiba XGT-5000 to verify thin section determination of degraded minerals.

Mineralogy was determined using x-ray diffraction (XRD) on a Rigaku D-MAX RAPID microdiffractometer with 3-dimensional image plate. Powdered sample was packed into 0.7 mm quartz tubes, which were then scanned for 3 minutes. The MDI Jade program was used to interpret the XRD diffraction patterns to determine which minerals were present in the sample.

Enrichment and depletion trends for major oxides are calculated using the following equation (Brimhall and Dietrich, 1987; Anderson et al., 2002):

$$\tau_{j,w} = (C_{j,w}C_{i,p}) / (C_{j,p}C_{i,w}) - 1$$

where $\tau_{j,w}$ is the dimensionless element-mass-transfer coefficient, $C_{j,w}$ is the weight percent of the element of interest in the weathered profile, $C_{i,p}$ is the weight percent of the immobile element in the parent material, $C_{j,p}$ is the weight percent of the element of interest in the parent material, and $C_{i,w}$ is the weight percent of the immobile element in the weathered profile. The immobile element used for this analysis was Ti, since it has the lowest mobility of all the elements investigated (Neaman et al., 2005b). Al has been used by some researchers in the past (Rye and Holland, 2000; Driese, 2004; Driese et al., 2007). However, evidence of clay translocation in some of the paleosol profiles indicates that Al, which is present in clays, is not an appropriate element for use in strain calculations for this study.

The chemical index of alteration (CIA) is typically calculated using oxide weight percents according to the following equation (Nesbitt and Young, 1982):

$$\text{CIA} = \text{Al}_2\text{O}_3 / (\text{Al}_2\text{O}_3 + \text{CaO} + \text{Na}_2\text{O} + \text{K}_2\text{O}) \times 100$$

The CIA indicates the extent of alteration in a weathered horizon. As major cations are lost, the CIA tends towards 100. However, CIA values can be depressed if any cations (particularly K) are later introduced through hydrothermal fluids or metasomatism, the latter of which has been previously noted for paleoweathering in the MRS region (Zbinden et al., 1988; Dott, 2003; Driese et al., 2007). The aluminum-calcium-sodium-potassium (A-CN-K) ternary plot method outlined by Fedo et al. (1995) can be used to correct for K-enrichment. In this method, unweathered parent material is plotted on the ternary diagram and an expected weathering trend is extrapolated from the parent material (determined by the loss of cations, with K trending towards zero). Weathered material that has been altered by K enrichment is then corrected back to the expected weathering trend to yield the true CIA.

3.6 Results

3.6.1 Harris

The Harris core can be divided into three major zones (Figure 3-2). Unweathered granite is present below 279.8 m (core depth). The granite transitions into a friable paleosaprolite over just a few centimeters above 279.8 m, and is present up to 278.3 m. Paleosaprolite is weak red (2.5YR 6/3) at its base, but becomes primarily light greenish gray, pale red, and pale green (10Y 8/1, 10R 7/4, 5G 7/2) up-section. It has fabric reminiscent of the underlying granite. Unconsolidated and poorly recovered sand is present between 278.3 m and 275.5 m, while lithified Mt. Simon Sandstone is present up-section. The sandstone, paleosaprolite, and unweathered granite zones were determined by visual inspection of the core and confirmed by geochemical and mineralogical trends.

XRD analysis indicates that the unweathered granite is composed primarily of anorthite, albite, and quartz (Figure 3-2). The overlying paleosaprolite shows complete loss of anorthite and albite and replacement with kaolinite, rutile, calcite, and siderite. Small quantities of apatite, as seen in XGT maps, are present in the paleosaprolite as well, but are lost towards the surface. The Mt. Simon Sandstone consists almost exclusively of quartz.

Analysis utilizing ICP-AES and EA yielded profiles for major oxides, C (bulk and organic), and S through the core (Figures 3a and 3b). A substantial depletion of soluble cations is evident up-section in this paleosaprolite. Na loss increases from 2% to 97% between 280.0 m and 279.5 m, and remains high (97-98% loss) up-section. Ca (83-91% loss), Mg (65-74% loss), and Mn (65-85% loss) likewise show depletion through the paleosaprolite, although not to the same extent as Na. K is slightly enriched in the paleosaprolite (21-34%, except at the paleosaprolite surface where it is enriched 160-235%). The paleosaprolite shows slight Fe enrichment at its base near the weathering front (5-8% enrichment), but otherwise shows losses up-section (17-34% loss). Al shows enrichment up-section (9-41% enrichment). P is enriched at depth (19-56% enrichment), but is almost completely lost near the surface (92-94% loss). The loss of P and Ca is incomplete at the very top of the paleosaprolite (50% and 63% loss, respectively). This surface layer also shows a sharp increase in Fe, Si, and Al compared to the paleosaprolite directly underneath this layer. There is no S present in the Harris core. Total C is enriched up to 0.8 wt% at the base of the paleosaprolite. Organic C content is very low in this core (~0.02 wt%), with the highest content (~0.06 wt%) at the very top of the paleosaprolite where loss of P and Ca is incomplete. Organic C content of the Mt. Simon Sandstone is very low (~0.02 wt%). CIA values (after correction for K-metasomatism) increase from the base of the saprolite (75) to its surface (>85).

3.6.2 Elk Point

The most in-depth analyses were performed on the Elk Point core. The core study section is divided into four major zones (Figure 3-4). Unweathered metagabbro is

present at the base of this core. Above 278.3 m, it transitions into a paleosaprolite that is present up to 276.7 m with a variable light greenish gray, weak red, pink color (10GY 7/2, 10R 4/2, 5YR 8/4) with a mineral fabric that mimics that of the underlying metagabbro. Between 276.7 m and 273.8 m, a friable, poorly lithified paleosol is present. This paleosol has a weak red color (10R 4/2) and tends to have a granular structure. A 5-cm-thick greenish gray sediment (10Y 6/1) is present between the paleosol and the basal conglomerate of the Mt. Simon Sandstone, which lies above 273.4 m. The sandstone, paleosol, paleosaprolite, and unweathered metagabbro zones were determined by visual inspection of the core and confirmed by geochemical and mineralogical trends.

Inspection of thin sections revealed soil micromorphological features, confirming that the Elk Point profile contains a paleosol. Clay infilling is visible throughout the paleosol and present in cracks through the paleosaprolite (Figure 3-5c). Near the top of the profile, these infillings are argillans, illuvial clay that form when clay was translocated to deeper horizons by water (Figure 3-5b). These argillans are microlaminated, but the barely noticeable extinction pattern under cross-polarized light indicates that the clay is not well oriented. In modern soils, fresh illuvial clay is typically well-oriented and strongly birefringent, but this orientation and associated extinction pattern degrades with time as argillans age and become incorporated into the soil matrix (McCarthy and Plint, 1998).

Dolomite is visible within the base of the paleosol as individual rhombs (Figure 3-5d) and throughout the paleosaprolite as larger amalgamations of rhombs. The unweathered metagabbro consists of plagioclase, biotite, and hornblende (Figure 3-5e), and these minerals appear to persist into the paleosaprolite, although they degrade substantially up-section (particularly biotite via delamination) and become replaced with clays in the paleosol. Thin section and visual inspection of the core indicate that the entire paleosol is a weathering product of the underlying metagabbro.

XRD analysis confirms thin section observations. The metagabbro mineralogy is dominated by anorthite and albite, with minor amounts of cummingtonite, ilmenite, and grunerite (Figure 3-4). Siderite and pyrite are present just below the transition from

paleosaprolite to unweathered parent material. The paleosaprolite is characterized by a complete loss of metagabbro mineralogy and the enrichment of dolomite, which is present from 278.3 m up to 276.5 m. Siderite is present at the paleosol-paleosaprolite transition and hematite is present within the paleosol. Illite is the dominant clay in the Elk Point paleosol and was presumably formed by K enrichment of pedogenic smectite. Pyrite and illite are present in the sediment between the basal conglomerate and the top of the paleosol. Quartz dominates the Mt. Simon Sandstone with pyrite present in the basal conglomerate.

ICP-AES results show a substantial depletion of soluble cations (Figures 6a and 6b). Na loss is high below the visible base of the paleosaprolite (60% loss), but returns to parent material concentrations below this zone. Na loss increases from 2% to 98% between 279.8 m and 278.3 m and remains high throughout the weathered section (97-100% loss). Mn has been lost from the weathered profile as well (45-96% loss). Ca and Mg are enriched in portions of the paleosaprolite (36-60% and 27-133% enrichment, respectively) and depleted in the overlying paleosol (43-70% and 5-47% loss, respectively) compared to the parent material. K is substantially enriched in the weathered sections of this core (175-762% enrichment), indicating significant K-metasomatism. Fe is depleted in the paleosaprolite (38-50% loss) and varies between slight enrichment and depletion in the paleosol (30% loss to 26% enrichment). Al remains comparable to parent material in the paleosaprolite and is enriched in the paleosol (0-50% enrichment). P values tend to remain similar to the parent material with some enrichment in the paleosol (0-38% enrichment), but the element is significantly depleted at the top of the profile (90-97% loss). EA results show that small amounts of S are present in the metagabbro (visible as pyrite in thin section), but the lack of this S in the weathered section indicates that it was most likely lost during pedogenesis. S is considerably enriched (8.3 wt%) at the base of the overlying Mt. Simon Sandstone and visual observations indicate that it is present in the form of encrusting pyrite. This S enrichment penetrates into the upper few centimeters of the paleosol (Figure 3-5a), indicating that the paleosol was permeable and uncemented when it was buried. Total C is enriched up to 5 wt% in the paleosaprolite, which is consistent with the Ca and Mg

enrichment as well as the carbonates visible in thin section (Figure 3-5d). Organic C is present (up to 0.11 wt%) in the paleosol and tends to increase up-section. CIA values (after correction for K-metasomatism) are 92-100.

3.6.3 Camp Quest

The Camp Quest core can be divided into three zones (Figure 3-7). Unweathered bedrock is present below 338.6 m (core depth). The transition from unweathered granitic gneiss to paleosaprolite is difficult to distinguish because the visible textures throughout the core are unchanged. The primary difference between the weathered and unweathered sections is the brittleness of the paleosaprolite and the presence of fractures, some of which are coated in clay. Weak red (2.5YR 5/3) and light greenish gray (10GY 8/1) clays can be found coating some fractures, with the greenish-white clay being the more common of the two at depth. The frequency of clay-coated fractures increases with depth. The paleosaprolite is not nearly as friable as the paleosaprolite in other cores. A thin light olive gray (5Y 6/2) sediment is present between the sandstone and the paleosaprolite, which is visually similar to the one found between the paleosol and sandstone in the Elk Point core. The Mt. Simon Sandstone is present above 323.8 m. Unlike the Elk Point core, no basal conglomerate is present at the base of the Mt. Simon Sandstone in the core.

XRD observations of mineral phases reveal that anorthite, albite, and quartz are present in the granitic gneiss, along with minor apatite and calcite (Figure 3-7). Apatite and calcite become more abundant in the paleosaprolite, along with rutile, although all three mineral phases disappear towards the surface. Illite is present throughout the paleosaprolite and kaolinite exists towards the top of the profile.

Major oxide results show similarities to the Harris and Elk Point profiles (Figures 8a and 8b). The paleosaprolite is characterized by complete loss of Na and Ca throughout most of the profile (96-99% and 86-98% loss, respectively). Mn, Mg, and Fe vary in concert, displaying zones of depletion at depth (78%, 55%, and 36% loss, respectively) and

enrichment up-section (20%, 40%, and 53% enrichment, respectively). K is enriched throughout the profile (86-433% enrichment). Al is slightly depleted in the paleosaprolite (15-30% loss). P is mostly depleted in the paleosaprolite (16-95% loss), with enrichment at the very top of the paleosaprolite (109% enrichment). A geochemically interesting zone is present between 329.5 m and 331.6 m, which is not apparent in visual inspection of the core. Within this interval, Na and Ca show incomplete loss (70% and 25% loss respectively) and P is considerably enriched (up to 133% enrichment). S is enriched (0.9 wt%) at the base of the sandstone and in the top few centimeters of the paleosaprolite, but otherwise is absent from most of the weathered profile. Total C is enriched up to 0.5 wt% in the paleosaprolite. Organic C is present in very small quantities (~0.02 wt%) throughout most of the paleosaprolite, although it is slightly enriched (~0.06 wt%) near the top of the weathered zone. CIA values (after correction for K-metasomatism) increase from the base of the saprolite (73) to the top (>88).

3.6.4 LaFleur

The LaFleur core, located just to the east of Elk Point, is present only in the form of well cuttings, so detailed visual descriptions are limited. The section can be divided into three zones based on the core log and mineralogy, which was determined by XRD (Figure 3-9). The abundance of rutile and the absence of anorthite and albite denote the lower boundary of the paleosaprolite at 314.9 m, below which unweathered granite is present. Paleosaprolite is present between 314.9 m and 313.0 m. The Mt. Simon Sandstone is present above 313.0 m, which was determined based on the prevalence of quartz and pyrite, distinguishing characteristics of the sandstone in the Elk Point core.

Major oxide results (Figure 3-10) show that Na loss is 89% below the base of the paleosaprolite, a pattern that is seen at the nearby Elk Point site. Na loss above this zone increases from 4% to 96% between 316.5 m and 314.3 m. Like the previously described profiles, Na is completely lost from the paleosaprolite (96-98%). Ca has a similar depletion pattern as Na, with 77% loss just below the base of the paleosaprolite, a slight

enrichment (20% enrichment) at the boundary, and high losses (82-84% loss) within the paleosaprolite. Mg is enriched in the paleosaprolite (15-68% enrichment). Mn is substantially enriched at the paleosaprolite-parent material boundary (157% enrichment), and slightly depleted in the paleosaprolite (0-25% loss). Fe is enriched throughout the profile (18-91% enrichment), with the highest enrichment at the base of the paleosaprolite. Al is depleted throughout the profile (38-92% loss). Si is depleted throughout the profile (47-93% loss), except in the paleosaprolite, where it is enriched up to 23%. P is lost from the entire profile (67-92% loss) and the loss is less substantial within the paleosaprolite (56-58% loss). CIA values, after correction for K-metasomatism, are typically >85. There is considerable scatter of the unweathered granite on the A-CN-K plot, which indicates it does not have a uniform composition or alternatively, may be an artifact of the depth-averaged nature of the well cuttings.

3.6.5 Sharp

The Sharp core can be divided into four zones (Figure 3-11). Minimally weathered basalt is present below 667.2 m. Paleosaprolite lies between 661.4 m and 659.0 m. The paleosaprolite contains fine fractures and mottles between 662.0 m and 661.4 m, which may indicate the top of an older basalt flow (R. Anderson, personal communication 2/07). No paleosol is present at this interface and many of the chemical trends (discussed subsequently) indicate that any earlier weathered features are heavily overprinted by subsequent weathering that formed the overlying paleosol and paleosaprolite. A weak red (10R 5/3) friable, unlithified paleosol lies between 659.0 m and 657.5 m and tends to have angular blocky structure. The paleosol becomes dusky red (10R 3/3) up-section. In contrast to the previous cores, the Mt. Simon Sandstone, which lies above 657.5 m in this core, is darker in color with some large clasts and cross-stratification. The zones were determined by visual inspection and confirmed by geochemical and mineralogical trends.

Inspection of thin sections confirms that a majority of the core has undergone intense alteration. The deepest analyzed sample contains biotite crystals, some of which are embedded in plagioclase. Some of the crystals are cracked, with carbonate infilling.

Biotite crystals do not appear fresh and showed considerable degradation. XRD results (Figure 3-11) indicate that illite, diopside, anorthite, albite, and magnetite are present at this depth. Up-section, biotite crystals disappear and are replaced by clay formed *in situ* (based on the lack of translocation features). There is almost no evidence of relict crystal structures in the paleosol and paleosaprolite. The mineral phases present throughout this portion of the profile and detected by XRD are magnetite, hematite, kaolinite, and smectite. Calcite veins are present near the top of the older basalt flow, but they appear heavily degraded and fractured in thin section. Unlike the Elk Point profile, there is no evidence of clay translocation in the Sharp profile. In thin section, the overlying Mt. Simon Sandstone is characterized by well-rounded quartz grains with minor calcite cementation, an observation that is confirmed by XRD.

Major oxides reveal similar trends as observed in previous cores (Figures 12a and 12b). Na is completely lost from the entire weathered section (95-98% loss). Ca, Mg, and Mn show almost complete depletion (95-100% loss, 97-99% loss, and 80-92% loss, respectively), with incomplete depletion at the boundary between basalt flows (80-90% loss, 69-82% loss, and 71-77% loss, respectively). K shows strong depletion in the older basalt flow (90-98% loss) with incomplete depletion in the younger one (60-80% loss). Fe is depleted in the older flow (1-46% loss) and enriched in the younger flow (12-55% enrichment). Al is comparable to unweathered basalt, although it does show slight enrichment in the older flow (5-25% enrichment). Si is enriched in the older flow (8-33% enrichment) and depleted in the younger flow (50-56% loss). P is partially depleted throughout the profile (43-51% loss), except at the base of the paleosaprolite and the boundary between basalt flows where it is enriched 95-316% and the paleosol-paleosaprolite boundary where it is enriched 156%. No S is present in this core. Bulk C is present in low concentrations (up to 0.04 wt%), except at the base of the paleosaprolite and the base of the Mt. Simon Sandstone, where it is present up to 0.4 wt%. After decarbonation, the C content of the paleosol and paleosaprolite remains unchanged through a majority of the profile. CIA values for the entire weathered portion of the Sharp profile are between 93-100 before and after correction for K-metasomatism.

3.6.6 Hummell/Nelson

The Hummell and Nelson cores have been grouped together because they were drilled close to one another (2.5 km separation). Neither core contains unweathered basalt, but the base of the Nelson core is the least weathered, based both on visual inspection and geochemical analysis. The Hummell core can be divided into three zones (Figure 3-13). Paleosaprolite is present below 846.7 m down to the total depth drilled for this core. The basalt from which the paleosaprolite is derived contains mm- to cm-scale calcite-infilled fractures. A light olive brown (2.5Y 5/3), extremely friable, unlithified paleosol with a platy structure is present between 846.7 m and 846.1 m. The Mt. Simon Sandstone, present above 846.1 m, is similar to the sandstone found in the Sharp core. The sandstone is darker and contains large clasts and cross-stratification. A basal conglomerate is present in this core and coloration indicates that some of the underlying paleosol may have been incorporated into the base of the Mt. Simon Sandstone. The Nelson core does not contain any visible paleosol (Figure 3-14). Minimally weathered basalt is present below 861.4 m. Paleosaprolite is presumably present between 861.4 m and 859.8 m, although only a small section of the paleosaprolite is present in the core section. The Mt. Simon Sandstone in the Nelson core is similar to that found in the Hummell and Sharp cores, with darker colors, larger well-rounded and well-sorted clasts, and cross-lamination. It is present above 859.8 m. The base of the sandstone and any paleosol that may have been present in this core is missing. For purposes of strain calculations, the base of the Nelson core was used for calculations of oxide depletion and enrichment in the Hummell core.

The Hummell core contains albite and anorthite at the base (Figure 3-13). Hematite and clays such as kaolinite and illite are present as well, indicating that the base of the core is partially weathered. A hydrothermal zone is present in the basalt, as indicated by an increased abundance of hedenbergite, chlorite, and serpentine in XRD between 848.3 m and 847.0 m. In addition, chlorite and serpentine are present in thin sections from these depths. Veins of chlorite and calcite are heavily fractured and degraded (Figures 15a and 15b), indicating that they are weathered. Above the hydrothermal zone, the dominant

minerals present are clays such as kaolinite and illite. In addition, goethite is present in the paleosol. In thin sections, clay dominates in the paleosol and there are almost no relict crystals present. The clay is deformed in places but has not formed the types of argillans that are found at Elk Point. The Nelson core is mostly unweathered, as indicated by the presence of anorthite and albite throughout the profile (Figure 3-14). These minerals are lost towards the top of the profile and more clays are visible in thin section, indicating that a weathered section may have existed between the basalt and the overlying sandstone, but either was not preserved or was not recovered during drilling. Kaolinite and illite increase up-section. The Mt. Simon Sandstone in both cores is dominated by quartz, although in the Hummell core, it is cemented by small amounts of calcite and pyrite. Hematite is also present at the base of the Mt. Simon Sandstone in the Hummell core and in thin section, clay-rich clasts that are visually similar to the Hummell paleosol are mixed with quartz grains (Figure 3-15c).

Major oxide and elemental results for the Hummell (Figures 16a and 16b) and Nelson (Figures 17a and 17b) cores reveal trends similar to previous sites. Like in all previous cores, Na is completely lost from a majority of the weathered section in the Hummell core (98-99% loss). The zone between the sandstone and minimally weathered basalt in the Nelson core is likewise completely Na-depleted (98% loss). Ca, Mg, and Mn are substantially depleted in the Hummell core (88-97% loss, 73-82% loss, and 76-79% loss respectively), and slightly less so in the weathered hydrothermally altered zone (55-80% loss, 35-62% loss, and 22-63% loss, respectively). K is substantially enriched in both cores (65-447% enrichment). Fe is slightly depleted in the Hummell paleosaprolite (4-33% loss) and becomes enriched in the paleosol (24% enrichment). Fe is slightly enriched in the Nelson core (16-25% enrichment). Al is depleted in the Hummell paleosaprolite (6-60% loss) and becomes slightly enriched in the paleosol (4% enrichment). Al remains mostly unchanged in the Nelson core, although it becomes somewhat enriched up-section (21% enrichment). Si is slightly depleted in the Hummell core (42-63% loss) and unchanged in the Nelson core. P is slightly enriched in the Hummell paleosaprolite (3-50% enrichment) and almost completely lost in the paleosol (97% loss). In the Nelson core, P content remains unchanged. S is slightly enriched in

the Hummell core hydrothermal zone (0.02 wt%) and at the base of the Mt. Simon Sandstone (0.14 wt%). There is no S present in the Nelson core. Total C is enriched in the hydrothermal zone of the Hummell core (1.64 wt%) and in the Mt. Simon Sandstone (0.73 wt%). Total C is highest in the zone between the basalt and the Mt. Simon Sandstone in the Nelson core (0.27 wt%). After decarbonation, organic C is present up to 0.08 wt% in the Hummell core and 0.22 wt% in the Nelson core. CIA values for the weathered portion of the Hummell and Nelson cores fall between 95-100, after correction for K-metasomatism.

3.7 Discussion

3.7.1 Age Constraints

A critical step in paleopedology is determining the time of formation of a paleosol or paleosaprolite. The basement material in the study region ranges in age from 1800 Ma (Harris Granite) to 1100 Ma (Keweenawan flood basalts), placing a lower boundary on potential ages of the paleoweathering features within that time span. As with most basal Cambrian sandstones, the Mt. Simon Sandstone is difficult to date due to a lack of body and trace fossils in the lower portions of the sandstone. However, biostratigraphy of formations overlying the Mt. Simon Sandstone can constrain the youngest possible date for sandstone deposition. The oldest fossils in the Elk Point and Camp Quest cores are *Aphelaspis* zone trilobites (McCormick, 2005; Runkel et al., 2007), which are present in the Bonneterre Formation that overlies the Mt. Simon Sandstone in both cores. Older faunal zones have been reported in additional cores in the study area, including *Crepicephalus* zone trilobite fossils in the Rhinehart A-1 core located close to the Hummell/Nelson cores (Runkel et al., 1998); and even older *Cedaria* zone trilobites at the base of the Bonneterre Formation in the Quimby core, located to the southwest of the Elk Point-LaFleur-Camp Quest area (Runkel et al., 2007). The *Cedaria*, *Crepicephalus*, and *Aphelaspis* faunal zones cover a period of time between 503-500 Ma (Shergold and Cooper, 2004). Because these faunal zones are located in the formations that overlie the

Mt. Simon Sandstone or at the very top of the Mt. Simon Sandstone throughout the study area, the formation itself is most likely older than 503 Ma.

Paleoweathering features present in cores from this region could have developed anytime between 1800 to 1100 and 503 Ma. Previous paleosol studies in the MRS region have assumed that the age of formation for paleosols is most likely closer to that of the overlying sandstone than the underlying basement material (Driese et al., 2007). As long as a weathering surface is exposed to the atmosphere, it will be subject to weathering reactions. A surface that is overlain by Middle Cambrian sediments was mostly likely exposed to the Middle Cambrian atmosphere prior to burial and so would likely reflect weathering conditions at that time. In the unlikely event that older Proterozoic paleosols present within the study area were exhumed during the Cambrian, the older weathering patterns would most likely have been quickly overprinted by younger weathering in a warm Cambrian world, unless exposed for only a brief period of time. Although the possibility exists for a much older age for the paleosols in the study region, in the absence of any compelling evidence for such an older age, a late Middle Cambrian age is the most conservative estimate.

3.7.2 Pedogenic Features

The first step in determining whether the weathered sections in the study area are useful for reconstructing weathering conditions during the Middle Cambrian is to determine if they are in fact a result of pedogenic processes. A variety of processes can affect paleosols after burial (Chapter 2), obscuring weathering signatures. Despite post-burial diagenetic effects (detailed later), several primarily pedogenic features are present throughout the study area.

3.7.2.1 Sodium Mobilization

The most noticeable pattern across the entire study area is the near-complete loss of Na in all alteration zones. Na is a highly mobile cation that is easily lost during hydrolysis, a

soil weathering reaction that releases cations such as Na^+ from primary minerals such as albite. This pattern of complete Na loss has been observed in other Middle Cambrian paleosols near the study area by other researchers (Driese et al., 2007) and in weathering horizons developed on granites and basalts of varying ages (Zbinden et al., 1988; Driese et al., 2007; Zhang et al., 2007; Jutras et al., 2009), indicating that it is a common feature in many paleosols.

3.7.2.2 Calcium Mobilization and Carbonate Precipitation

In the soil environment, Ca is easily mobilized via dissolution reactions, which release Ca^{2+} cations from calcite. In humid climates, water flow through well-drained soils is sufficient to remove Ca from the weathering horizon. However, in drier environments where water cannot penetrate deep into the soil before evaporating, Ca can precipitate at the average depth of wetting (Retallack, 2001) and can incorporate Mn and Mg due to their ability to substitute for the Ca^{2+} ion. The dominant pattern in the study area is strong depletion, as seen in the Harris, Sharp, and Hummell/Nelson cores. Ca loss is significant, although incomplete, at depth in the Sharp and Hummell cores where calcite-enriched zones are present in the paleosaprolite. In the Sharp core, this occurs at the top of an older basalt flow and in the Hummell core, this occurs in a hydrothermal vein. The calcite is not pedogenic, as the calcite veins are visibly degraded and fractured in thin sections of these profiles and are associated with geogenic features that were likely present prior to the onset of weathering. Significant Ca losses indicate that in a majority of the study region, well-drained soil conditions contributed to significant losses of Ca.

The Elk Point profile differs from this pattern in that there are significant amounts of dolomite present throughout the paleosaprolite and at the base of the paleosol, a feature that is not observed elsewhere in the study area. The dolomite is present in two primary forms: as individual rhombs and as pore infillings and concretions. The 0.5-1 mm rhombs consist of a core dolomite crystal and a secondary layer, indicating several phases of growth. Within the paleosaprolite, dolomite is present as larger concretions. Rhombs are occasionally visible, but most are present as part of larger concretions. No dolomite

is present elsewhere in the section. Pedogenic dolomite is extremely rare, but can form under saline soil conditions and in soils derived from Mg-rich parent material (El-Sayed et al., 1991; Kessler et al., 2001). Dolomite precipitated from marine fluids typically incorporates significant amounts of Sr (El-Sayed et al., 1991; Bone et al., 1992), but this is not the case at Elk Point where dolomite contains low Sr contents (<100 ppm), hence precluding a significant marine influence during carbonate precipitation, especially during the Cambrian when ocean Sr levels are expected to have been high due to high continental weathering rates (Montanez et al., 1996). The Mg content of the Elk Point metagabbro is not particularly high (3-5 wt%), especially compared to the Keweenaw basalts (5-8 wt%), which weathered to dolomite-free paleosols. A purely pedogenic explanation for dolomite at Elk Point, therefore, is not favored. The dolomite is most likely a result of post-burial recrystallization of pre-existing pedogenic carbonate by dolomitizing fluids known to have affected the MRS region (discussed later) (Luczaj, 2006). The presence of pedogenic carbonate (prior to post-burial dolomitization) more than 2 m below the surface of the paleosol indicates that this soil formed in a slightly drier environment than the other sites, which allowed for Ca^{2+} precipitation at depth, rather than complete removal as seen at other sites in the study region.

3.7.2.3 Iron Mobility

Iron mobility in soils has been used frequently in the past as an indicator of soil and, by extrapolation, paleosol redox state to determine the oxidation state of the atmosphere, especially for the Precambrian (Holland, 1984, 1992; Ohmoto, 1996; Holland et al., 1997). In general Fe is immobile in oxidizing and alkaline conditions and mobile in reducing and acidic conditions. All weathering profiles are posited to have developed primarily during the Middle Cambrian under an oxygenated atmosphere (Canfield et al., 2006).

In the Elk Point, Sharp, and Hummell profiles, Fe is most strongly enriched in the paleosol. However, the patterns of enrichment and depletion differ between these three paleosols. In the Elk Point paleosol, Fe is barely enriched in the paleosol and

consistently depleted in the paleosaprolite, which is indicative of transient reducing conditions at depth. Siderite is present in minor quantities at the interface between paleosol and paleosaprolite, which is also consistent with transient reducing conditions at depth. In both the Elk Point and Sharp paleosols, Fe is present as hematite, which gives both paleosols a bright red coloration. In the Hummell paleosol, however, Fe in the paleosol is present primarily as goethite, which gives that paleosol a brown coloration. Post-burial alteration can dehydrate goethite to hematite (Retallack, 2001), so it may be possible that the hematite in the Elk Point and Sharp paleosols is a result of diagenesis rather than pedogenesis. Regardless, the high abundance of goethite and hematite in these highly weathered paleosols is consistent with soil development in tropical and subtropical weathering regimes (Kabata-Pendias, 2001; Retallack, 2001; Schaetzl and Anderson, 2005). The presence of goethite at the Hummell site in particular is indicative of moister soil conditions than were present at the Elk Point and Sharp sites, provided that the hematite at those two sites is primary. Minor Fe depletion at depth in all three profiles may be a result of transient reducing conditions as a result of soil saturation, but not long enough to result in considerable depletion of Fe.

In the study area, the vast majority of the soil profiles show a pattern of Fe enrichment near the surface and Fe depletion deeper in the profile. The only site where this pattern does not hold is at the Harris site, where Fe is partially lost throughout the profile, though the magnitude of depletion decreases with depth. In the Harris core, Fe is partially depleted and present in siderite. Siderite can be precipitated in soils that are water-saturated and poorly-oxygenated (Retallack, 2001). Siderite is often accompanied by pyrite in reducing soil conditions, provided that a source of sulfur is present either from weathered parent material or a later influx of sulfate-rich ocean water. Siderite will not precipitate until all S has been precipitated as pyrite in reducing conditions. No sulfur or pyrite is present in the Harris profile, either in the granite or the overlying paleosaprolite, indicating no marine influence on the profile during weathering.

3.7.2.4 Clay Mineralogy and Mobility

Clay mineralogy in the study area is dominated by illite and kaolinite. Illite has two potential origins in paleosols: pedogenic formation from acidic igneous rocks (such as granites and granitic gneisses) and alteration of smectite by K-rich fluids after burial (Grathoff et al., 2001; Retallack, 2001; Schaetzl and Anderson, 2005). K-enrichment patterns throughout the study area suggest that a majority of the illite is a result of post-burial illitization of pedogenic smectites. The Sharp site is the only one within the study area that was not affected by K-metasomatism, and so retains some pedogenic smectite. Smectites are relatively cation-rich clays and under more intense weathering conditions, are replaced by more heavily leached clays such as kaolinite. Kaolinite is present in small quantities at the surface of the Camp Quest site. It is present at comparable or greater quantities than smectite/illite at the Sharp, Hummell, and Nelson sites and is the only clay present at the Harris site. In modern environments, smectite forms in drier areas where leaching is incomplete, while kaolinite forms in warm, humid climates as a result of intense leaching (Schaetzl and Anderson, 2005). The abundance of smectite (later altered to illite) at the Elk Point, LaFleur, and Camp Quest site suggests that this half of the study area was slightly drier compared to the eastern half, where considerable leaching resulted in the systematic destruction of smectite and formation of kaolinite as a result of more humid conditions. This interpretation is consistent with previously discussed paleoclimatic indicators, such as pedogenic carbonates at the Elk Point site indicating drier conditions, and goethite at the Hummell site indicating wetter conditions. The presence of kaolinite as the only form of clay at the Harris site indicates intense leaching, which is consistent with iron leaching and siderite precipitation due to frequent water-saturated conditions.

Clays within the study area were mostly formed *in situ*, which is evident by the lack of clay translocation features and the distribution of clays, which often mimic the fabric of the parent material from which they weathered, especially in the Sharp, Hummell, and Nelson paleosaprolites. Clay translocation is readily identifiable at the Elk Point site and is most noticeable near the surface, where argillans are present between 13 and 37 cm

paleosol-depth, and dominate the soil microfabric at 28 cm paleosol-depth. Clay translocation involves dispersion in zones of low base saturation, downward transport by water, and flocculation in lower zones as a result of desiccation, the presence of base-rich pore water, or decreased soil pore sizes (Schaetzl and Anderson, 2005). The depth of carbonate deposition at Elk Point (~2 m) and the presence of clay-coated fractures within the paleosaprolite indicate that water percolated deeply into the profile and was not restricted to the top 30 cm of the paleosol. Argillans at Elk Point overlap with the zone of active apatite dissolution and are especially prominent 5 centimeters above the last appearance of apatite. Active dissolution of apatite, which is present in quantities of 2-5 wt% throughout the paleosol, may have released Ca^{2+} ions that aided in clay flocculation and formation of argillans near the top of the paleosol.

3.7.3 Post-Burial Alteration

K is a highly mobile cation that is easily lost from modern weathering horizons, much like Na. However, within the study area, K is substantially enriched in a majority of the profiles (with the exception of the LaFleur and Sharp profiles) and present within illite. This enrichment is likely the result of K-metasomatism, which has been reported in many paleosols and alteration profiles beneath Cambrian sandstones in the MRS region (Zbinden et al., 1988; Dott, 2003; Liu et al., 2003; Driese et al., 2007). K-metasomatism in this region has been previously associated with brine migration during the Acadian (Devonian) and Alleghenian (Permian) orogenies (Grathoff et al., 2001; Liu et al., 2003). The few studies that have investigated the age of K-metasomatism in central Iowa suggest a Permian date for illitization in this area (Grathoff et al., 2001). None have investigated the composition of brines and direction of flow in the study area, which is within and north of the Forest City Basin (Anderson and Wells, 1968; Luczaj, 2006). Contemporaneous brine migration has, however, been thoroughly studied in the nearby Illinois Basin and Wisconsin Arch due to its likely contribution to Mississippi Valley-Type (MVT) Pb-Zn deposit formation (Grathoff et al., 2001; Pannalal et al., 2004; Luczaj, 2006). These studies may provide insights into the nature of post-burial alteration of weathered zones in the study area.

MVT deposit-associated brine migration has been previously linked to dolomitization and illitization within the MRS region (Sverjensky, 1986; Duffin et al., 1989; Grathoff et al., 2001; Liu et al., 2003; Luczaj, 2006). Studies of fluid inclusions preserved in minerals precipitated from the brine indicate a Na-Ca-Mg-Cl-H₂O composition with salinities between 8-28 wt% NaCl equivalent (Liu et al., 2003; Luczaj, 2006). One potential source of this fluid is evolved seawater mobilized from thrust zones with increasing meteoric water contributions at increasing distances away from the thrust zone (Ziegler and Longstaffe, 2000). Brines of similar composition migrating through the study area would explain several notable non-pedogenic features, such as high K and illite contents (illitization of pedogenic smectites) and the presence of low-Sr dolomite at Elk Point (dolomitization of pedogenic carbonates).

Within the study area, S content of parent material is negligible and is only present in parent material that was metamorphosed or hydrothermally altered prior to weathering (Elk Point and Hummell, respectively). During weathering, S was lost as the pyrite was oxidized, as no S is present in any of the weathered profiles. Substantial amounts of pyrite, however, are present at the top of the Elk Point profile (up to 8 wt%), where it encrusts the basal Mt. Simon Sandstone conglomerate. Nodular pyrite is present in the drab, reduced upper few centimeters of the paleosol (Figure 3-5a) and is not present deeper in the profile. Smaller surface pyrite enrichments are present at the Camp Quest and Hummell sites. Within the Mt. Simon Sandstone in the Hummell core, pyrite is present only in clay clasts that bear a striking resemblance to the underlying paleosol (Figure 3-15c). No pyrite is present at the surface of the Harris paleosol, which was previously demonstrated to have lost Fe as a result of reducing soil conditions. The Sharp paleosol, which was not metasomatized, likewise shows no surface pyrite enrichment. Pyrite within the studied cores is most likely diagenetic and tends to occur at the surface of metasomatized profiles that contain pedogenic iron oxides. Pyrite may have been precipitated shortly after the weathering horizon was buried by transgression of the sea and deposition of the Mt. Simon Sandstone, with pyrite precipitating in surface zones where pedogenic iron oxides reacted with marine S. Alternatively, S-rich reducing

fluids may have flowed preferentially along the paleosol/paleosaprolite-sandstone contact, allowing S to react with pedogenic Fe-oxides mobilized by reducing conditions. Pyrite precipitation in the MRS region, especially within basal conglomerates at the Precambrian-Cambrian boundary, has been previously noted and attributed to brine migration (Sverjensky, 1986; Luczaj, 2006). The pyritizing event was most likely separate from the K-metasomatic event, as K enrichment is present throughout the weathered section, while pyrite is present only at the paleoweathered surface at select sites (Elk Point, Camp Quest, and Hummell).

Although brine migration throughout the study region has resulted in pervasive K enrichment, probable dolomitization of pedogenic carbonates, and potentially pyrite precipitation at the paleosol/paleosaprolite-sandstone contact, a majority of the geochemistry within the weathered profiles is unaffected. Pyrite precipitation only affects the uppermost centimeters of the paleoweathered surface, as evidenced by the absence of pyrite below the top few centimeters of the weathered profile. Dolomitization only affects pre-existing carbonates, as evidenced by the absence of dolomite at other metasomatized sites. Aside from extensive K enrichment, comparison of the un-metasomatized Sharp geochemical profiles to those at other sites in the study region indicates no appreciable overprinting or alteration of the chemical composition of paleoweathered zones, an observation previously made by Driese et al. (2007) in relation to penecontemporaneous weathered profiles to the north of the study area.

3.7.4 Paleosol Classifications

Classification of paleosols using modern soil classification schemes can be difficult, as paleosols have often undergone erosion, compaction, and geochemical reactions as a result of burial and post-burial fluid flow. Nonetheless, preliminary classifications based on remaining B horizons, which are the most important horizons for classifying a soil, can aid in purposes of interpretation.

3.7.4.1 Weathering on Granitic Parent Materials

In modern environments, granites and granitic gneisses tend to weather to nutrient-poor sandy residuum (*grus*) due to the high quartz content of the parent material (Retallack, 2001; Schaetzl and Anderson, 2005). The quartz-rich Mt. Simon Sandstone has been previously attributed to redistribution of chemically weathered *grus* by the transgressing Cambrian seas (Dott et al., 1986; Dott, 2003; Driese et al., 2007). Non-lithified sandy residuum rich in titanium oxides has been previously reported at the LaFleur site (McCormick, 2005) and may be present at the Harris site (personal observation). No such sandy residuum has been noted for the Camp Quest site. Because of the loose nature of the sandy residuum at these sites, there is a high probability that the upper horizons of the paleoweathered zones may have been lost and that only the deeper horizons remain.

Middle Cambrian weathering on the Harris granite is consistent with modern granite weathering profiles. At the Harris site, only a C horizon is present. The Harris paleosaprolite is capped by a thin, silica rich layer (based on oxide analysis and personal observations) that may be a thin duricrust. A duricrust is a soil horizon cemented by illuvial silica, and its presence here may have prevented further loss of the paleoweathered zone during the Cambrian transgression. Silica is not typically mobile in soils, but can become so under wetter, high-pH conditions (Schaetzl and Anderson, 2005). The profile is thoroughly leached, as evidenced by loss of major cations, the presence of kaolinite, and high CIA values (>85). The paleosaprolite was likely water-saturated and experienced frequent reducing conditions, resulting in the mobilization of Fe and siderite precipitation beneath the purported duricrust. The Harris paleosaprolite can be classified as the truncated based of an Ultisol that developed in an aquic moisture regime.

The Camp Quest paleosaprolite is directly overlain by the Mt. Simon Sandstone. There is no indication either from the core log or core observations of a granitic gneiss-derived sandy residuum or *grus*. If such a residuum was present at the site, it was lost either

during the weathering process or to the transgressing seas. The remaining material is heavily weathered, as evidenced by high CIA values (>88) and the loss of major cations throughout the profile. The illite present in the paleosaprolite may have been the direct weathering product of the Camp Quest granitic gneiss, but K-enrichment throughout the profile suggests that the illite is most likely diagenetic and was probably smectite prior to illitization. Kaolinite present at the surface may indicate more intense surface weathering. Clay coatings on fractures throughout the paleosaprolite may be a result of downward transport of pedogenic clays by water percolating along joints between corestones. The Camp Quest paleosaprolite is likely a truncated paleosaprolite, with only the C horizon remaining. The absence of *grus* between the paleosaprolite and the overlying Mt. Simon Sandstone may indicate that the Camp Quest paleosaprolite developed on steep topography, resulting in continual loss of *grus* during pedogenesis. Alternatively, the *grus* may have become incorporated into the Mt. Simon Sandstone or was stripped away during the transgression. The Camp Quest paleosaprolite is best classified as the truncated remains of an Alfisol or Ultisol that developed in a xeric (Mediterranean) moisture regime, resulting in more intense weathering at the surface and heavy leaching at depth, but incomplete weathering of clays.

Classification of the LaFleur site is difficult because samples from the site are present as well cuttings rather than as core. The geochemistry and mineralogy of the core suggests that a paleosaprolite is present between the unweathered granite and the overlying Mt. Simon Sandstone, based on cation loss patterns, high CIA values (>85), and the presence of illite and rutile. K is not particularly enriched at the LaFleur site, so illite may be pedogenic in origin, rather than diagenetic. The paleosaprolite present at this site could potentially be classified as an Alfisol or Ultisol that developed in a xeric or ustic (semi-arid) moisture regime, resulting in incomplete clay weathering.

3.7.4.2 Weathering on Mafic Parent Materials

In modern environments, soils derived from mafic materials tend to be redder due to higher parent material Fe content; more nutrient-rich due to high parent material contents

of Ca, K, Na, and Mg; and more clay-rich due to lower parent material quartz abundances (Retallack, 2001; Schaetzl and Anderson, 2005). Within the study area, mafic material is present primarily in the zone of Precambrian rifting in the eastern half of the study area. Mafic material is also present as intrusions in older terranes, such as the metagabbro at Elk Point.

Weathering at the Elk Point site is characterized by the development of a thick, clay-rich paleosol (Bt horizon) overlying a carbonate-rich paleosaprolite (Ck horizon). The persistence of apatite, a mineral that is soluble in acidic conditions, indicates that the soil was likely alkaline during the course of its development. Accumulation of clays above the zone of apatite dissolution suggests that the top few centimeters of the paleosol were likely acidic and heavily leached, which aided in apatite dissolution and clay dispersion near the soil surface. K-enrichment patterns suggest the presence of illitized smectite. This paleosol is best classified as an Alfisol, based on incomplete clay weathering, the presence of clay-rich horizons, and the persistence of apatite (indicating alkaline soil conditions). The presence of a carbonate horizon at depth indicates that the paleoweathered section likely developed in an ustic moisture regime.

The Sharp profile shows intense weathering and complete cation loss down to considerable depths. The clay-rich surface layer is likely a Bt horizon. The paleosaprolite can be classified as a C horizon. The major clays present include smectite and kaolinite, indicating intense weathering and partial destruction of smectite. The Sharp paleoweathered zone is best classified as an Ultisol. The depth of weathering and the absence of a zone of carbonate enrichment indicate that paleoweathering most likely took place in an udic (wet) moisture regime.

The Hummell/Nelson profiles likewise show intense weathering and complete cation loss. The Hummell paleosol is likely a Bt horizon, and both the Hummell and Nelson cores contain significantly altered C horizons. Both cores contain kaolinite and illite (likely a result of K-enrichment of smectites), indicating weathering conditions similar to those at the Sharp site. Classification of the Nelson core is difficult due to the poorly

recovered nature of the paleosaprolite. The Hummell profile is best classified as an Ultisol, and likely developed in a perudic (very wet) moisture regime based on the presence of the hydrated Fe-oxide goethite and Al loss (potentially as a result of biological activity, which will be discussed later).

3.7.5 Soil-Forming Factors

The Alfisols and Ultisols that developed in the study area show considerable cation loss and high CIA values, indicating intense alteration, which is consistent with development in warm, generally humid climates. The alteration was incomplete at all sites based on the persistence of clays (which are typically destroyed in tropical Oxisols, generally considered the endpoint of soil formation) and is most consistent with a subtropical climate. The eastern sites (Sharp, Hummell, and Nelson) contain more weathered clays (kaolinite) and evidence of higher soil moisture content (goethite) than sites to the west (Elk Point, Camp Quest, and LaFleur), which tend to contain illite and carbonates (particularly at the Elk Point site). The Harris site is unusual in that although it is in the western half of the study area, it probably developed in an aquic moisture regime. Paleogeographic reconstructions place the study area at or near the equator during the Middle Cambrian, with the drier sites (Elk Point, Camp Quest, and LaFleur) located to the north of the wetter sites (Sharp, Hummell, and Nelson). The intense weathering that characterizes the study area is consistent with previous studies of weathering in this region (Driese et al., 2007). A warm, humid subtropical climate for the study area based on the observed weathering patterns is not entirely consistent with the hot, humid climate that would be predicted for an equatorially located area during a time of high CO₂ levels (>10 PAL), and consequently high temperatures (Berner, 2006; Came et al., 2007) and that there is some evidence for from the carbon isotope record (Brasier and Sukhov, 1998; Saltzman et al., 2004). The discrepancy between predicted and observed weathering in the study region (based on climate models and paleogeography) has several possible explanations. Most Paleozoic climate research has been focused on the Precambrian-Cambrian transition and the climate effects of the post-Ordovician rise of terrestrial ecosystems (Mora et al., 1996; Berner, 2003, 2006). As a result, Middle

Cambrian climate has not been well-studied, and so Paleozoic climate and CO₂ models are not well-constrained during this period of time. Despite this problem, models of the Cambrian do not tend to predict low CO₂ levels or temperatures, and so the Middle Cambrian tropical environment would be expected to have been highly leaching and conducive to Oxisol formation, rather than Alfisol and Ultisol formation. The subtropical climate in the study area (with a drier northern region and a wetter southern region) during a high-CO₂ world can potentially be better explained by a more northerly location for the study area than is predicted by paleogeographic reconstructions. Paleogeographic reconstructions during the Cambrian have been problematic, although most agree that Laurentia was moving from high southern latitudes towards and across the equator just prior to and during the Cambrian (Torsvik and Rehnstrom, 2001; McCausland et al., 2007). Alternatively, the study site is located in the continental interior. In a world without substantial plant cover and low evapotranspiration rates, the centrally located study area may have been somewhat drier despite a low paleolatitude, resulting in substantial, but less intense, leaching than in modern, vegetated tropical environments.

In addition to climate, topography and time of exposure can contribute significantly to the formation of weathered profiles. Cambrian sediments above the Precambrian basement in the MRS region are relatively flat-lying today, and elevation variability of the Precambrian basement is limited to about 100 m (Runkel et al., 1998; Runkel et al., 2007). Assuming that the top of the Mt. Simon Sandstone was relatively flat-lying at the time of deposition, which is reasonable given the lack of tectonic deformation in the study region, the thickness of the Mt. Simon Sandstone overlying the Precambrian basement throughout the study area may give an indication of relative topography at the time of burial. In general, drier sites tend to be overlain by thinner Mt. Simon Sandstone sediments, indicating that they may have been located at a slightly higher elevation with better drainage. The Elk Point paleosol (the driest in the study area) is overlain by 2.7 m of sandstone, while the Hummell paleosol (the wettest non-flooded paleosol in the study area) is overlain by 37.5 m of sandstone. Aside from the strong west-east climate signal, topographic variability may have resulted in further weathering heterogeneity within the study area. Within the generally dry western half of the study area, a higher

paleoelevation at the Elk Point site may have resulted in drier soil conditions allowing the precipitation of carbonates, with a lower paleoelevation resulting in frequent water-saturated conditions at the Harris site. Within the generally wet eastern half of the study area, a higher elevation and possibly more well-drained conditions at the Sharp site may have resulted in slightly drier soil conditions that favored the formation of hematite (assuming that the hematite is pedogenic), as opposed to the lower elevation at Hummell where poorer drainage conditions may have resulted in wetter conditions that favored the formation of goethite.

3.7.6 Terrestrial Biota?

A few interesting geochemical patterns within the study area are not easily explained by weathering reactions and may indicate biological influence. Previous studies of granite and basalt weathering indicate that P, Si, and Al mobility can be enhanced in the presence of organic acids (Neaman et al., 2005a, b, 2006).

3.7.6.1 Silicon and Aluminum

Si is not typically mobile in soil environments, except under highly alkaline conditions (Kabata-Pendias, 2001). However, organic ligands may help mobilize Si, especially in basalts for reasons that are not yet fully understood (Neaman et al., 2005b). Throughout a majority of the study region, Si content remains unchanged through the weathered profiles. This is not the case for the LaFleur core, especially through the unweathered bedrock, and may be a result of heterogeneity in the parent material or mixing of samples from various depths during well drilling and cuttings retrieval. Si is also partially depleted in the Sharp and Hummell profiles, which developed on basalts, and may be a result of mobilization by organic ligands.

Like Si, Al is not typically mobile in soil environments. However, it can be mobilized in acidic soils or by organic acids (Kabata-Pendias, 2001; Neaman et al., 2005b). In a majority of the paleoweathered surfaces, Al content is either unchanged or slightly

enriched, indicating loss of other mobile cations, leaving Al relatively enriched compared to the parent material. Al loss is seen in the LaFleur core, and again, may be a result of heterogeneity in the granite. Al is also depleted in the Hummell paleosaprolite, but not in the overlying paleosol. This may be a result of differences in the Hummell basalt and the Nelson basalt, the latter of which is used to normalize both profiles. However, even when the Hummell profile is normalized to the lowermost available sample (which is weathered), Al still shows minor depletion, with the strongest depletion at the base of the Hummell paleosol. This indicates that the Al depletion in this profile is real and may have been a result of mobilization by organic acids and loss resulting from considerable water flow through this paleosol (Neaman et al., 2005a).

3.7.6.2 Phosphorus

P in soils is typically present as apatite and is relatively stable in basic and slightly acidic soil conditions (Neaman et al., 2005b). P cycling in the environment does not include an atmospheric component, and so P is a limiting resource for terrestrial life, as the only source of P is through weathering of apatite present in parent material or through P input via atmospheric dust (Chadwick et al., 1999). As a result, bacteria and fungi have adapted to the paucity of P in the terrestrial realm by evolving certain organic acids that strongly leach P from apatite (Welch et al., 2002), an adaptation that is especially important in weathering of fresh parent material when organic-bound P is not present (Crews et al., 1995). In modern soils, apatite-associated P decreases with time as organic-associated P increases until the apatite source is depleted, at which time organic P begins to decrease as it is lost through surface run-off (Crews et al., 1995). In the oldest soils, P can become immobilized by Fe and Al (Crews et al., 1995), except in arid environments, where it can become incorporated into carbonates instead (Lajtha and Schlesinger, 1988).

P contents throughout the study area are generally low, typically <0.3 wt%, except at Elk Point, where P contents are 1-2 wt%. Geogenic (pre-existing non-pedogenic) features within the Sharp and Hummell profiles likewise show high P contents (~1 wt% at the

contact between basalt flows and ~0.5 wt% in the hydrothermal vein respectively). P patterns in most profiles (except LaFleur and Nelson) tend to show strong depletion up-section. This pattern is especially prominent at Elk Point, which has a higher initial apatite concentration than any other site in the study region. Apatite is present throughout a majority of the Elk Point profile and is completely absent in the top 30 cm of the Elk Point profile, as can be seen in XGT maps (Figure 3-18). There is no evidence from thin sections of secondary phosphate precipitation at depth. The apparent enrichment of P within the paleosol may be a result of minor variability in the original parent material. The persistence of apatite throughout a majority of the Elk Point profile despite considerable chemical alteration indicates pedogenesis under alkaline conditions. The complete and abrupt dissolution of apatite in the top 30 cm of the profile, as well as the previously discussed clay mobilization in the same horizon, is strongly indicative of acidic surface conditions. Apatite and P depletion, especially in dry soils, has been previously attributed to the activity of organic ligands (Neaman et al., 2005a) and is the most likely explanation for abrupt surficial P loss at Elk Point and is further detailed in Chapter 4.

3.7.6.3 Organic Carbon

Organic carbon is present in all of the studied cores, but is typically present in concentrations of less than 0.2 wt%. Organic C tends to increase up-section in all weathered horizons, particularly in the Elk Point, Sharp, and Nelson cores. In the Harris core, organic C content is highest in the purported duricrust. A more thorough analysis of organic C distributions, isotopic composition, and implications for potential Middle Cambrian terrestrial biota are further detailed in Chapter 4.

3.8 Conclusions

Weathering in the MRS region during the Middle Cambrian is characterized by extensive loss of mobile cations and high CIA values, resulting in the formation of Alfisols and Ultisols. However, the persistence of clays and apatite at some sites indicates that

weathering is incomplete, as these minerals tend to be destroyed in intensely altered tropical soils (Oxisols) in the modern world. The extent and intensity of weathering in the study region indicates likely formation in a subtropical climate, which is not consistent with an equatorial paleolocation in a high-CO₂ world. Possible explanations for this discrepancy include a cooler Middle Cambrian world than predicted by climate models, a more northerly paleolatitude than predicted by paleogeographic reconstructions, or drier continental interior environments due to the absence of widespread vegetation and its effect on continental humidity. Western (paleo-northern) sites tend to be drier than the eastern (paleo-southern) sites. Illite (likely illitized smectite) and pedogenic carbonates are present in the western sites (Elk Point, Camp Quest, and LaFleur), while more intensely weathered kaolinite and goethite tend to be present in eastern sites (Sharp, Hummell, and Nelson). The Harris profile is unusual in that even though it is located in the western half of the study area, it was frequently water-saturated.

Secondary controls on paleosol and paleosaprolite formation include topography and parent material. Although a majority of the study area was flat-lying, drier sites tend to be overlain by thinner Mt. Simon Sandstone sequences, indicating that they may have been located at slightly higher elevations and may have experienced more well-drained conditions. Within the drier western half of the study region, the Elk Point paleosol (the driest, based on pedogenic carbonates) is at a higher paleoelevation than the Harris paleosaprolite (the wettest, based on Fe mobilization and siderite precipitation). Likewise, within the wetter eastern half of the study region, the Sharp paleosol (likely the driest, based on pedogenic hematite) is at a higher paleoelevation than the Hummell paleosol (the wettest, based on Al mobilization and pedogenic goethite). Differences in paleoelevation may have resulted in different drainage conditions, with sites at lower paleoelevations being poorly drained compared to sites developed at higher paleoelevations. Weathered profiles are further differentiated from each other by the parent materials from which they weathered. Granitic basements tend to yield paleosaprolites with thin sandy mantles (most of which were lost prior to or during the transgression), while mafic basements tend to yield thick clay-rich paleosols developed

on top of distinctive paleosaprolites. This is consistent with modern weathering patterns of granitic and mafic parent materials.

As noted by many previous studies, sandstones and weathered basement material in the MRS region have been affected by post-burial brine migration. Brine migration and metasomatism in the study area resulted in K-enrichment of pedogenic smectites, dolomitization of pedogenic carbonates, and pyrite precipitation at the paleosol/paleosaprolite-sandstone boundary. Comparisons of metasomatized cores (Harris, Elk Point, Camp Quest, Hummell, and Nelson) to an unmetasomatized core (Sharp) indicate that a majority of the pedogenic geochemical signatures were not affected by brine migration.

Potential biotic weathering signatures have been detected in the study area. Increased Si, Al, and P mobility has been linked to the presence of organic ligands by previous researchers. Si has been lost in the Sharp and Hummell profiles, and Al has been lost from the Hummell profile. P is very strongly depleted at the surface of the Elk Point profile, and also displays loss up-section at other sites throughout the study area. These patterns hint at the presence of a terrestrial ecosystem that was affecting soil formation in the study area during the Middle Cambrian.

3.9 Acknowledgements

This research was funded by the NASA Astrobiology Institute and the Pennsylvania State University Department of Geosciences. Special thanks to Y. Watanabe, H. Gong, E. Altinok, I. Johnson, and D. Hummer for analytical assistance; A. Morales and R. Quintero for field and lab assistance; T. Haggar, P. Morath, and R. Anderson for sample collection assistance; and R. Anderson, Y. Watanabe, and E. Altinok for useful discussion.

3.10 References

- Anderson, K.H., and Wells, J.S., 1968, Forest City Basin of Missouri, Kansas, Nebraska, and Iowa: AAPG Bulletin, v. 52, p. 264-281.
- Anderson, R.R., 2006, Geology of the Precambrian Surface of Iowa and surrounding area, Iowa Geological Survey.
- Anderson, R.R., and McKay, R.M., 1997, Clastic Rocks Associated with the Midcontinent Rift System in Iowa, *in* Interior, U.D.o.t., ed., US Geological Survey, p. I1-I44.
- Anderson, S.P., Dietrich, W.E., and Brimhall, J., G. H., 2002, Weathering profiles, mass-balance analysis, and rates of solution loss: Linkages between weathering and erosion in a small, steep catchment: GSA Bulletin, v. 114, p. 1143-1158.
- Battistuzzi, F.U., Feijao, A., and Hedges, S.B., 2004, A genomic timescale of prokaryote evolution: insights into the origin of methanogenesis, phototrophy, and the colonization of land: BMC Evolutionary Biology, v. 4, p. 44.
- Berner, R.A., 2003, The rise of trees and their effects on Paleozoic atmospheric CO₂ and O₂: Comptes Rendus Geosciences, v. 335, p. 1173-1177.
- , 2006, GEOCARBSULF: A combined model for Phanerozoic atmospheric O₂ and CO₂: Geochimica et Cosmochimica Acta, v. 70, p. 5653-5664.
- Bone, Y., James, N.P., and Kyser, T.K., 1992, Synsedimentary detrital dolomite in Quaternary cool-water carbonate sediments, Lacepede shelf, South Australia: Geology, v. 20, p. 109-112.
- Brasier, M.D., and Sukhov, S.S., 1998, The falling amplitude of carbon isotopic oscillations through the Lower to Middle Cambrian: northern Siberia data: Canadian Journal of Earth Sciences, v. 35, p. 353-373.
- Brimhall, G.H., and Dietrich, W.E., 1987, Constitutive mass balance relations between chemical composition, volume, density, porosity, and strain in metasomatic hydrochemical systems: Results on weathering and pedogenesis Geochimica et Cosmochimica Acta, v. 51, p. 567-587.
- Came, R.E., Eiler, J.M., Veizer, J., Azmy, K., Brand, U., and Weidman, C.R., 2007, Coupling of surface temperatures and atmospheric CO₂ concentrations during the Palaeozoic era: Nature, v. 449, p. 198-201.
- Canfield, D.E., Poulton, S.W., and Narbonne, G.M., 2006, Late-Neoproterozoic Deep-Ocean Oxygenation and the Rise of Animal Life: Science, v. 315, p. 92-95.
- Chadwick, O.A., Derry, L.A., Vitousek, P.M., Huebert, B.J., and Hedin, L.O., 1999, Changing sources of nutrients during four million years of ecosystem development: Nature, v. 297, p. 491-497.
- Condon, D.J., and Prave, A.R., 2000, Two from Donegal: Neoproterozoic glacial episodes on the northeast margin of Laurentia: Geology, v. 28, p. 951-954.
- Crews, T.E., Kitayama, K., Fownes, J.H., Riley, R.H., Herbert, D.A., Mueller-Dombois, D., and Vitousek, P.M., 1995, Changes in Soil Phosphorus Fractions and Ecosystem Dynamics across a Long Chronosequence in Hawaii: Ecology, v. 76, p. 1407-1424.
- Dalziel, I.W.D., 1997, Neoproterozoic-Paleozoic geography and tectonics: Review, hypothesis, environmental speculation: GSA Bulletin, v. 109, p. 16-42.

- Davis, D.W., and Paces, J.B., 1990, Time resolution of geologic events on the Keweenaw Peninsula and implications for development of the Midcontinent Rift system: *Earth and Planetary Science Letters*, v. 97, p. 54-64.
- Dott, R.H., 2003, The Importance of Eolian Abrasion in Supermature Quartz Sandstones and the Paradox of Weathering on Vegetation-Free Landscapes: *Journal of Geology*, v. 111, p. 387-405.
- Dott, R.H., Byers, C.W., Fielder, G.W., Stenzel, S.R., and Winfree, K.E., 1986, Aeolian to marine transition in Cambro—Ordovician cratonic sheet sandstones of the northern Mississippi valley, USA: *Sedimentology*, v. 33, p. 345-367.
- Driese, S.G., 2004, Pedogenic translocation of Fe in modern and ancient vertisols and implications for interpretations of the Hekpoort paleosol (2.25 Ga): *Journal of Geology*, v. 112, p. 543-560.
- Driese, S.G., Medaris, L.G., Ren, M., Runkel, A.C., and Langford, R.P., 2007, Differentiating Pedogenesis from Diagenesis in Early Terrestrial Paleoweathering Surfaces Formed on Granitic Composition Parent Materials: *Journal of Geology*, v. 115, p. 387-406.
- Driese, S.G., Simpson, E.L., and Eriksson, K.A., 1995, Redoximorphic Paleosols in Alluvial and Lacustrine Deposits, 1.8 Ga Lochness Formation, Mount Isa, Australia: Pedogenic Processes and Implications for Paleoclimate: *Journal of Sedimentary Research*, v. A65, p. 675-689.
- Duffin, M.E., Lee, M., Klein, G.d., and Hay, R.L., 1989, Potassic Diagenesis of Cambrian Sandstones and Precambrian Granitic Basement in UPH-3 Deep Hole, Upper Mississippi Valley, USA: *Journal of Sedimentary Petrology*, v. 59, p. 848-861.
- El-Sayed, M.I., Fairchild, I.J., and Spiro, B., 1991, Kuwaiti dolocrete: petrology, geochemistry and groundwater origin: *Sedimentary Geology*, v. 73, p. 59-75.
- Fedo, C.M., Nesbitt, H.W., and Young, G.M., 1995, Unraveling the effects of potassium metasomatism in sedimentary rocks and paleosols, with implications for paleoweathering conditions and provenance: *Geology*, v. 23, p. 921-924.
- Grathoff, G.H., Moore, D.M., Hay, R.L., and Wemmer, K., 2001, Origin of illite in the lower Paleozoic of the Illinois basin: Evidence for brine migrations: *GSA Bulletin*, v. 113, p. 1092-1104.
- Gutzmer, J., and Beukes, N.J., 1998, Earliest laterites and possible evidence for terrestrial vegetation in the Early Proterozoic: *Geology*, v. 26, p. 263-266.
- Heckman, D.S., Geiser, D.M., Eidell, B.R., Stauffer, R.L., Kardos, N.L., and Hedges, S.B., 2001, Molecular Evidence for the Early Colonization of Land by Fungi and Plants: *Science*, v. 293, p. 1129-1133.
- Hodych, J.P., Cox, R.A., and Kosler, J., 2004, An equatorial Laurentia at 550 Ma confirmed by Grenvillian inherited zircons dated by LAM ICP-MS in the Skinner Cove volcanics of western Newfoundland: implications for inertial interchange true polar wander: *Precambrian Research*, v. 129, p. 93-113.
- Hoffman, P.F., Kaufman, A.J., Halverson, G.P., and Schrag, D.P., 1998, A Neoproterozoic Snowball Earth: *Science*, v. 281, p. 1342-1346.
- Holland, H.D., 1984, Oxygen in the Precambrian Atmosphere: Evidence from Terrestrial Environments, *in* Holland, H.D., ed., *The Chemical Evolution of the Atmosphere and Oceans*: Princeton, NJ, Princeton University Press, p. 277-336.

- , 1992, Distribution and Paleoenvironmental Interpretation of Proterozoic Paleosols, *in* Schopf, J.W., and Klein, C., eds., *The Proterozoic Biosphere*: Cambridge, Cambridge University Press, p. 153-155.
- Holland, H.D., Rye, R., and Ohmoto, H., 1997, Evidence in pre-2.2 Ga paleosols for the early evolution of atmospheric oxygen and terrestrial biota: Comment and Reply: *Geology*, v. 25, p. 857-859.
- Holm, D.K., Van Schmus, W.R., MacNeill, L.C., Boerboom, T.J., Schweitzer, D., and Schneider, D., 2005, U-Pb zircon geochronology of Paleoproterozoic plutons from the northern midcontinent, USA: Evidence for subduction flip and continued convergence after geon 18 Penokean orogenesis: *GSA Bulletin*, v. 117, p. 259-275.
- Horodyski, R.J., and Knauth, L.P., 1994, Life on Land in the Precambrian: *Science*, v. 263, p. 494-498.
- Jutras, P., Quillan, R.S., and LeForte, M.J., 2009, Evidence from Middle Ordovician paleosols for the predominance of alkaline groundwater at the dawn of land plant radiation: *Geology*, v. 37, p. 91-94.
- Kabata-Pendias, A., 2001, *Trace Elements in Soils and Plants*: Boca Raton, CRD Press, 413 p.
- Kessler, J.L.P., Soreghan, G.S., and Wacker, H.J., 2001, Equatorial Aridity in Western Pangea: Lower Permian Loessite and Dolomitic Paleosols in Northeastern New Mexico, USA: *Journal of Sedimentary Research*, v. 71, p. 817-832.
- Lajtha, K., and Schlesinger, W.H., 1988, The Biogeochemistry of Phosphorus Cycling and Phosphorus Availability Along a Desert Chronosequence: *Ecology*, v. 69, p. 24-39.
- Liu, J., Hay, R.L., Deino, A., and Kyser, T.K., 2003, Age and origin of authigenic K-feldspar in uppermost Precambrian rocks in the North American Midcontinent: *GSA Bulletin*, v. 115, p. 422-433.
- Luczaj, J.A., 2006, Evidence against the Dorag (mixing-zone) model for dolomitization along the Wisconsin arch - A case for hydrothermal diagenesis: *AAPG Bulletin*, v. 90, p. 1719-1738.
- McCarthy, P.J., and Plint, A.G., 1998, Recognition of interfluvial sequence boundaries: Integrating paleopedology and sequence stratigraphy: *Geology*, v. 26, p. 387-390.
- McCausland, P.J.A., Van der Voo, R., and Hall, C.M., 2007, Circum-Iapetus paleogeography of the Precambrian–Cambrian transition with a new paleomagnetic constraint from Laurentia: *Precambrian Research*, v. 156, p. 125-152.
- McCormick, K.A., 2005, Drilling of an Aeromagnetic Anomaly in Southeastern South Dakota: Results from Analysis of Paleozoic and Precambrian Core, *in* Resources, D.o.E.a.N., ed., Volume 2005, Geological Survey, p. 1-19.
- McCormick, K.A.H., R. H., 2004, Geology of Lincoln and Union Counties, South Dakota, *in* Resources, D.o.E.a.N., ed., Volume 2004, Geological Survey, p. 1-43.
- McKerrow, W.S., Scotese, C.R., and Brasier, M.D., 1992, Early Cambrian continental reconstructions: *Journal of the Geological Society, London*, v. 149, p. 599-606.
- Montanez, I.P., Banner, J.L., Osleger, D.A., Borg, L.E., and Bosserman, P.J., 1996, Integrated Sr isotope variations and sea-level history of Middle to Upper

- Cambrian platform carbonates: Implications for the evolution of Cambrian seawater $87\text{Sr}/86\text{Sr}$: *Geology*, v. 24, p. 917-920.
- Mora, C.I., Driese, S.G., and Colarusso, L.A., 1996, Middle to Late Paleozoic Atmospheric CO_2 Levels from Soil Carbonate and Organic Matter: *Science*, v. 271, p. 1105-1107.
- Neaman, A., Chorover, J., and Brantley, S.L., 2005a, Element mobility patterns record organic ligands in soils on early Earth: *Geology*, v. 33, p. 117-120.
- , 2005b, Implications of the Evolution of Organic Acid Moieties for Basalt Weathering over Geological Time: *American Journal of Science*, v. 305, p. 147-185.
- , 2006, Effects of Organic Ligands on Granite Dissolution in Batch Experiments at pH 6: *American Journal of Science*, v. 306, p. 451-473.
- Nesbitt, H.W., and Young, G.M., 1982, Early Proterozoic climates and plate motions inferred from major element chemistry of lutites: *Nature*, v. 299, p. 715-717.
- Ohmoto, H., 1996, Evidence in pre-2.2 Ga paleosols for the early evolution of atmospheric oxygen and terrestrial biota: *Geology*, v. 24, p. 1135-1138.
- Ojakangas, R.W., and Dickas, A.B., 2002, The 1.1-Ga Midcontinent Rift System, central North America: sedimentology of two deep boreholes, Lake Superior region: *Sedimentary Geology*, v. 147, p. 13-36.
- Ojakangas, R.W., Morey, G.B., and Green, J.C., 2001, The Mesoproterozoic Midcontinent Rift System, Lake Superior Region, USA: *Sedimentary Geology*, v. 141-142, p. 421-442.
- Pannalal, S.J., Symons, D.T.A., and Sangster, D.F., 2004, Paleomagnetic dating of Upper Mississippi Valley zinc-lead mineralisation, WI, USA: *Journal of Applied Geophysics*, v. 56, p. 135-153.
- Retallack, G.J., 1991, Untangling the Effects of Burial Alteration and Ancient Soil Formation: *Annual Review of Earth and Planetary Sciences*, v. 19, p. 183-206.
- , 2001, *Soils of the Past: An Introduction to Paleopedology*: Oxford, Blackwell Science, 404 p.
- Runkel, A.C., McKay, R.M., and Palmer, A.R., 1998, Origin of a classic cratonic sheet sandstone: Stratigraphy across the Sauk II-Sauk III boundary in the Upper Mississippi Valley: *GSA Bulletin*, v. 110, p. 188-210.
- Runkel, A.C., Miller, J.F., McKay, R.M., Palmer, A.R., and Taylor, J.F., 2007, High-resolution sequence stratigraphy of lower Paleozoic sheet sandstones in central North America: The role of special conditions of cratonic interiors in development of stratal architecture: *GSA Bulletin*, v. 119, p. 860-881.
- Rye, R., and Holland, H.D., 2000, Geology and geochemistry of paleosols developed on the Hekpoort Basalt, Pretoria Group, South Africa: *American Journal of Science*, v. 300, p. 85-141.
- Saltzman, M.R., Cowan, C.A., Runkel, A.C., Runnegar, B., Stewart, M.C., and Palmer, A.R., 2004, The Late Cambrian SPICE ($\delta^{13}\text{C}$) Event and the Sauk II-Sauk III Regression: New Evidence from Laurentian Basins in Utah, Iowa, and Newfoundland: *Journal of Sedimentary Research*, v. 74, p. 366-377.
- Schaetzl, R.J., and Anderson, S., 2005, *Soils: Genesis and Geomorphology*, Cambridge University Press.

- Shergold, J.H., and Cooper, R.A., 2004, The Cambrian Period, *in* Gradstein, F.M., Ogg, J.G., and Smith, A.G., eds., *A Geologic Time Scale 2004*, Cambridge University Press, p. 147-164.
- Soofi, M.A., and King, S.D., 2002, Post-rift deformation of the Midcontinent rift under Grenville tectonism: *Tectonophysics*, v. 359, p. 209-223.
- Suhr, N.H., and Ingamells, C.O., 1966, Solution Technique for Analysis of Silicates: *Analytical Chemistry*, v. 338, p. 730-734.
- Sverjensky, D.A., 1986, Genesis of Mississippi Valley-Type Lead-Zinc Deposits: *Annual Review of Earth and Planetary Sciences*, v. 14, p. 177-199.
- Torsvik, T.H., and Rehnstrom, E.F., 2001, Cambrian palaeomagnetic data from Baltica: implications for true polar wander and Cambrian palaeogeography: *Journal of the Geological Society, London*, v. 158, p. 321-329.
- Trindade, R.I.F., and Macouin, M., 2007, Palaeolatitude of glacial deposits and palaeogeography of Neoproterozoic ice ages: *Comptes Rendus Geosciences*, v. 339, p. 200-211.
- Van Schmus, W.R., 1987, Early and Middle Proterozoic provinces in the central United States, *in* Kroner, A., ed., *Proterozoic lithospheric evolution*, Volume 17, American Geophysical Union Geodynamics Series, p. 43-68.
- , 1992, Tectonic setting of the Midcontinent Rift system: *Tectonophysics*, v. 213, p. 1-15.
- Van Schmus, W.R., Schneider, D.A., Holm, D.K., Dodson, S., and Nelson, B.K., 2007, New insights into the southern margin of the Archean–Proterozoic boundary in the north-central United States based on U–Pb, Sm–Nd, and Ar–Ar geochronology: *Precambrian Research*, v. 157, p. 80-105.
- Watanabe, Y., Martini, J.E.J., and Ohmoto, H., 2000, Geochemical evidence for terrestrial ecosystems 2.6 billion years ago: *Nature*, v. 408, p. 574-578.
- Welch, S.A., Taunton, A.E., and Banfield, J.F., 2002, Effect of Microorganisms and Microbial Metabolites on Apatite Dissolution: *Geomicrobiology journal*, v. 19, p. 343-367.
- Whitmeyer, S.J., and Karlstrom, K.E., 2007, Tectonic model for the Proterozoic growth of North America: *Geosphere*, v. 3, p. 220-259.
- Zbinden, E.A., Holland, H.D., and Feakes, C.R., 1988, The Sturgeon Falls Paleosol and the Composition of the Atmosphere 1.1 Ga BP: *Precambrian Research*, v. 42, p. 141-163.
- Zhang, G.-L., Pan, J.-H., Huang, C.-M., and Gong, Z.-T., 2007, Geochemical features of a soil chronosequence developed on basalt in Hainan Island, China: *Revista Mexicana de Ciencias Geologicas*, v. 24, p. 261-269.
- Ziegler, K., and Longstaffe, F.J., 2000, Multiple Episodes of Clay Alteration at the Precambrian/Paleozoic Unconformity, Appalachian Basin: Isotopic Evidence for Long-Distance and Local Fluid Migrations: *Clays and Clay Minerals*, v. 48, p. 474-493.

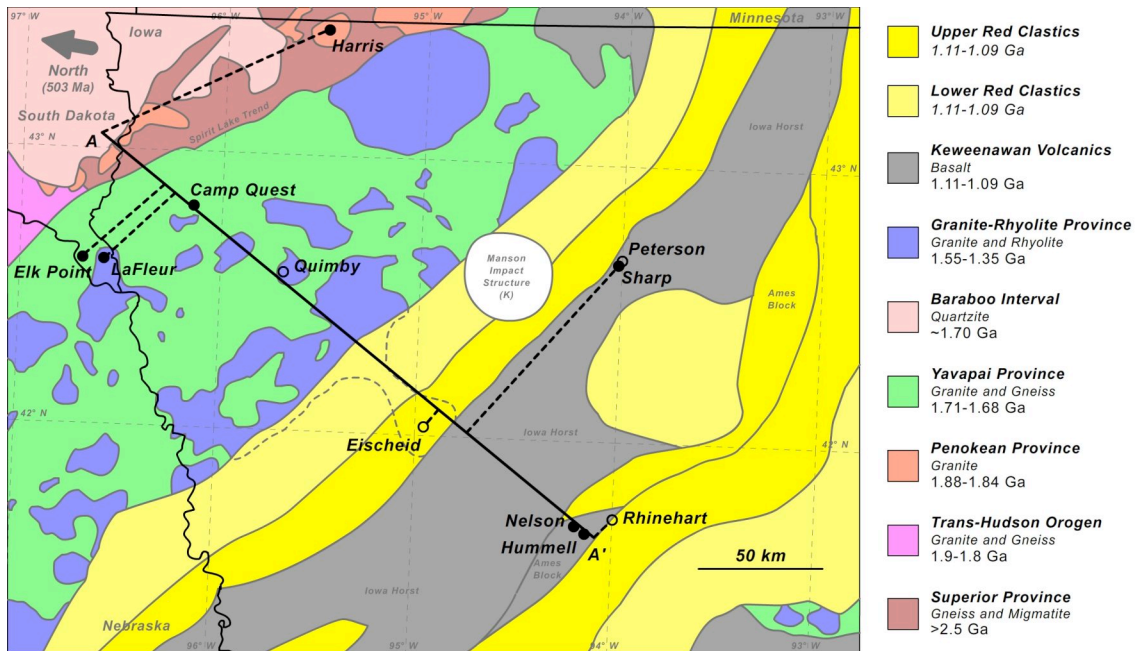


Figure 3-1a: Detailed bedrock map of the study region, showing the variety of terranes upon which paleoweathering features developed (solid circles). Open circles indicate additional cores that were used to constrain the age of the overlying Middle Cambrian Mt. Simon Sandstone and differentiate older "Red Clastics" from the Mt. Simon Sandstone. Modified from Anderson (2006).

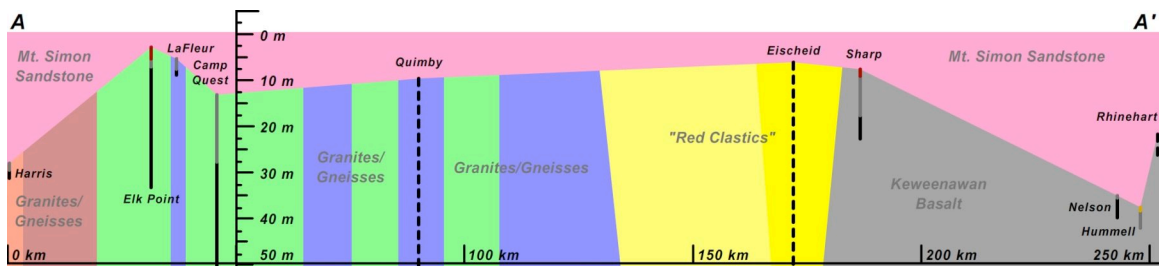


Figure 3-1b: Cross-section (A-A') of the study region. Core depths are normalized to the top of the Mt. Simon Sandstone, which was relatively flat-lying when deposited and remains so today. Cores are represented by lines: red/yellow for paleosols, gray for paleosaprolites, black for unweathered parent material, and dotted for cores utilized for stratigraphic control but not otherwise investigated in this study.

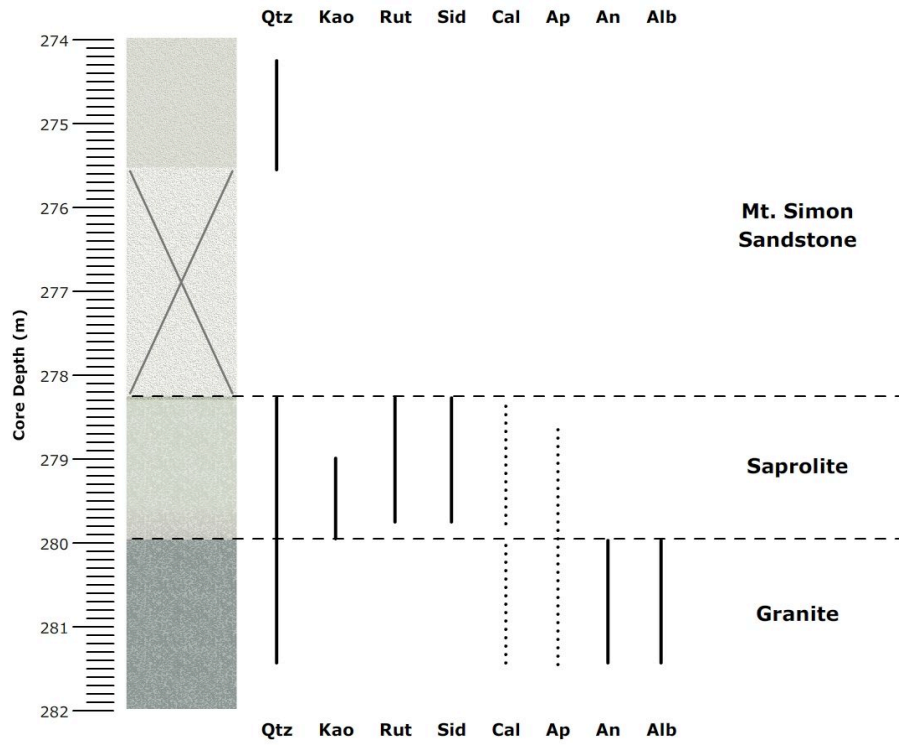


Figure 3-2: Mineral abundances based on XRD scans of the Harris core (qtz = quartz, kao = kaolinite, rut = rutile, sid = siderite, cal = calcite, ap = apatite, an = anorthite, alb = albite; dotted lines indicate likely trace abundances)

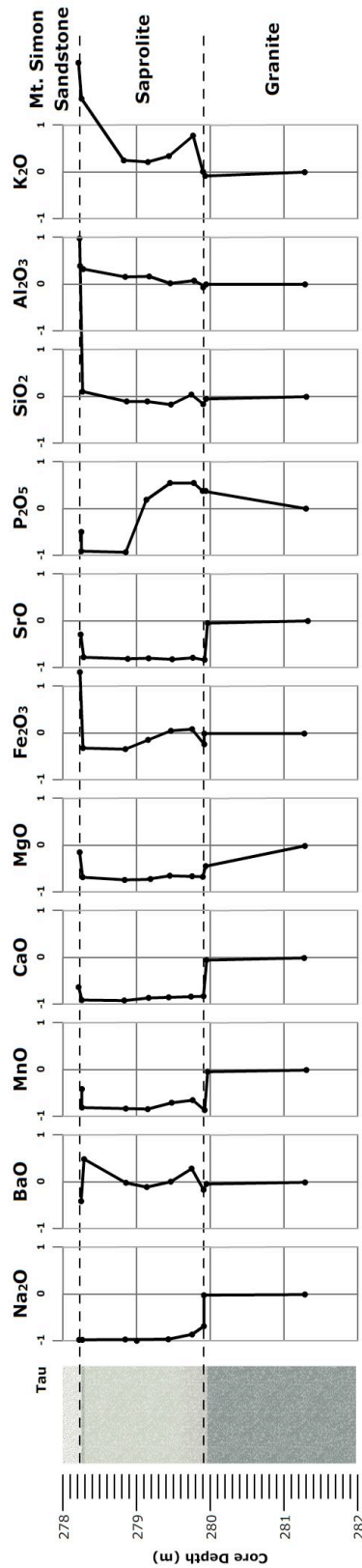


Figure 3-3a: Oxide enrichment and depletion for the Harris core, normalized to Ti.

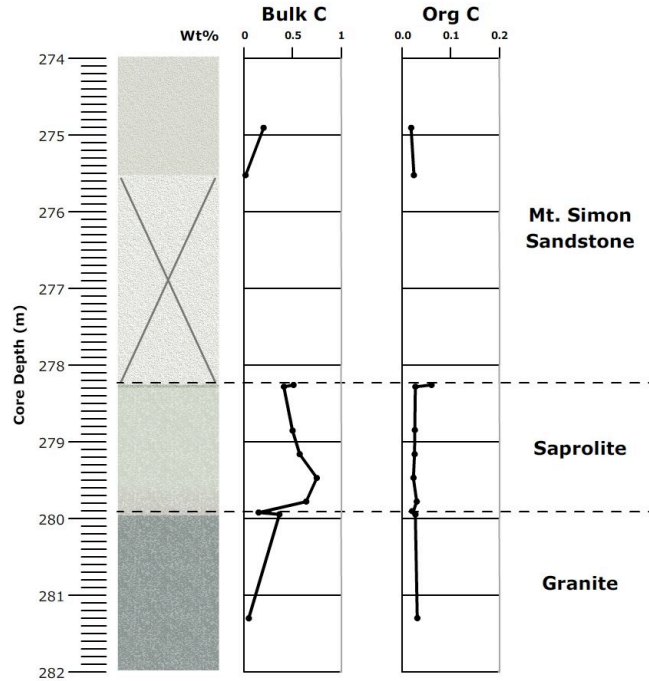


Figure 3-3b: Total C and organic C through the Harris profile. "X" indicates missing portions of the core.

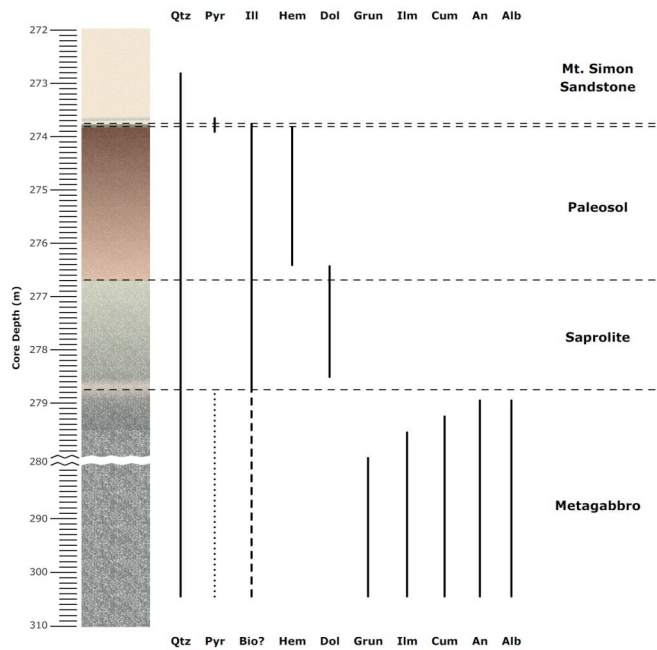


Figure 3-4: Mineral abundances based on XRD scans of the Elk Point core (qtz = quartz, pyr = pyrite, ill = illite, bio? = probable biotite, hem = hematite, dol = dolomite, grun = grunerite, ilm = ilmenite, cum = cummingtonite, an = anorthite, alb = albite; dotted line indicates likely trace abundances)

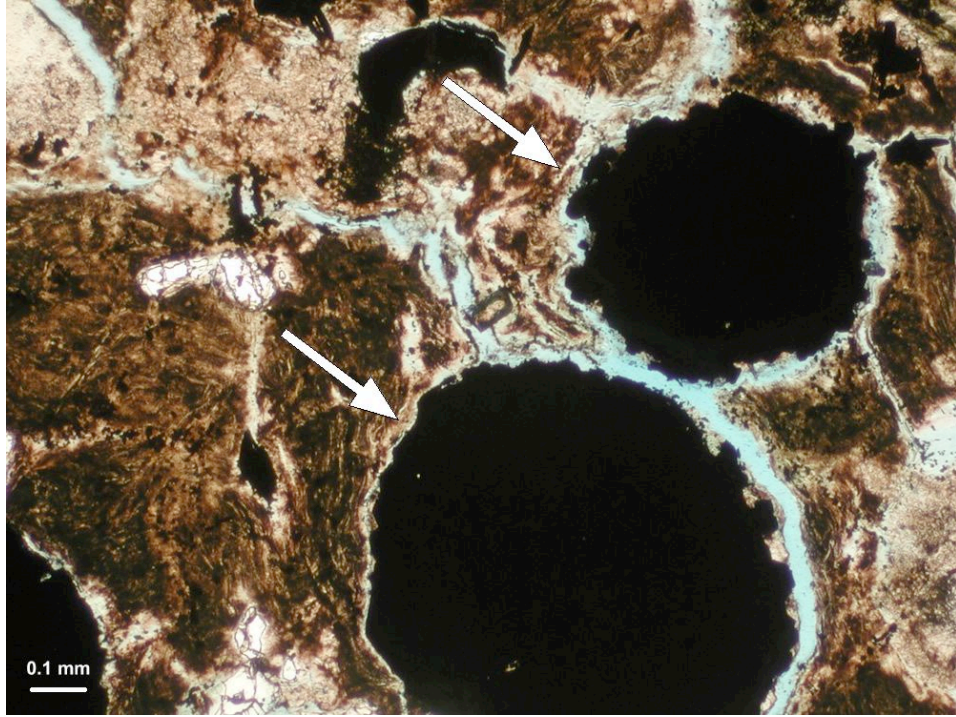


Figure 3-5a: The top of the Elk Point paleosol, showing growth of pyrite nodules (273.7 m).

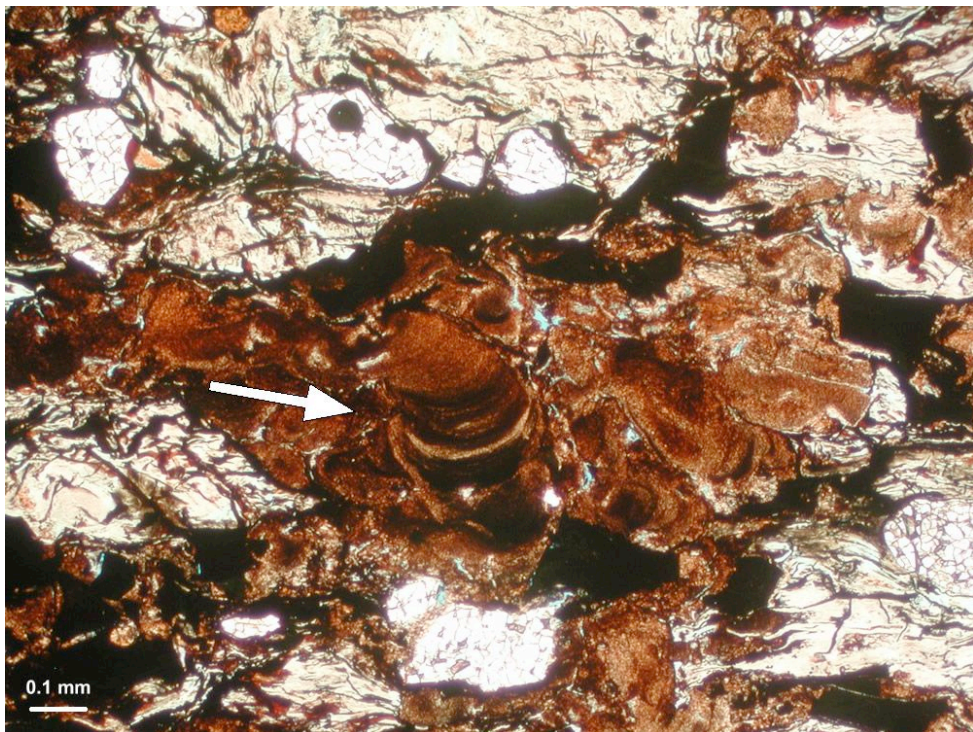


Figure 3-5b: Illuvial clay present near the top of the Elk Point paleosol (274.0 m).

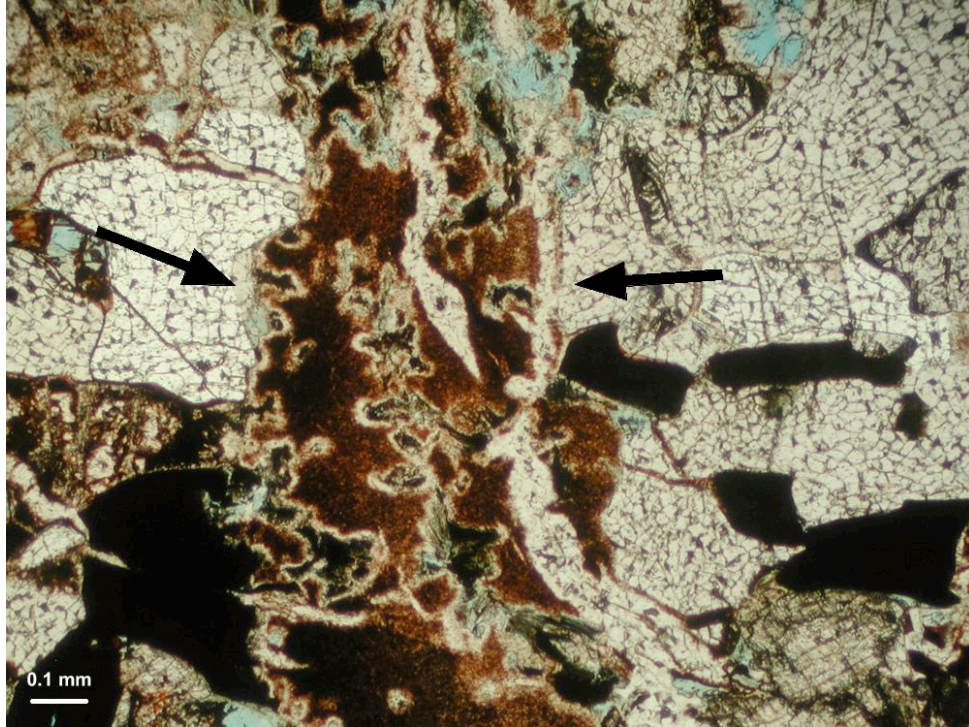


Figure 3-5c: Clay infilling in a crack through the paleosaprolite zone (276.8 m).

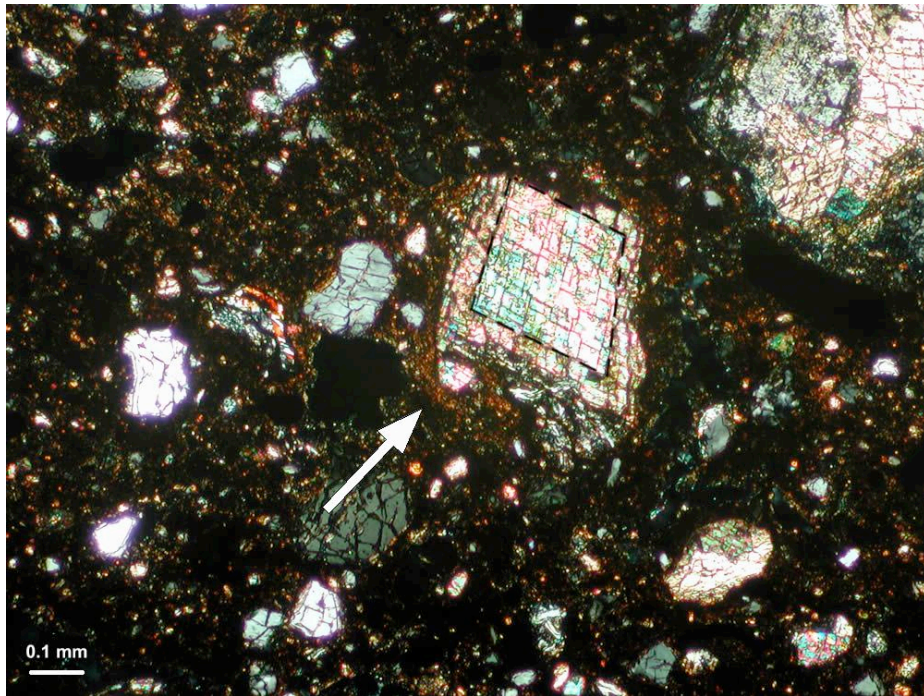


Figure 3-5d: A dolomite rhomb at the base of the paleosol, showing two stages of replacement growth (dotted line) and displacement of surrounding clay fabric (arrow) (276.8 m).



Figure 3-5e: Unweathered metagabbro. Major phases include biotite, hornblende, and plagioclase (278.9 m).

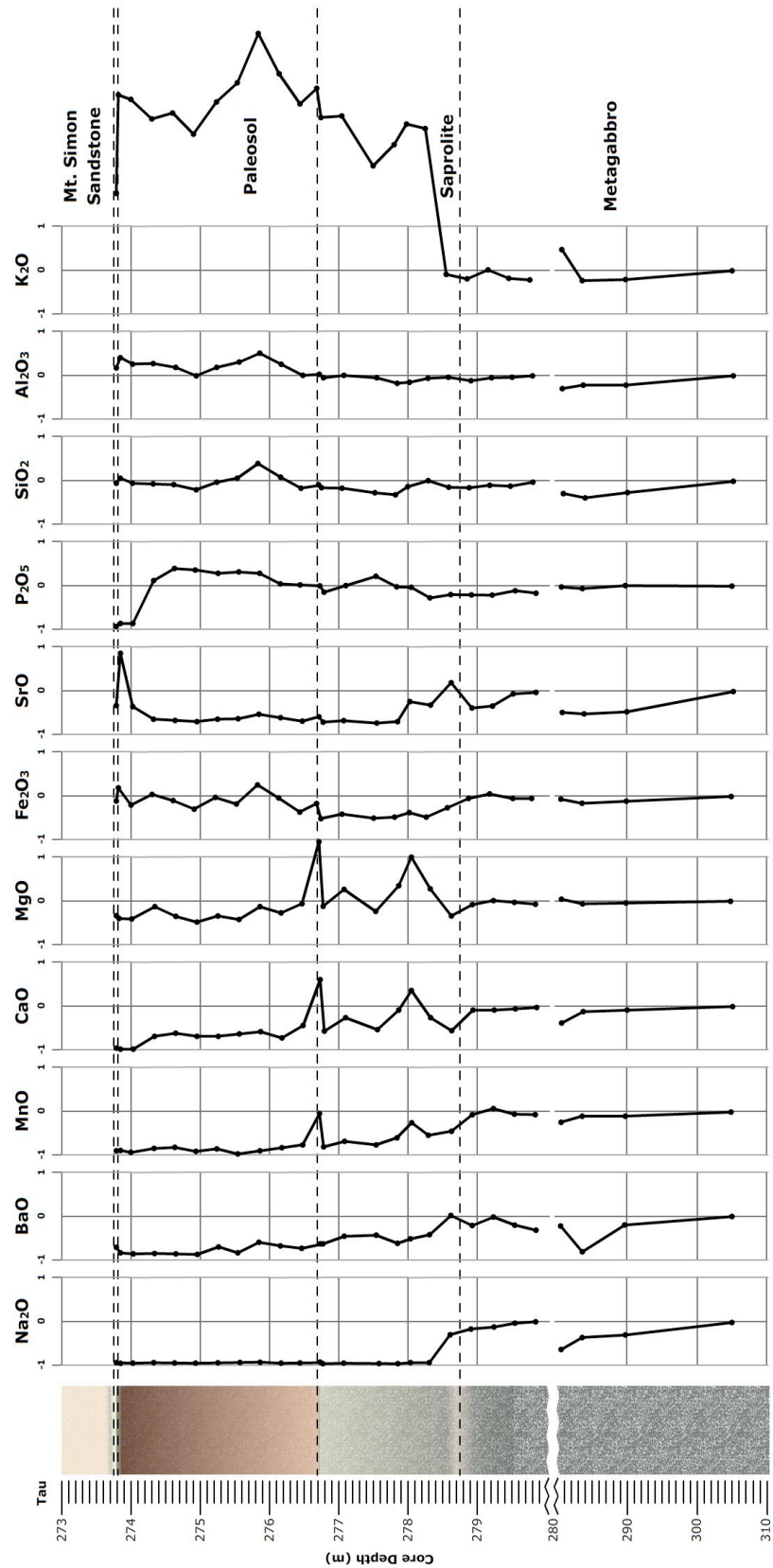


Figure 3-6a: Oxide enrichment and depletion for the Elk Point core, normalized to Ti.

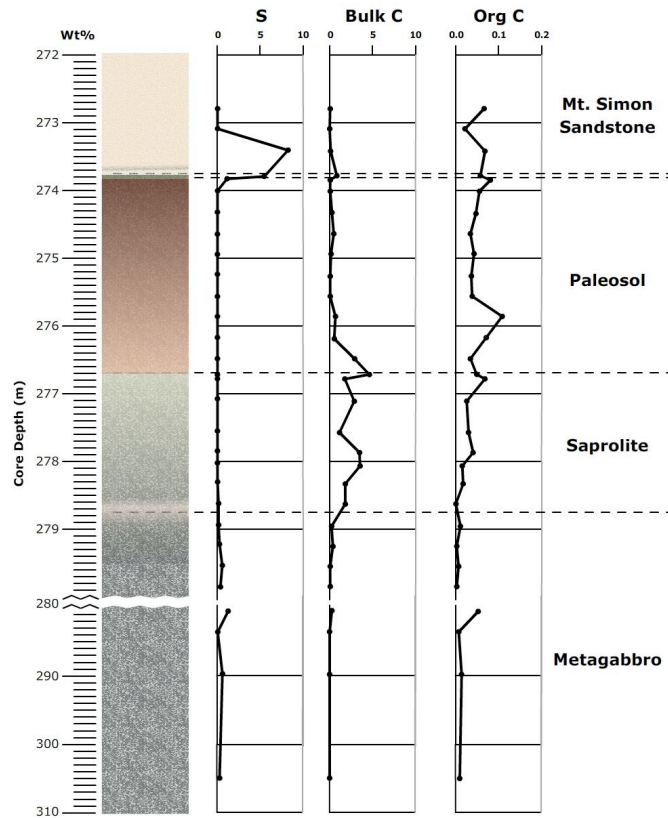


Figure 3-6b: S, bulk C, and organic C through the Elk Point profile.

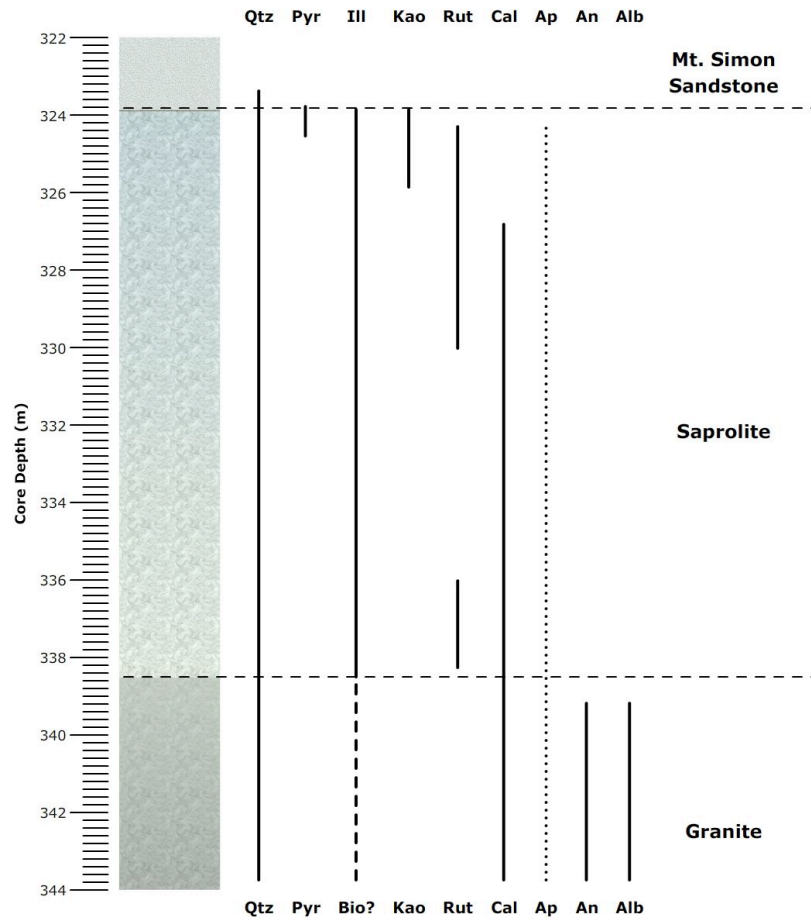


Figure 3-7: Mineral abundances based on XRD scans of the Camp Quest core (qtz = quartz, pyr = pyrite, ill = illite, bio? = probable biotite, kao = kaolinite, rut = rutile, cal = calcite, ap = apatite, an = anorthite, alb = albite; dotted line indicates likely trace abundances)

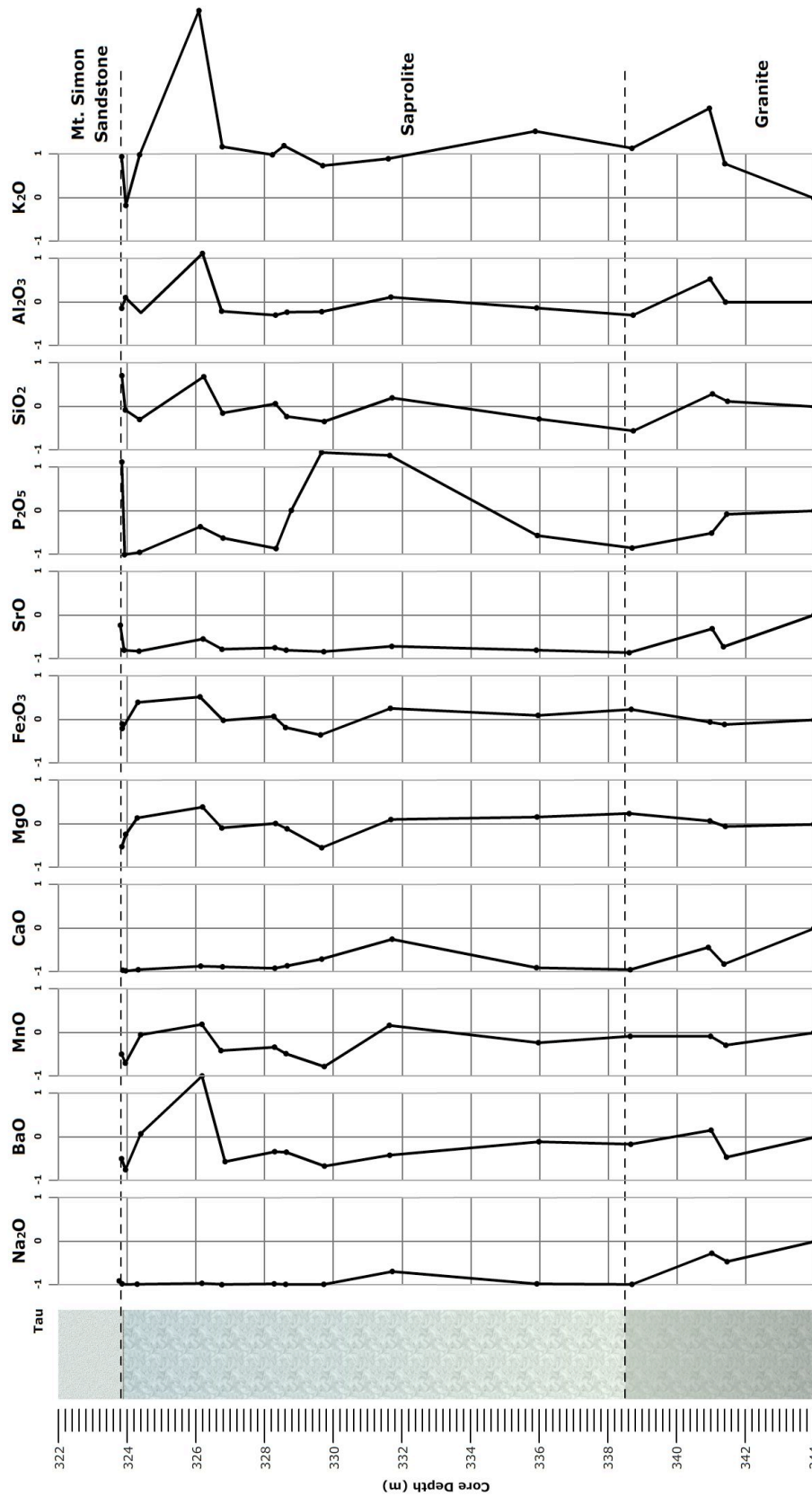


Figure 3-8a: Oxide enrichment and depletion for the Camp Quest core, normalized to Ti.

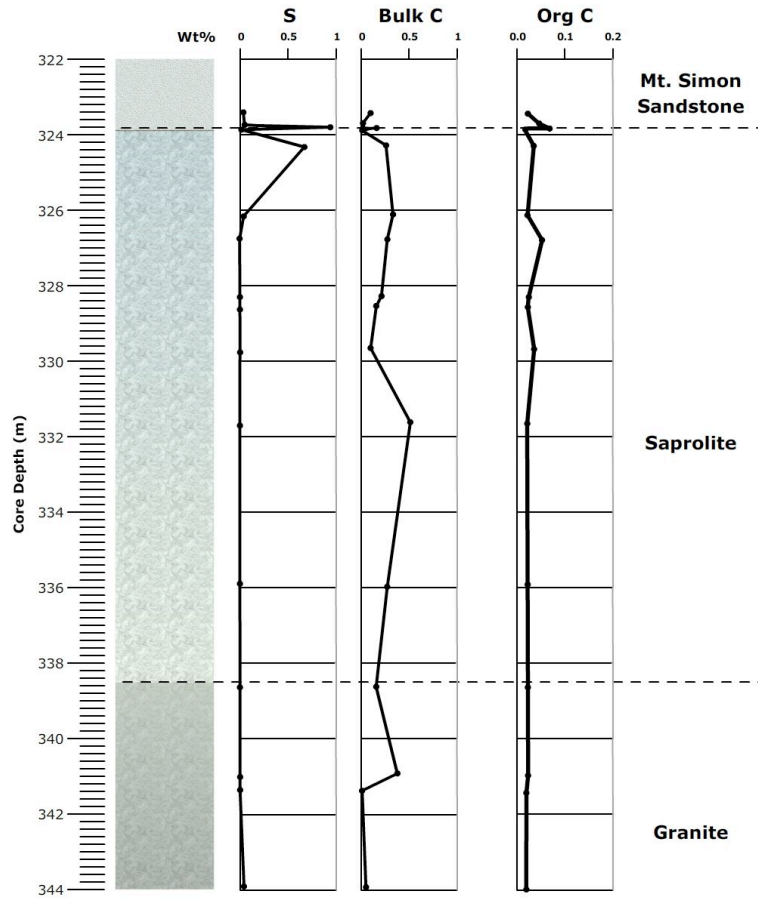


Figure 3-8b: S, bulk C, and organic C through the Camp Quest profile.

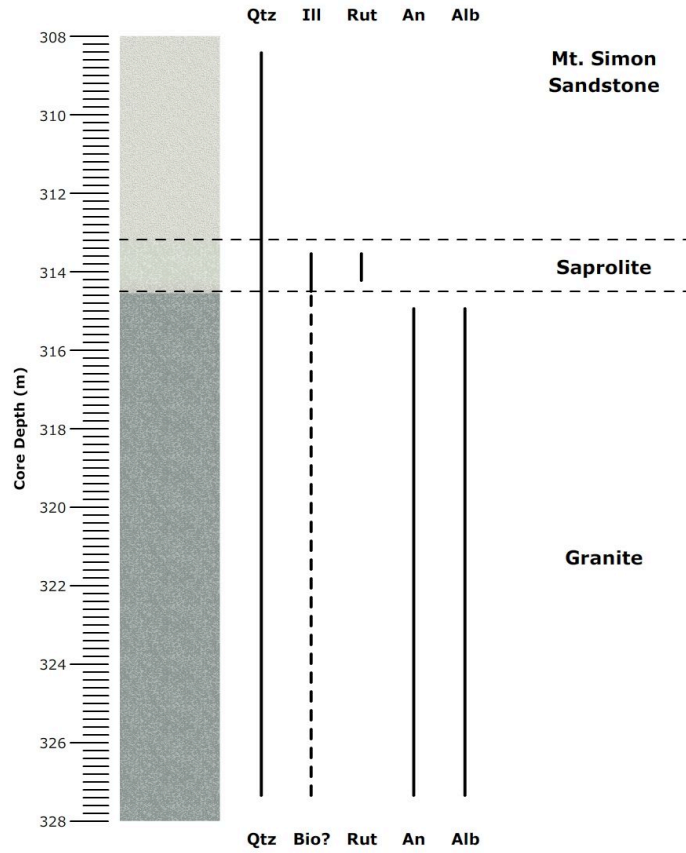


Figure 3-9: Mineral abundances based on XRD scans of the LaFleur well cuttings (qtz = quartz, ill = illite, bio? = probable biotite, rut = rutile, an = anorthite, alb = albite)

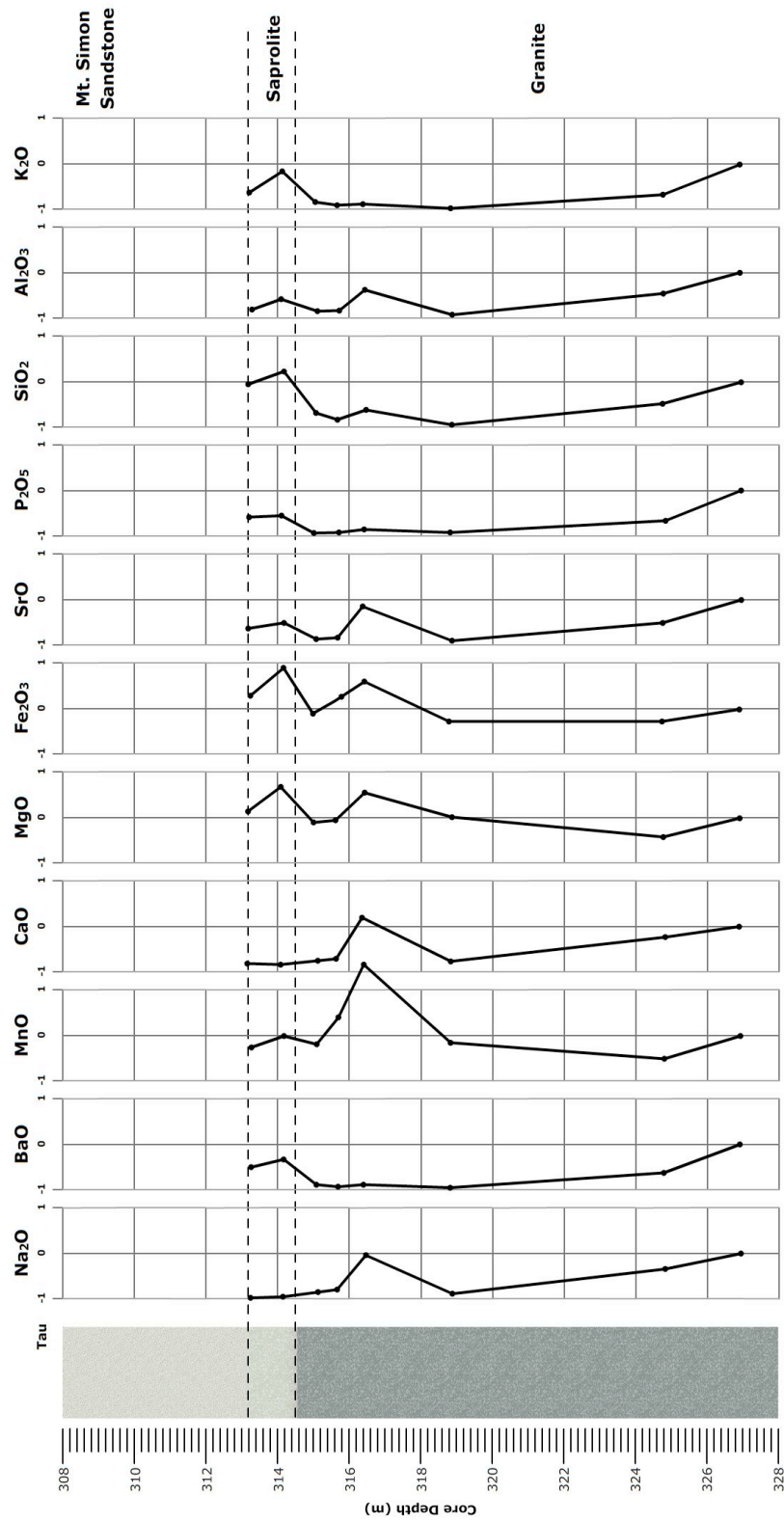


Figure 3-10: Oxide enrichment and depletion for the LaFleur well cuttings, normalized to Ti.

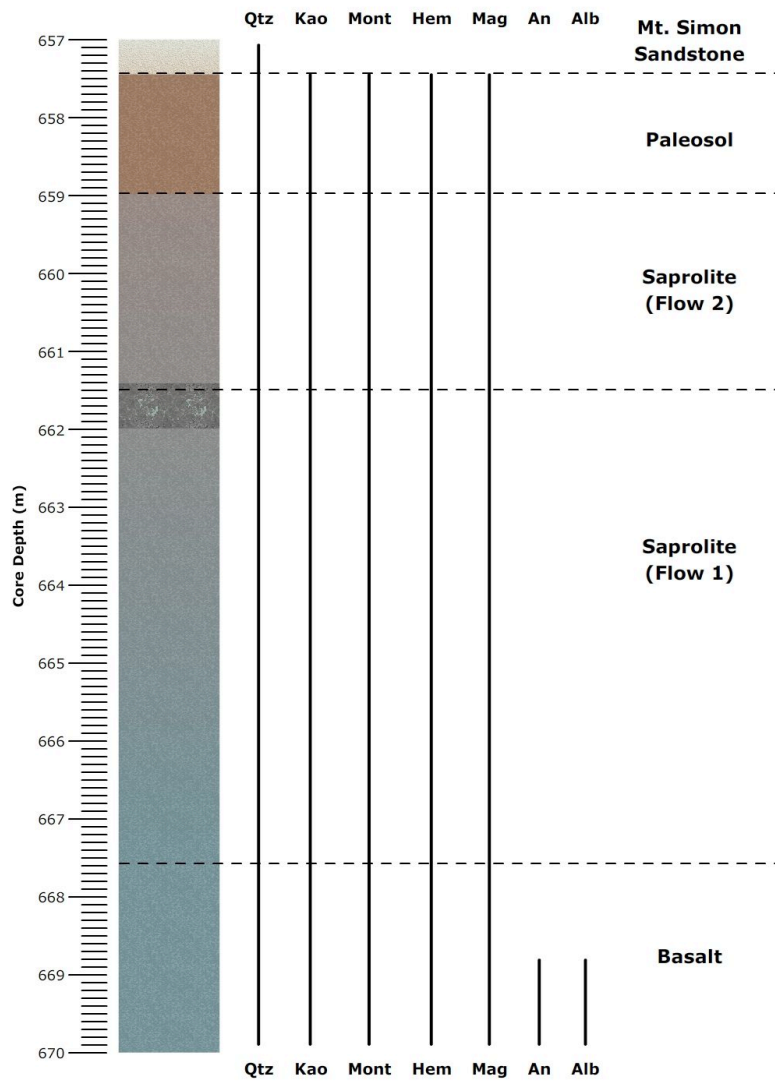


Figure 3-11: Mineral abundances based on XRD scans of the Sharp core (qtz = quartz, kao = kaolinite, mont = montmorillonite, hem = hematite, mag = magnetite, an = anorthite, alb = albite)

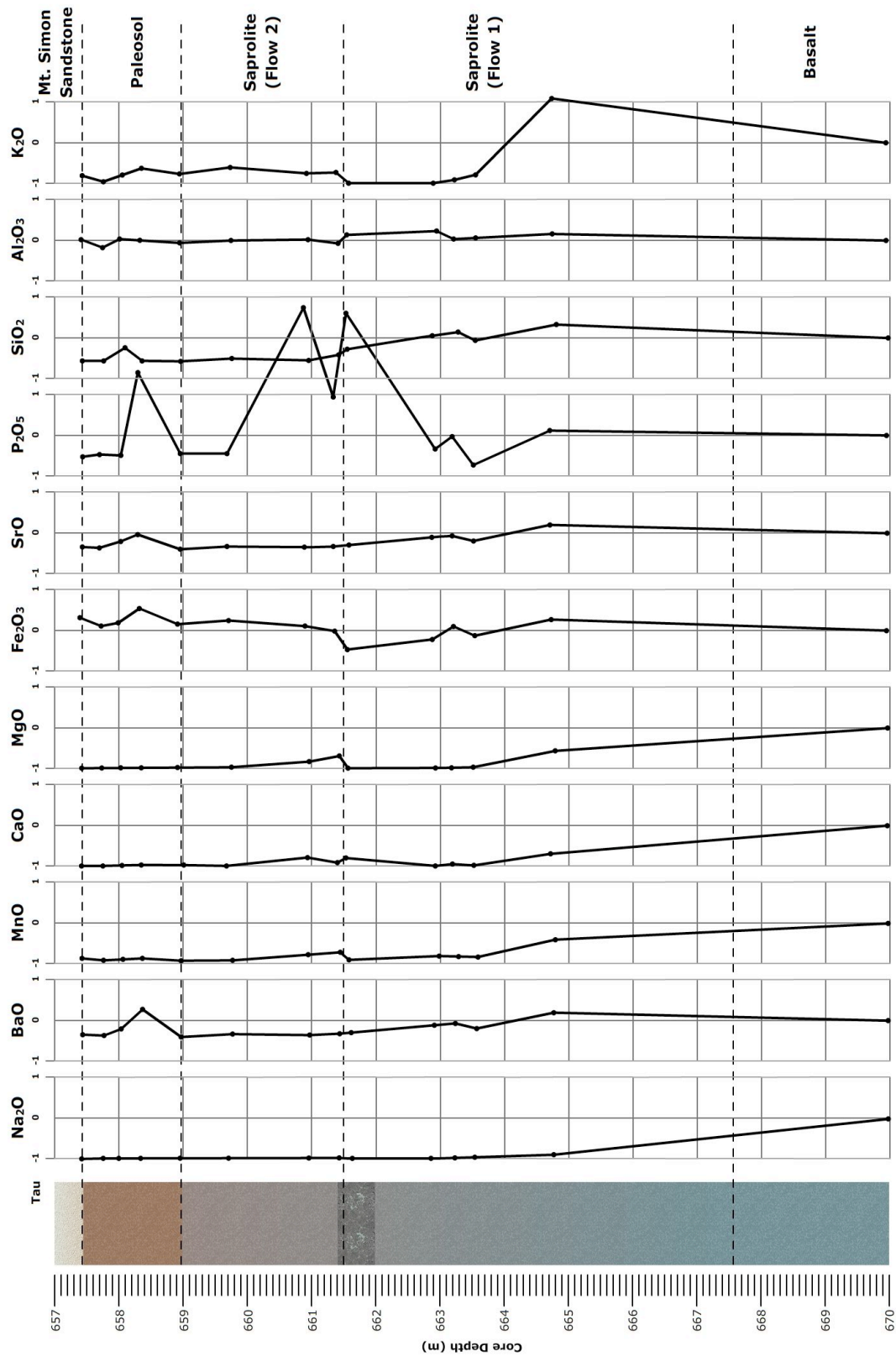


Figure 3-12a: Oxide enrichment and depletion for the Sharp core, normalized to Ti.

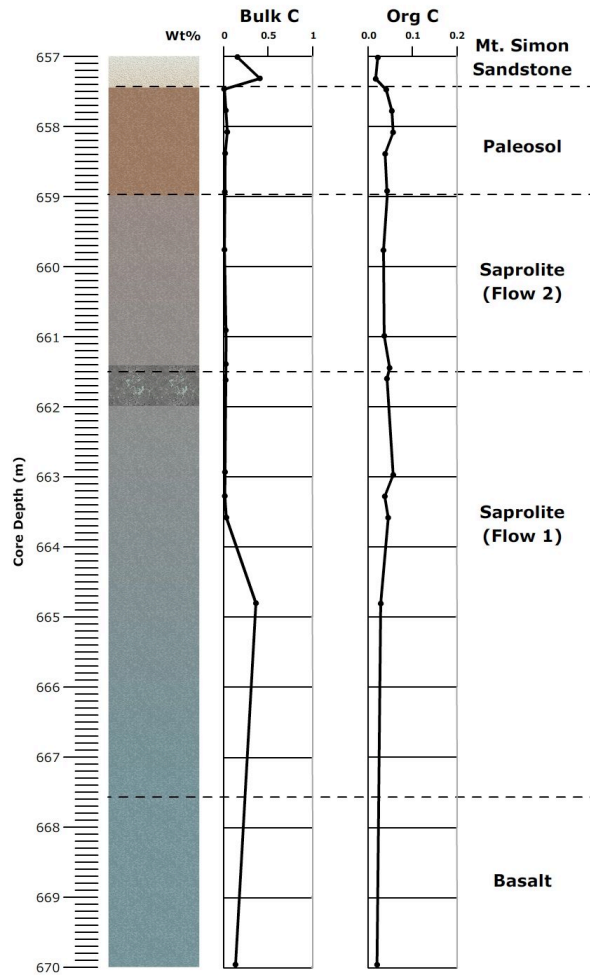


Figure 3-12b: Bulk C and organic C through the Sharp profile.

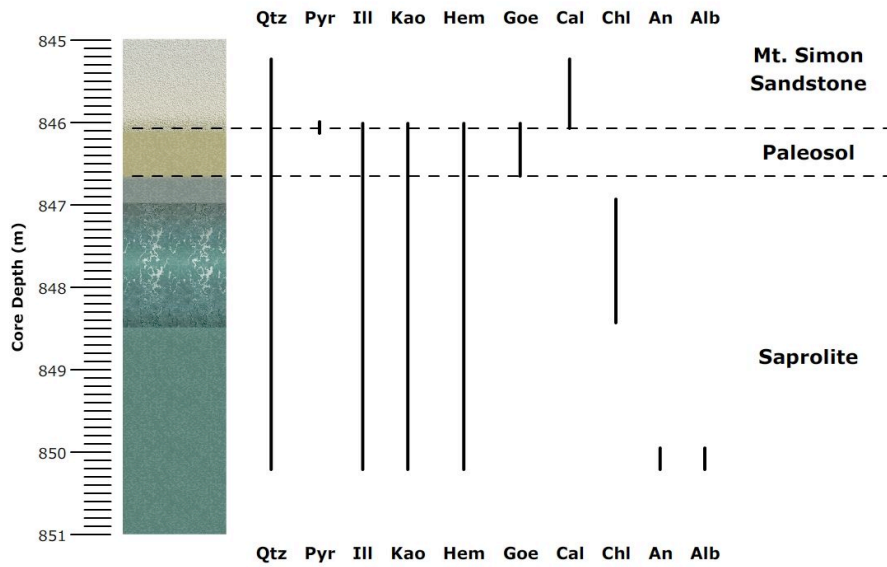


Figure 3-13: Mineral abundances based on XRD scans of the Hummell core (qtz = quartz, pyr = pyrite, ill = illite, kao = kaolinite, hem = hematite, goe = goethite, cal = calcite, chl = chlorite, an = anorthite, alb = albite)

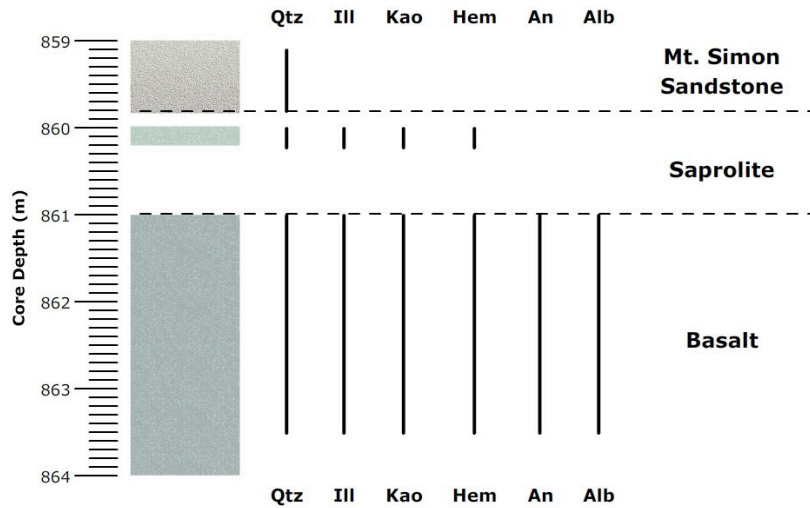


Figure 3-14: Mineral abundances based on XRD scans of the Nelson core (qtz = quartz, ill = illite, kao = kaolinite, hem = hematite, an = anorthite, alb = albite)



Figure 3-15a: Image of the hydrothermally altered basalt in the Hummell core. Note that the entire section of the core is friable.

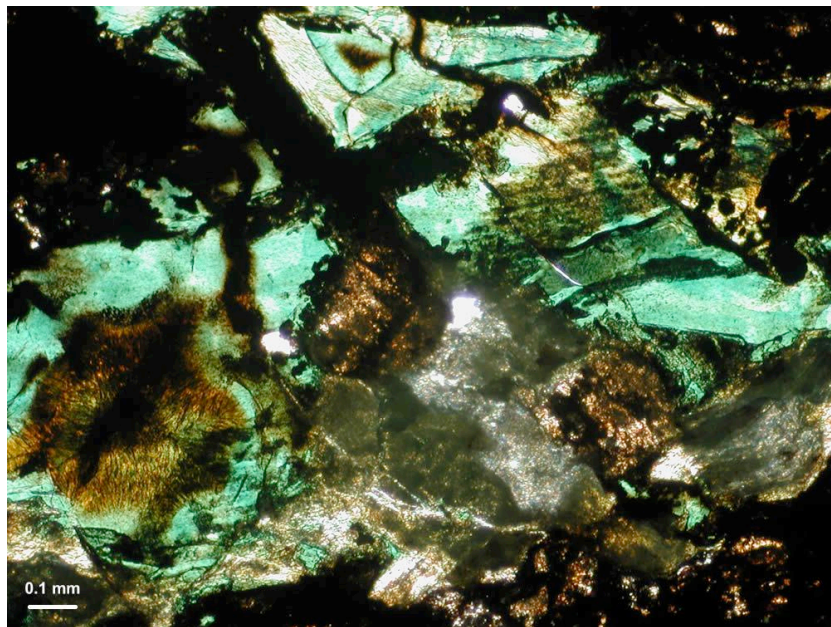


Figure 3-15b: Thin section image of fractured and degraded chlorite in the Hummell weathering section (846.7 m).

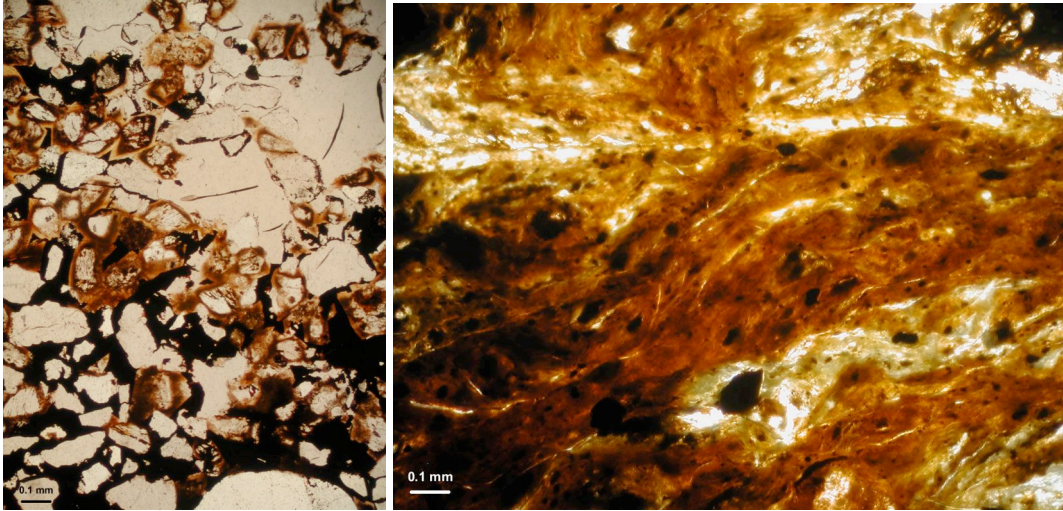


Figure 3-15c: Thin section images of Hummell paleosol-type clasts in the Mt. Simon Sandstone (846.1 m, left image) compared to the Hummell paleosol (846.4, right image). Pyrite (black, left image) is associated only with the clay-rich clasts.

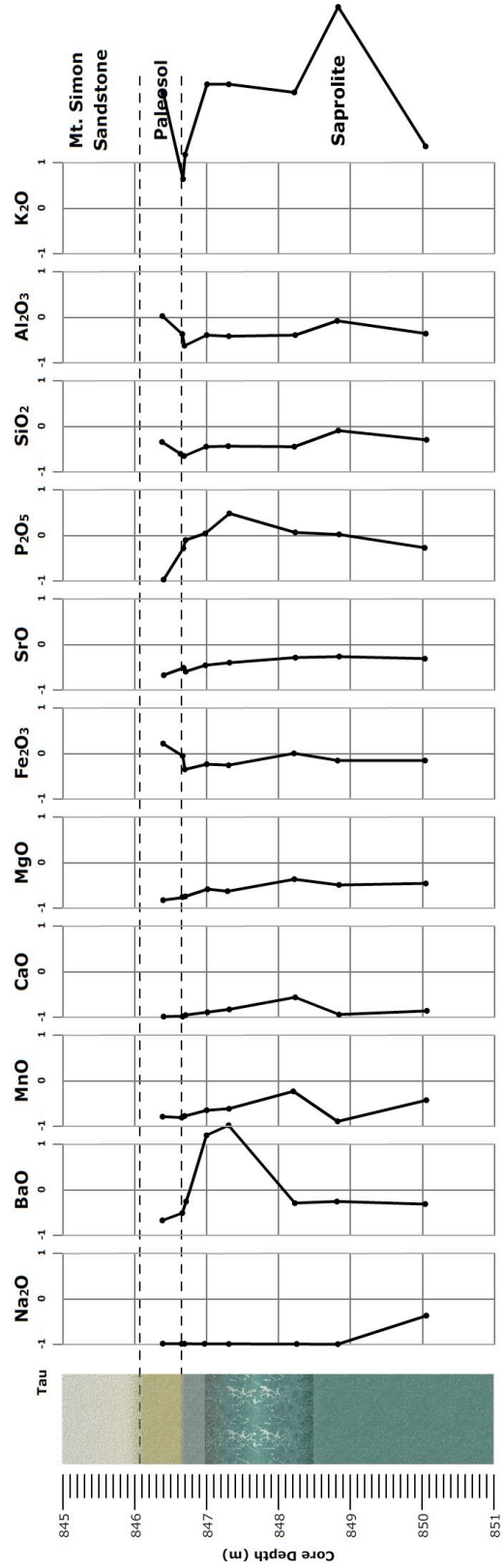


Figure 3-16a: Oxide enrichment and depletion for the Hummell core, normalized to Ti (in the Nelson core).

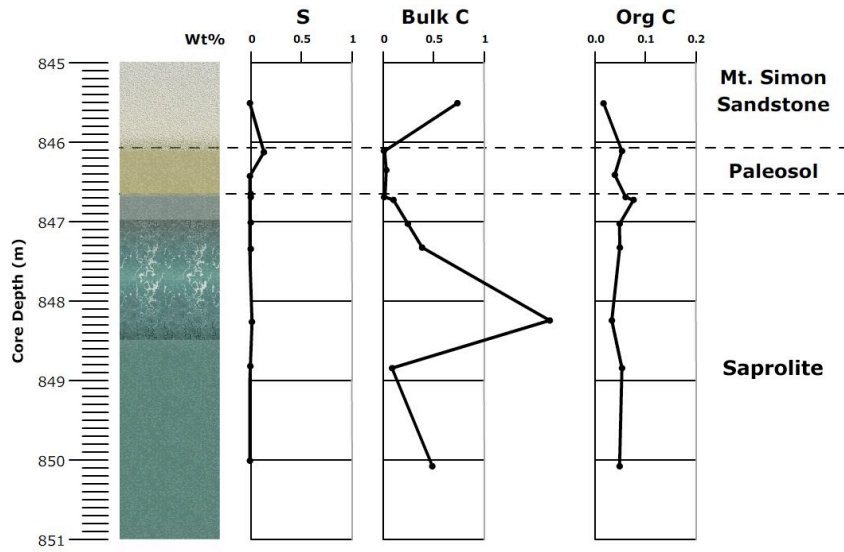


Figure 3-16b: S, bulk C, and organic C through the Hummell profile.

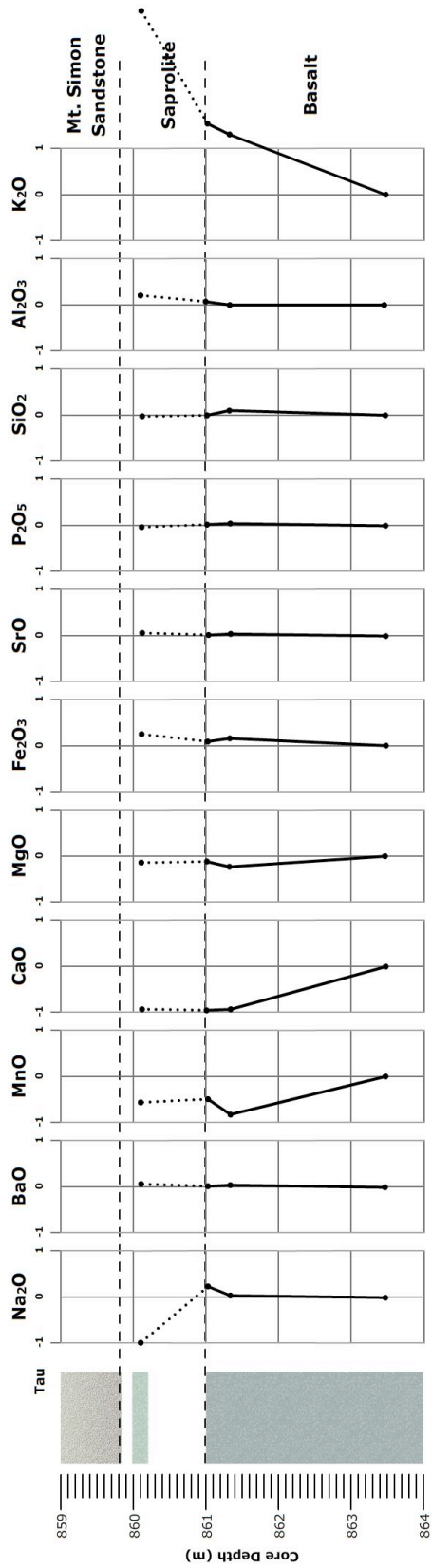


Figure 3-17a: Oxide enrichment and depletion for the Nelson core, normalized to Ti.

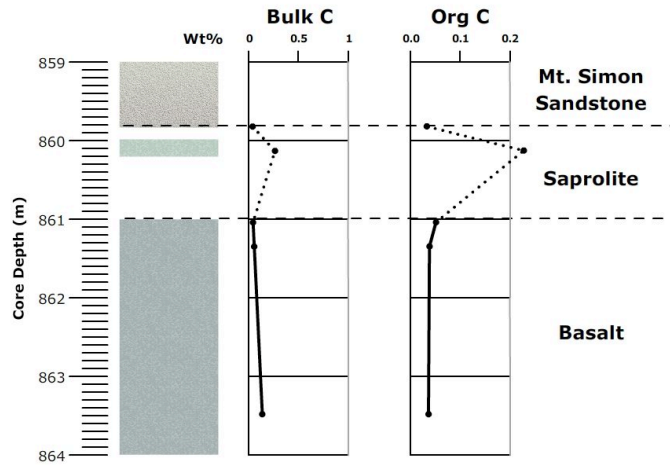


Figure 3-17b: Bulk C and organic C through the Nelson profile.

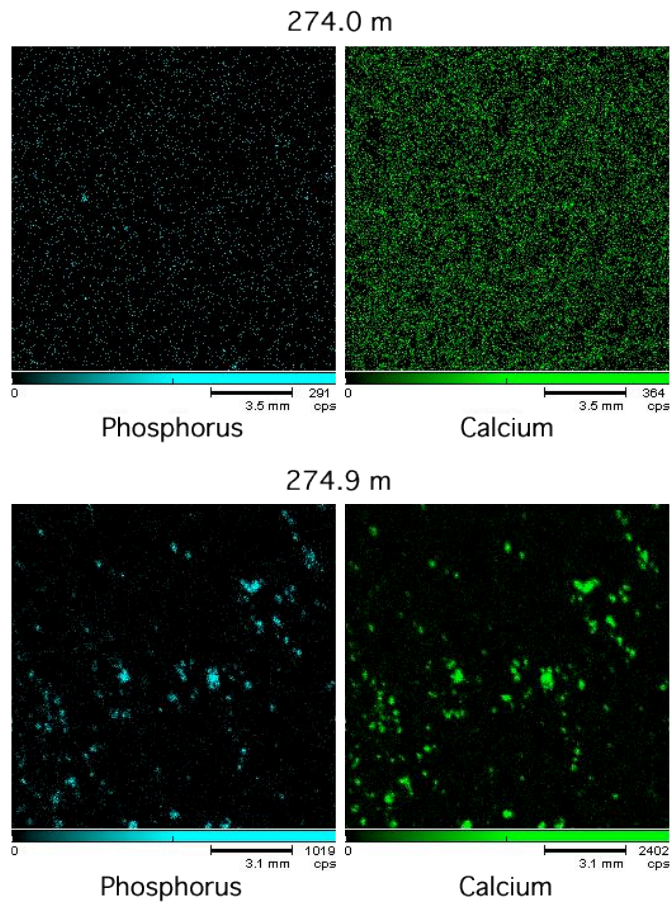


Figure 3-18: XGT maps of the Elk Point paleosol show loss of apatite up-section.

CHAPTER 4

Biosignatures in Middle Cambrian Paleosols: Fungal Weathering at Elk Point?

4.1 Abstract

Cambrian terrestrial ecosystems have been the subject of much speculation because few fossil-bearing strata exist and hence little is known about them. Terrestrial microbial mats are known from the Precambrian paleosol record and bryophytes are known from the mid-Ordovician palynological record. However, the intervening time is more enigmatic. In this study, six Middle Cambrian paleosols and paleosaprolites from the Iowa and South Dakota subsurface were investigated for biosignatures of early terrestrial ecosystems. These paleoweathered surfaces developed in a subtropical climate near the equator during the Middle Cambrian. The weathered horizons show various organic C trends ranging from surface enrichment to enrichment at depth. Average organic C contents (0.03-0.06 wt%) are low, but higher than for previously reported Proterozoic paleosols (<0.01 wt%). Carbon isotope results (-30‰ to -23‰) are consistent with a photosynthetic origin. At one particularly well-preserved site (Elk Point), the depth of complete apatite dissolution (down to 30 cm), the lack of substantial secondary phosphates or oxide- or carbonate-bound P, and the general persistence of apatite at depth through a majority of the paleosol are consistent with dissolution of apatite and uptake of P by surficial biological activity. The presence of argillans in the zone of apatite dissolution indicates a likely high soil solution concentration of Ca resulting in clay flocculation. P uptake coupled with increasing Ca concentrations as a result of apatite dissolution is consistent with the past presence of mycorrhizal fungi. Enigmatic tunnel structures in some apatite grains may be a result of biological activity, possibly fungal in origin. The presence of a shallow terrestrial ecosystem dominated by fungi (perhaps symbiotically associated with terrestrial primary producers) in Middle Cambrian paleosols would be consistent with molecular clock studies that suggest an earlier origin for terrestrial denizens. Enhanced apatite weathering due to the presence of a more deeply weathering Middle Cambrian terrestrial ecosystem may have, over time, increased

the P flux to the oceans and eventually become an important contributing factor in the Steptoean carbon isotope excursion recorded in Upper Cambrian sediments all over the world.

4.2 Introduction

Traditionally, the history of terrestrial life and ecosystems has been documented through study of macrofossils, with the appearance of *Cooksonia* during the mid-Silurian marking the first-recognized appearance of vascular plants (Edwards and Feehan, 1980; Kenrick and Crane, 1997). Vascular plants, however, were likely preceded by non-vascular plants (bryophytes) such as mosses, hornworts, and liverworts as evidenced by palynological studies, which show a diverse suite of spore tetrads and dyads in the fossil record starting in the mid-Ordovician (Strother et al., 1996; Wellman et al., 2003) and perhaps as early as the mid-Cambrian (Strother et al., 2004). Many modern plants form symbiotic associations with mycorrhizal fungi, which aid in nutrient acquisition. Because of the ubiquity of the plant-fungus symbiosis in the modern world, many researchers speculate that it is an ancient adaptation critical to the successful colonization of the terrestrial realm by plants (Selosse and Le Tacon, 1998; Redecker et al., 2000; Schussler, 2002). Fungi can form mycorrhiza-like associations with liverwort and hornwort rhizoids, both of which are considered the likely earliest terrestrial plants (Read et al., 2000; Renzaglia et al., 2007). Fossil evidence for mycorrhizal fungi is present in rocks as old as 460 Ma (Redecker et al., 2000). Prior to the colonization of land by plants and their fungal associates, the terrestrial realm was the domain of cyanobacteria, terrestrial bacteria, and lichens, which likely formed low-lying surface crusts (Labandeira, 2005).

Molecular clock studies suggest that terrestrial ecosystems are of considerable antiquity, with terrestrial bacteria present as early as the Archean (Battistuzzi et al., 2004; Battistuzzi and Hedges, 2009) and fungi and land plants diverging potentially as early as the Neoproterozoic (Heckman et al., 2001). These results are at odds with the fossil record. Studies of Proterozoic and Cambrian paleosol and terrestrial surface geochemistry may help illuminate changes in terrestrial flora that are not otherwise

recorded in the fossil record and may aid in resolving the discrepancy between molecular clock predictions and observations from the fossil record. To date, carbon and oxygen isotope geochemistry (Horodyski and Knauth, 1994; Gutzmer and Beukes, 1998; Knauth, 2008), biotic enhancement of element mobility (Neaman et al., 2005a, b, 2006), and changes in P mobility during the Proterozoic and Phanerozoic (Driese et al., 2007; Horodyski et al., 2008) have hinted at a systematic "greening" of the terrestrial landscape during the Neoproterozoic and Cambrian. Some researchers speculate that the Cambrian may have been a critical turning point in regards to the development of Phanerozoic terrestrial ecosystems, with the emergence of cryptospores hinting at a potential bryophyte presence in addition to previously existing biological crusts (Labandeira, 2005). In this study, six Middle Cambrian paleosols from central Laurentia have been analyzed for organic carbon contents, carbon isotope ratios, and element mobilization patterns (particularly P) to determine the potential composition and weathering impact of hypothesized Middle Cambrian terrestrial flora. Previous investigations of the Elk Point (South Dakota, US) core (Chapter 3) revealed a possible biosignature in the form of complete surface P loss. As a result, this core was selected for a more thorough investigation.

4.3 Geological Setting

Paleosols and paleosaprolites in the study region (the subsurface of central and western Iowa and southeast South Dakota) developed on a variety of Proterozoic basement material in the central region of Laurentia, an area known as the Midcontinental Rift System (MRS) (Chapters 2 and 3). For the purposes of this study, a paleosaprolite is defined as the portion of the paleoweathered zone that has been chemically altered, yet retains the textures of the parent material. A paleosol is defined as the portion of the paleoweathered zone that is characterized by pedogenic features and complete destruction of parent material textures. All paleosols are overlain by the Middle Cambrian Mt. Simon Sandstone, which in the study area is older than 500 Ma and likely older than 503 Ma (Chapter 3). Geochemical and mineralogical patterns, previously described (Chapter 3), indicate that the preserved horizons were zones of active weathering just prior to

burial. Aside from metasomatism affecting K concentrations at most sites, the paleosols and paleosaprolites tend to preserve Middle Cambrian weathering signatures. During this period of time, the study region was subjected to subtropical climate conditions. Subtle differences in geochemistry from site to site indicate that variability in bedrock and local relief contributed to the type of weathered horizons present at each location. Several trends, most notably P mobilization, hinted at biological effects, which will be explored in more detail here.

4.4 Sample Locations and Descriptions

The cores of interest were drilled by a variety of agencies between 1954 and 1979 in northwestern and central Iowa and southeast South Dakota and are stored at the Iowa Geological Survey core repository in Coralville, Iowa, and the South Dakota Geological Survey core repository in Vermillion, South Dakota. For this study, six cores were sampled and analyzed (Figure 4-1). The analyzed cores can be grouped into two regions. The Harris, Elk Point, and Camp Quest cores are located on pre-MRS terrane in northwest Iowa and southeast South Dakota. The Sharp, Hummell, and Nelson cores are located on the Iowa Horst. These cores were selected for analysis because all display visible evidence of parent material alteration beneath the Mt. Simon Sandstone. In all core profiles, the degree of alteration decreases with depth below the apparent top of the paleoweathered zone.

4.4.1 IGS-USGS D-13; Harris (Harris)

The Harris core was drilled in Osceola County in northwest Iowa (T100N R39W Sec. 17 SE SW SW SW). The basement material in this core is the Harris granite. A 2 m-thick paleosaprolite is developed on this granite, which was previously determined to have developed under reducing conditions as a result of persistent water saturation (Chapter 3). Unconsolidated and poorly recovered sandstone is present above the paleosaprolite, which may or may not be Mt. Simon Sandstone. More lithified Mt. Simon Sandstone is present above this unconsolidated zone.

4.4.2 R-20-2002-1 Elk Point Core (Elk Point)

The Elk Point core was drilled south of Elk Point, South Dakota (T90N R50W Sec. 13 NW NW NW NE). The basement material in this core is a strongly foliated metagabbro. The weathered section can be divided into two distinct zones: a paleosaprolite (1.6 m) that is enriched in dolomite and a red paleosol (3 m) showing clay translocation. This paleosol was previously determined to have formed under drier conditions, which resulted in pervasive carbonate precipitation in the paleosaprolite, which was later dolomitized by metasomatic fluids (Chapter 3). The overlying Mt. Simon Sandstone contains a basal conglomerate enriched in diagenetic pyrite. This core was selected for in-depth analysis due to its thickness, organic carbon contents, high apatite contents, and strong P depletion near the surface.

4.4.3 Lemars School District D-21; Camp Quest (Camp Quest)

The Camp Quest core was drilled in Plymouth County in northwest Iowa (T92N R45W Sec. 2 SW NW SW NW) and is located approximately 40 km northeast of Elk Point and approximately 90 km southwest of Harris. The basement material in this core is granitic gneiss. No paleosol is present in this core, but a thick paleosaprolite zone (18 m) is developed on the parent material. The Mt. Simon Sandstone overlies the paleosaprolite in this core.

4.4.4 Sharp #1 (Sharp)

The Sharp core was drilled in Webster County in central Iowa (T90N R27W Sec. 10 NW W NW NW) on the western edge of the Iowa Horst. The weathered section, likely developed in moderately humid conditions (Chapter 3), is present above basalt. A red paleosol (1.5 m) is located above a thick paleosaprolite zone (8.5 m). Mt. Simon Sandstone overlies the paleosol.

4.4.5 Hummell, Henry #1 and Nelson #1 (Hummell/Nelson)

The Hummell and Nelson cores were drilled in Dallas County in central Iowa (T79N R28W Sec. 18 NW NE NW and T79N R29W Sec. 12 SW SE NW, respectively). Both cores are similar to the Sharp core, with darker sandstone present above the basalt. In the Hummell core, a brown paleosol (1 m) is present above a paleosaprolite, and was previously determined to have formed under warm, humid conditions (Chapter 3). No unweathered basalt is present, although alteration is incomplete at the base of this core. The Nelson core, which is located near the Hummell core, may have a very thin alteration zone near the top of the basalt, but most of the basalt is poorly weathered. Mt. Simon Sandstone is present above the weathered sections in both cores.

4.5 Methodology

All work subsequent to core description, which was completed at the core repositories, was undertaken at the Pennsylvania State University. Cores were sampled from the overlying sandstone down through unweathered parent material (or the deepest available sample if unweathered material was not available) at regular intervals that varied from site to site depending on the thickness of weathered zones. Paleosols were typically sampled at finer intervals (<30 cm). Retrieved samples were cut with a water-lubricated rock saw to remove exterior surfaces on lithified sandstones and parent material. Exterior surfaces were removed manually on poorly lithified paleosol and paleosaprolite samples, which would have otherwise disaggregated under the water-lubricated rock saw. Samples were sonicated in deionized (DI) water for 2-3 minutes 3 times to remove surface contaminants, unless the sample began to disaggregate. Samples were dried, then ground to -100 mesh (149 μm). Powders were split into two aliquots. One aliquot was retained for bulk analysis while the other was reacted with 2 N hydrochloric acid for 48 hours to remove carbonate, then rinsed three times in DI water, dried in an oven, homogenized to create uniform powder for analysis, and weighed to determine mass loss during decarbonation.

Organic carbon content of samples was determined using a CE Instruments NA 2500 elemental analyzer (EA). The detection limit was 0.01 wt% and precision on replicate analysis was better than ± 0.01 wt% for C for decarbonated samples. Results for the decarbonated powders were corrected to account for mass loss during decarbonation.

Decarbonated samples were run on a Costech Analytical ECS 4010 elemental analyzer connected to a Thermo-Finnegan Delta Plus XP mass spectrometer via a ConFlo III interface to determine organic carbon isotope composition. The ANU sucrose standard was used, which is calibrated to NBS 19. All results are reported relative to the VPDB standard. Precision was typically better than 0.1‰.

Fresh samples were utilized for hydrofluoric acid dissolution. Samples from the Elk Point core were ground to -160 mesh (93 μm). Powders were then reacted with 10% HCl for 24 hours, decanted, and reacted with HF for 48 hours. Remaining organic matter was centrifuged, decanted, rinsed three times in DI water, and filtered. After drying for 24 hours, organic matter was rinsed off filter paper with acetone into vials for storage. The organic matter was investigated in transmitted light and photographed extensively. After transmitted light microscopy, samples were washed back into storage vials, dried, and embedded in epoxy for reflected light microscopy. Additional whole core samples from Elk Point were sent to Global Geolab Ltd. for separate extraction and preparation for observation in transmitted light.

Major oxides were determined for bulk samples using a Perkin-Elmer Optima 5300 inductively-coupled plasma atomic emission spectroscope (ICP-AES). Major oxide results are presented in a prior chapter (Chapter 3), but P results will be further discussed here.

Samples were sent to National Petrographic Service, Inc. for thin section preparation. Cut surfaces and thin sections were used for quantitative x-ray mapping of elemental distributions on a Horiba XGT-5000 to verify thin section determination of degraded minerals.

A normative mineral analysis was performed on the Elk Point weathered horizons to determine partitioning of oxides in minerals determined by XRD (Chapter 3). All oxide weight percents were initially converted to mole proportions. S was attributed to pyrite, and Fe molar proportions were decreased accordingly. P was attributed to apatite, and Ca was reduced accordingly. Remaining Ca was attributed to dolomite and Mg reduced accordingly, unless Mg contents were too low, in which case all Mg was attributed to dolomite and Ca was reduced accordingly. Remaining Ca (if present) was attributed to calcite. Fe was attributed to hematite. Remaining P (if present) was attributed to hematite-associated P. All Al was attributed to illite, and K and Si were reduced accordingly. All remaining Si was attributed to quartz. Ti was attributed to titanium oxides. The main purpose of the normative mineral analysis was to determine the partitioning of P in soil minerals. Additional mineralogy was used to ensure that the calculations were balanced (total wt% of minerals was ~100%).

4.6 Results

4.6.1 Organic Carbon

Organic carbon contents are low throughout the study area and are generally <0.1 wt%. Paleosols and paleosaprolites tend to be enriched in organic carbon compared to both the overlying sandstone and underlying parent material (Table 4-1). The highest organic carbon contents are present in the Nelson paleosaprolite (0.23 wt%). Lower organic carbon contents are present in the Elk Point paleosol (0.06 ± 0.02 wt%), Sharp paleosol (0.05 ± 0.01 wt%), and Hummell paleosol (0.05 ± 0.02 wt%). The lowest amounts are present in the Harris (0.03 ± 0.01 wt%) and Camp Quest paleosaprolites (0.03 ± 0.02 wt%).

Paleosaprolites (Harris and Camp Quest) are low in organic carbon throughout the profile, with slight enrichment at the surface (Figures 2a and 2c). Paleosols (Elk Point, Sharp, and Hummell) show two organic carbon profiles. The Sharp paleosol shows a broad zone of organic carbon enrichment (down to 0.5 m, as opposed to the surficial

enrichment that is seen in the paleosaprolites) (Figure 4-2d). The Elk Point and Hummell paleosols contain low organic carbon contents, with minor accumulation at depth (typically near or just above the paleosol-paleosaprolite boundary) (Figures 2b and 2e). The Nelson paleosaprolite is anomalous and shows the highest organic carbon content of all the sites (Figure 4-2f). Because this paleosaprolite is represented by one sample, it is impossible to determine more precisely how organic carbon is distributed through the weathered section that was likely once present at the site.

4.6.2 Organic $\delta^{13}\text{C}$

Despite similarities in organic carbon content throughout the study area, carbon isotope values for the organic matter are quite variable (Table 4-1). Organic matter in the Mt. Simon Sandstone present in the Elk Point core has anomalously ^{13}C -depleted carbon isotope values ($-52.7 \pm 2.2\text{‰}$). Organic matter in the Mt. Simon Sandstone from the western portion of the study area, excluding Elk Point, tends to be more depleted ($-25.4 \pm 0.4\text{‰}$, $n = 4$) than organic matter in sandstone from the eastern portion of the study area ($-23.9 \pm 0.4\text{‰}$, $n = 5$). Carbon isotope values tend to be enriched in the paleosol compared to the sandstone in the Elk Point (by $\sim 25\text{‰}$), Camp Quest (by $\sim 1\text{‰}$), Sharp (by $\sim 0.5\text{‰}$), and Hummell (by $\sim 0.5\text{‰}$) cores. In the Harris and Nelson cores, the paleosol carbon isotope values tend to be depleted compared to the overlying sandstone (by $\sim 0.5\text{‰}$ in the Harris core and $\sim 5\text{‰}$ in the Nelson core). The west-east dichotomy present in sandstone isotope results is not present in the weathered sections ($-24.8 \pm 1.6\text{‰}$, $n = 18$ for western sites excluding Elk Point and $-24.1 \pm 1.4\text{‰}$, $n = 22$ for eastern sites). The Elk Point core shows the most variability in carbon isotope results (Figure 4-2b). Its paleosol isotopic composition is typically around -25‰ , with lighter values at the top ($\sim -30\text{‰}$) and an anomalous heavy value at depth ($\sim -20.0\text{‰}$). The paleosaprolite shows more variability, with values between $\sim -17\text{‰}$ and $\sim -42\text{‰}$. The Camp Quest core contains some variability near the top of the paleosaprolite, with values ranging between $\sim -21\text{‰}$ and $\sim -27\text{‰}$ (Figure 4-2c). This level of variability is not present at the other sites.

4.6.3 Extracted Organic Matter

Organic matter was extracted from the Elk Point core and utilized in transmitted and reflected light microscopy. In general, sandstone organic matter tends to be black and clumps together during microscopic work, while paleosol organic matter is light brown and tends to flake apart more easily during microscopic work (Figures 3a and 3b). Organic matter in all samples is mostly amorphous, with very few, if any, structures visible. Most organic matter is light brown, although a few fragments are darker. The dark fragments are typically embedded in the lighter material. Separate extractions by Global Geolabs Ltd. yielded very little material. Morphologically identifiable material was mostly light-colored and immature, and likely to be modern contamination, probably introduced during drilling, recovery, or storage of the core. Darker-colored organic matter, which is more likely to be relict Cambrian organic matter, was not identifiable and was mostly amorphous.

4.6.4 Phosphorus Content and Depletion Patterns

As described previously (Chapter 3), P contents throughout the study area are low, typically <0.3 wt%. The Elk Point site contains the highest P contents (1-2 wt%). Geogenic (pre-existing non-pedogenic) features within the Sharp and Hummell profiles likewise show high P contents (~1 wt% at the contact between basalt flows in Sharp and ~0.5 wt% in a hydrothermal vein at Hummell). P patterns tend to show strong surface depletion, with the exception of the Nelson site. This pattern is especially prominent at Elk Point, which had higher initial P contents than any other site in the study region.

4.6.5 Apatite Dissolution

Apatite was most thoroughly investigated at Elk Point, as the site contains high P contents relative to the rest of the studied sites. Normative mineral analysis results suggest apatite content ranging between 2.2-4.9 wt% (average 3.4 wt%) (Table 4-2). All P can be accounted for in apatite, indicating that there is little, if any, oxide- or carbonate-

bound P present at Elk Point. These results are consistent with XGT maps of thin sections, which show P primarily associated with Ca in apatite grains. P at Elk Point seems to be predominately present in the form of apatite.

Apatite in thin sections shows little change up-section through a majority of the profile. Apatite is present throughout the metagabbro, typically in close association with biotite (Figure 4-4a). Moving up-section into the weathered zone, biotite becomes intensely altered, but apatite remains minimally altered, with some fractures further up-section but otherwise remaining intact (Figure 4-4b). This pattern remains unchanged throughout the weathered zone, except near the surface. Rare tunnel-like features (Figures 4c-e) become visible starting at 140 cm soil-depth. These tunnels, when present, are long, irregular tubes with a diameter of $\sim 10 \mu\text{m}$. The tunnel at 140 cm soil-depth (Figure 4-4c) contains kerogen in clumps based on preliminary Raman spectroscopic observations (Bill Schopf, personal communication). Tunnels are exceedingly rare in the core. One is present at 140 cm soil-depth and may have been formed by a non-fungal endolith (an organism that can live within minerals and can include algae, bacteria, and fungi) (Bill Schopf, personal communication). Three may be present at 50 cm soil-depth, and they tend to be filled with hematite based on preliminary Raman spectroscopic observations (Bill Schopf, personal communication). Fractures and thin alteration rinds become more common up-section (Figure 4-4e). Intense degradation of apatite is not observed until 30 cm soil-depth. At this depth, apatite becomes highly fragmented. The fragments tend to be rounded and appear to have been subject to dissolution based on comparison to intact grains deeper in the paleosol and paleosaprolite (Figures 4f-g). Apatite abruptly disappears above this zone of dissolution and is completely absent in the top 30 cm of the soil. There is very little evidence of secondary phosphate precipitation anywhere in the paleosol. Biotite, which is intensely altered throughout the weathered section, shows no visible changes in its weathered state through the depths where apatite has dissolved.

4.7 Discussion

4.7.1 Organic Matter Sources

Metasomatic fluids affected all sites except Sharp (Chapter 3), so the possibility of a migrated hydrocarbon source must be considered. Very little work has been completed on hydrocarbon migration in association with brine migration in the MRS region, other than to suggest that it may be a possibility (Duffin et al., 1989). Potassic alteration has been previously reported throughout the study area, except at the Sharp site (Chapter 3). There are no considerable differences between organic carbon contents and carbon isotope values of metasomatized and unmetasomatized sites, indicating that the organic material present in the paleosols and paleosaprolites is not likely to be a result of hydrocarbon migration. Slight differences in carbon isotopic values between sandstone and paleosol/paleosaprolite (as well as differences in the physical appearance and consistency of organic matter in the Elk Point sandstone and paleosol) suggest that younger marine organic matter introduced during the Cambrian transgression is likely not an adequate explanation for the organic matter present in the weathered zones. The organic matter present throughout the weathered zones is likely relict terrestrial organic matter.

4.7.2 Organic C Patterns

Organic carbon is present in low concentrations throughout the study area, typically <0.1 wt%, so extraction and characterization of the organic matter is difficult. Nonetheless, three patterns of organic carbon are recognizable in the paleoweathered zones. In the Harris and Camp Quest paleosaprolites, the highest organic carbon contents are at the surface. As previously reported (Chapter 3), both paleosaprolites are likely the truncated remains of thicker weathered zones that were lost either during weathering or the subsequent transgression. The slight enrichment of organic matter at the top of the paleosaprolites may indicate a zone of accumulation due to a change in lithology from sandy *grus* to indurated paleosaprolite. In the Sharp profile, the highest organic carbon

contents are within the surface horizons, rather than concentrated at a lithologic boundary. This may indicate the ancient presence of a terrestrial biota in this horizon or slight downward illuviation of surficial organic matter. The Elk Point and Hummell paleosols show organic C enrichment at depth. In the Hummell core, the enrichment is at the base of the paleosol. In the Elk Point core, zones of enrichment are present at the base of the paleosaprolite, the base of the paleosol, and about 2 m below the surface of the paleosol. These results indicate either the presence of a subsurface terrestrial biota, illuviation of surficial organic matter to greater depths, or both.

Data on organic C contents of Precambrian and early Phanerozoic paleosols is sparse. Archean paleosol organic C content can be as high as 1.4 wt% (Watanabe et al., 2004) presumably as a result of poor decomposition of terrestrial organic matter due to likely reducing soil conditions and a lack of consumers (Retallack, 2001). Typically, however, paleosol organic C content can be as low as <0.1 wt% as a result of post-burial decomposition (Retallack, 2001) and has been found to be as low as <0.01 wt% in Paleoproterozoic and Neoproterozoic paleosols (Retallack and Mindszenty, 1994; Gutzmer and Beukes, 1998). Organic C contents in the Middle Cambrian paleosols of this study are higher than those of the Proterozoic studies and comparable to younger paleosols, indicating the possible presence of a more substantial surface biota than was present in the Proterozoic.

4.7.3 Carbon Isotopes

Paleosols and paleosaprolites in this study show a range in $\delta^{13}\text{C}_{\text{org}}$ (-30‰ to -23‰; average: ~-25‰) which encompasses the normal values of modern soil organic matter (-27‰ to -25‰) (Retallack, 2001) and is similar to previously reported Precambrian soil values (-25.6‰) (Retallack and Mindszenty, 1994). These results are consistent with a photosynthetic origin for the organic matter. Isotope trends are not consistent from site to site. At the Harris and Nelson sites, the organic matter in the weathered horizons is more ^{13}C -depleted than in the overlying sandstone. At the Elk Point, Camp Quest, Sharp, and Hummell sites, the organic matter within the sandstone is more ^{13}C -depleted than the

underlying weathered zones, up to 25‰ at Elk Point, but typically 0.5-1‰ at the other sites. The reason for this pattern is unclear, but may be related to different organic matter inputs into the Mt. Simon Sandstone during its deposition. The extremely negative $\delta^{13}\text{C}$ values for the Mt. Simon Sandstone organic matter at Elk Point ($\sim -53\text{‰}$) could indicate methanogenesis followed by methanotrophy. This signal is not seen in the Mt. Simon Sandstone at other sites. A pattern emerges when sandstones from the western sites (Harris and Camp Quest, excluding the anomalous Elk Point results) are compared to sandstones from the eastern sites (Sharp, Hummell, and Nelson). The eastern sites tend to be $\sim 1\text{‰}$ heavier than the western sites. These differences may reflect changes in marine $\delta^{13}\text{C}$ values and potentially that the sites are of slightly different ages, as marine $\delta^{13}\text{C}_{\text{carb}}$ varied between -1‰ and 0‰ just prior to the onset of the Steptoean positive carbon isotope excursion (SPICE) ~ 4 million years after initial deposition of Mt. Simon sandstone at these sites (Saltzman et al., 2004; Kouchinsky et al., 2008). Paleoweathered zones from the western and eastern portions of the study area show considerable overlap and are not distinguishable from each other.

4.7.4 Phosphorus and Apatite Dissolution at Elk Point

Typically, the inorganic source of P in terrestrial environments is weathering from apatite, although in some cases dust deposition can be significant (Chadwick et al., 1999). As a result, P is a limiting nutrient and over geologic time, organisms have developed adaptations that enhance apatite dissolution to aid in the release of P, as apatite is relatively weathering-resistant, except in acidic soil environments (Taunton et al., 2000b; Welch et al., 2002; Neaman et al., 2005b). Abiotic apatite dissolution in modern soil environments typically results in the precipitation of secondary phosphates in close proximity to the apatite grain (Taunton et al., 2000b). Like apatite, secondary phosphates are typically insoluble in alkaline soils and will persist in lower soil zones where biological dissolution is less intense than at the surface. Bacteria and fungal hyphae can either suppress secondary phosphate precipitation through the uptake of P or actively dissolve secondary phosphates that were previously precipitated (Taunton et al., 2000a). Over time, apatite-bound P decreases as P is incorporated into organic matter. Once the

apatite source is exhausted, the organic-P fraction begins to decrease as it is lost to run-off (Crews et al., 1995). Eventually, any soil P not lost to run-off can become immobilized by Fe and Al (Crews et al., 1995), except in arid environments, where it can become incorporated into carbonates instead (Lajtha and Schlesinger, 1988).

Apatite makes up a considerable portion of the Elk Point paleosol and paleosaprolite (2-5 wt%) and it is remarkably persistent, despite the heavily weathered nature of the Elk Point paleosol. The persistence of apatite throughout a majority of the Elk Point core indicates that the paleosol was never particularly acidic at depth (Chapter 3). This is not the case near the surface, where apatite is completely absent in the top 30 cm of the paleosol. Acidic conditions were therefore more likely to have been present in the top 30 cm of the Elk Point paleosol, resulting in apatite dissolution. The abruptness with which apatite disappears from the profile coupled with a lack of lithologic or geochemical discontinuities at this depth argue strongly against a purely abiological mechanism for apatite attack (in this case, surface acidic conditions restricted to the top 30 cm of the paleosol that affect only apatite stability) and is consistent with many previous studies that have attributed enhanced apatite dissolution and P mobilization in terrestrial environments to weathering in the presence of organic ligands (Neaman et al., 2005a, b, 2006; Driese et al., 2007).

Once released from apatite, P can have one of two fates in the soil environment. It can be removed from the soil solution by organisms, or alternatively, it may be mobilized down-section, where it can precipitate as secondary phosphates or become bound to oxides and carbonates if it is not flushed entirely from the system by water. There is very little evidence from thin sections of secondary phosphate precipitation anywhere in the Elk Point profile. There are almost no rinds or secondary growths on apatite in the zone of dissolution, which is inconsistent with apatite dissolution in the absence of biological activity. In addition, based on normative mineral analysis, all P in the Elk Point paleosol can be attributed to apatite, which is consistent with XGT maps that suggest very little oxide- or carbonate-associated P. This indicates that once P was released from apatite, it was removed from the soil solution relatively quickly, most likely by biological activity;

otherwise it would have been retained as oxide- or carbonate-bound P or as secondary phosphates. Carbonates present at depth at Elk Point indicate that calcium was not completely removed from the profile due to low rainfall at the site. As a result, complete flushing of P mobilized from apatite dissolution by rainwater is not likely.

Argillans, which are clay flow structures, are very prominent just above the zone of apatite dissolution (Chapter 3). In modern soil environments, clay translocation occurs in three steps: dispersion, translocation, and flocculation. Clays tend to disperse in soil horizons that are depleted in cations, and flocculate in horizons that are richer in cations such as Ca and Mg (Schaetzl and Anderson, 2005). The ubiquity of clay coatings and argillans in the zone of apatite dissolution is consistent with flocculation in a zone where the soil solution is enriched in Ca as a consequence of apatite dissolution. The removal of P and subsequent accumulation of Ca in soil solution during apatite dissolution has been previously attributed to the activities of mycorrhizal fungi (Ness and Vlek, 2000). Further evidence for the presence of mycorrhizal fungi in the Elk Point paleosol may include the possible tunnel features present in some of the apatite grains close to the zone of dissolution. The tunnel-like features are morphologically similar to modern fungal tunnels found in feldspars and hornblendes (van Breemen et al., 2000; Landeweert et al., 2001; Hoffland et al., 2002, 2003) and have not been previously reported in apatite. However, preliminary results from Raman spectroscopy indicate that some of the tunnels may be hematite-filled fractures (Figure 4-4e) or may have been generated by non-fungal endoliths (Figure 4-4c) (Bill Schopf, personal communication).

4.7.5 Cambrian Terrestrial Ecosystems and Consequences

Based on a comparison to a limited number of studies, P mobilization from ancient soil surface horizons appears to have intensified and become more complete from the Precambrian to the Cambrian (Driese et al., 2007; Driese and Medaris, 2008). This pattern may be the result of changes in the composition of terrestrial ecosystems, which resulted in higher nutrient demands (particularly P) and led to deeper and more efficient weathering of apatite. The increasing intensity of P depletion from the Precambrian to

the Cambrian may be a geochemical indicator of the increasing prominence of a rhizosphere-like ecosystem, perhaps associated with the rhizoids of very early bryophytes, as many fungi, both symbiotic and free-living, solubilize apatite quite readily (Rosling et al., 2007).

In the study area, the SPICE event is recorded in Upper Cambrian carbonates and has been linked to increased carbon burial during a fall in sea level (Saltzman et al., 2004) and high continental weathering rates (Kouchinsky et al., 2008). As mentioned previously, P in the paleoweathered zones is present predominantly as apatite, with little indication of oxide- or carbonate-associated P. This likely indicates that once liberated from apatite, P was most likely heavily recycled and mostly lost to surface run-off as organic-P before substantial quantities of it could have become incorporated into soil Fe- and Al-oxides. This increased nutrient flow from terrestrial to marine environments as a result of the increasing prominence of a more deeply weathering terrestrial soil biota during the Middle Cambrian may have gradually enhanced marine primary productivity and, in turn, increased rates of marine organic matter burial offshore and contributed to a nutrient build-up that led to the SPICE event in the Upper Cambrian. The SPICE event has also been previously linked to trilobite mass extinction (Saltzman et al., 1998; Saltzman et al., 2000) and potentially ocean anoxia (Gill et al., 2007) in a pattern that is remarkably similar to one described for the Devonian following the development of seeds and arborescence in terrestrial land plants, resulting in changes in the depth, intensity, and extent of pedogenesis and resulting nutrient flux to the ocean (Algeo and Scheckler, 1998). An earlier terrestrial ecosystem colonization attempt during the Middle Cambrian may have resulted in changes in weathering depth and intensity that may be related to the Upper Cambrian SPICE event.

4.8 Conclusions

Geochemical trends in paleoweathered surfaces of Middle Cambrian age in the MRS region have previously hinted at potential biological effects, particularly in P loss and apatite dissolution. Organic carbon contents at all sites, which are higher than previously

reported results for Proterozoic paleosols and similar to younger paleosols, indicate an ecosystem that was likely more substantial than older Proterozoic terrestrial ecosystems. The Harris and Camp Quest sites likely accumulated small amounts of organic matter at a lithologic discontinuity between sandy *grus* and the underlying indurated paleosaprolite. The Sharp, Hummell, and Elk Point paleosols likely contained more substantial surface biotas, with illuviation having redistributed organic matter down-section. Organic carbon isotope values for all weathered zones are consistent with a photosynthetic origin.

Apatite content is highest at the Elk Point site (2-5 wt%), but is completely absent from the top 30 cm of the paleosol. Normative mineral analysis, thin section analysis, and XGT maps indicate that the vast majority of P is present as apatite. Once dissolved, P was likely taken up by biological activity and became organically bound, and was thus unavailable for precipitation as secondary phosphates or binding to oxides or carbonates, which are not present in the Elk Point core. Biological apatite dissolution, resulting in P uptake and an increase in soil Ca concentrations, may have resulted in the flocculation of clays that were mobilized from the upper horizons of the paleosol. This is consistent with the behavior of modern mycorrhizal fungi. Further evidence for mycorrhizal fungi may be present in the form of apatite tunnel features, but these results are equivocal and are under further investigation. If mycorrhizal fungi were present at Elk Point and affecting apatite dissolution and clay flocculation, this would extend their record from the mid-Ordovician (~460 Ma) to the Middle Cambrian (>503 Ma) and would be consistent with molecular clock studies that predict their earlier origin. Enhanced apatite weathering as a result of the increasing prominence of more deeply weathering terrestrial ecosystems could have led to higher P fluxes to the Cambrian oceans as a result of run-off and may have, over time, enhanced marine productivity and organic matter burial, eventually contributing to the Upper Cambrian SPICE event, which has been previously linked to high continental weathering and marine organic matter burial rates.

4.9 Acknowledgements

This research was funded by the NASA Astrobiology Institute and the Pennsylvania State University Department of Geosciences. Special thanks to Y. Watanabe, H. Gong, E. Altinok, I. Johnson, D. Hummer, J. Fulton, C. Junium, D. van Niekirk, and G. Mitchell for analytical assistance; A. Morales and R. Quintero for field and lab assistance; T. Haggar, P. Morath, and R. Anderson for sample collection assistance; and R. Anderson, Y. Watanabe, and F. Battistuzzi for useful discussion.

4.10 References

- Algeo, T.J., and Scheckler, S.E., 1998, Terrestrial-Marine Teleconnections in the Devonian: Links between the Evolution of Land Plants, Weathering Processes, and Marine Anoxic Events: *Philosophical Transactions: Biological Sciences*, v. 353, p. 113-128.
- Anderson, R.R., 2006, Geology of the Precambrian Surface of Iowa and surrounding area, Iowa Geological Survey.
- Battistuzzi, F.U., Feijao, A., and Hedges, S.B., 2004, A genomic timescale of prokaryote evolution: insights into the origin of methanogenesis, phototrophy, and the colonization of land: *BMC Evolutionary Biology*, v. 4, p. 44.
- Battistuzzi, F.U., and Hedges, S.B., 2009, A major clade of prokaryotes with ancient adaptations to life on land: *Molecular Biology and Evolution*, v. 26, p. 335-343.
- Chadwick, O.A., Derry, L.A., Vitousek, P.M., Huebert, B.J., and Hedin, L.O., 1999, Changing sources of nutrients during four million years of ecosystem development: *Nature*, v. 297, p. 491-497.
- Crews, T.E., Kitayama, K., Fownes, J.H., Riley, R.H., Herbert, D.A., Mueller-Dombois, D., and Vitousek, P.M., 1995, Changes in Soil Phosphorus Fractions and Ecosystem Dynamics across a Long Chronosequence in Hawaii: *Ecology*, v. 76, p. 1407-1424.
- Driese, S.G., and Medaris, L.G., 2008, Evidence for Biological and Hydrological Controls on the Development of a Paleoproterozoic Paleoweathering Profile in the Baraboo Range, Wisconsin, USA: *Journal of Sedimentary Research*, v. 78, p. 443-457.
- Driese, S.G., Medaris, L.G., Ren, M., Runkel, A.C., and Langford, R.P., 2007, Differentiating Pedogenesis from Diagenesis in Early Terrestrial Paleoweathering Surfaces Formed on Granitic Composition Parent Materials: *Journal of Geology*, v. 115, p. 387-406.
- Duffin, M.E., Lee, M., Klein, G.d., and Hay, R.L., 1989, Potassic Diagenesis of Cambrian Sandstones and Precambrian Granitic Basement in UPH-3 Deep Hole, Upper Mississippi Valley, USA: *Journal of Sedimentary Petrology*, v. 59, p. 848-861.

- Edwards, D., and Feehan, J., 1980, Records of *Cooksonia*-type sporangia from late Wenlock strata in Ireland: *Nature*, v. 287, p. 41-42.
- Gill, B., Lyons, T., Kump, L.R., Young, S., and Saltzman, M.R., 2007, A Late Cambrian Ocean Anoxic Event: *GSA Abstracts with Programs*, v. 39, p. 304.
- Gutzmer, J., and Beukes, N.J., 1998, Earliest laterites and possible evidence for terrestrial vegetation in the Early Proterozoic: *Geology*, v. 26, p. 263-266.
- Heckman, D.S., Geiser, D.M., Eidell, B.R., Stauffer, R.L., Kardos, N.L., and Hedges, S.B., 2001, Molecular Evidence for the Early Colonization of Land by Fungi and Plants: *Science*, v. 293, p. 1129-1133.
- Hoffland, E., Giesler, R., Jongmans, T., and van Breemen, N., 2002, Increasing Feldspar Tunneling by Fungi across a North Sweden Podzol Chronosequence: *Ecosystems*, v. 5, p. 11-22.
- , 2003, Feldspar Tunneling by Fungi along Natural Productivity Gradients: *Ecosystems*, v. 6, p. 739-746.
- Horodyski, R.J., and Knauth, L.P., 1994, Life on Land in the Precambrian: *Science*, v. 263, p. 494-498.
- Horodyskyj, L.B., White, T.S., and Kump, L.R., 2008, Biosignatures in Middle Cambrian Paleosols: *Eos Trans. AGU, Fall Meeting Supplemental*, v. 89, p. Abstract P54A-03.
- Kenrick, P., and Crane, P.R., 1997, The origin and early evolution of plants on land: *Nature*, v. 389, p. 33-39.
- Knauth, L.P., 2008, Greening of the Late Precambrian Landscape: *Geological Society of America Abstracts with Programs*, v. 40, p. 96.
- Kouchinsky, A., Bengtson, S., Gallet, Y., Korovnikov, I., Pavlov, V., Runnegar, B., Shields, G., Veizer, J., Young, E., and Ziegler, K., 2008, The SPICE carbon isotope excursion in Siberia: a combined study of the upper Middle Cambrian–lowermost Ordovician Kulyumbe River section, northwestern Siberian Platform: *Geological Magazine*, v. 145, p. 609-622.
- Labandeira, C.C., 2005, Invasion of the continents: cyanobacterial crusts to tree-inhabiting arthropods: *TRENDS in Ecology and Evolution*, v. 20, p. 253-262.
- Lajtha, K., and Schlesinger, W.H., 1988, The Biogeochemistry of Phosphorus Cycling and Phosphorus Availability Along a Desert Chronosequence: *Ecology*, v. 69, p. 24-39.
- Landeweert, R., Hoffland, E., Finlay, R.D., Kuyper, T.W., and van Breemen, N., 2001, Linking plants to rocks: ectomycorrhizal fungi mobilize nutrients from minerals: *TRENDS in Ecology and Evolution*, v. 16, p. 248-254.
- Neaman, A., Chorover, J., and Brantley, S.L., 2005a, Element mobility patterns record organic ligands in soils on early Earth: *Geology*, v. 33, p. 117-120.
- , 2005b, Implications of the Evolution of Organic Acid Moieties for Basalt Weathering over Geological Time: *American Journal of Science*, v. 305, p. 147-185.
- , 2006, Effects of Organic Ligands on Granite Dissolution in Batch Experiments at pH 6: *American Journal of Science*, v. 306, p. 451-473.
- Ness, R.L.L., and Vlek, P.L.G., 2000, Mechanism of Calcium and Phosphate Release from Hydroxy-Apatite by Mycorrhizal Hyphae: *Soil Science Society of America Journal*, v. 64, p. 949-955.

- Read, D.J., Duckett, J.G., Francis, R., Ligrone, R., and Russell, A., 2000, Symbiotic fungal associations in 'lower' land plants: *Philosophical Transactions of the Royal Society of London B*, v. 355, p. 815-831.
- Redecker, D., Kodner, R., and Graham, L.E., 2000, Glomalean Fungi from the Ordovician: *Science*, v. 289, p. 1920-1921.
- Renzaglia, K.S., Schuette, S., Duff, R.J., Ligrone, R., Shaw, A.J., Mishler, B.D., and Duckett, J.G., 2007, Bryophyte phylogeny: Advancing the molecular and morphological frontiers: *The Bryologist*, v. 110, p. 179-213.
- Retallack, G.J., 2001, *Soils of the Past: An Introduction to Paleopedology*: Oxford, Blackwell Science, 404 p.
- Retallack, G.J., and Mindszenty, A., 1994, Well Preserved Late Precambrian Paleosols from Northwest Scotland: *Journal of Sedimentary Research*, v. A64, p. 264-281.
- Rosling, A., Suttle, K.B., Johansson, E., van Hees, P.A.W., and Banfield, J.F., 2007, Phosphorous availability influences the dissolution of apatite by soil fungi: *Geobiology*, v. 5, p. 265-280.
- Saltzman, M.R., Cowan, C.A., Runkel, A.C., Runnegar, B., Stewart, M.C., and Palmer, A.R., 2004, The Late Cambrian SPICE (d13C) Event and the Sauk II-Sauk III Regression: New Evidence from Laurentian Basins in Utah, Iowa, and Newfoundland: *Journal of Sedimentary Research*, v. 74, p. 366-377.
- Saltzman, M.R., Ripperdan, R.L., Brasier, M.D., Lohmann, K.C., Robison, R.A., Chang, W.T., Peng, S., Ergaliev, E.K., and Runnegar, B., 2000, A global carbon isotope excursion (SPICE) during the Late Cambrian: relation to trilobite extinctions, organic-matter burial and sea level: *Palaeogeography, Palaeoclimatology, Palaeoecology*, v. 162, p. 211-223.
- Saltzman, M.R., Runnegar, B., and Lohmann, K.C., 1998, Carbon isotope stratigraphy of Upper Cambrian (Steptoean Stage) sequences of the eastern Great Basin: Record of a global oceanographic event: *GSA Bulletin*, v. 110, p. 285-297.
- Schaetzl, R.J., and Anderson, S., 2005, *Soils: Genesis and Geomorphology*, Cambridge University Press.
- Schussler, A., 2002, Molecular phylogeny, taxonomy, and evolution of *Geosiphon pyriformis* and arbuscular mycorrhizal fungi: *Plant and Soil*, v. 244, p. 75-83.
- Selosse, M.A., and Le Tacon, F.L., 1998, The land flora: a phototroph-fungus partnership: *Trends in Ecology and Evolution*, v. 13, p. 15-20.
- Strother, P.K., Al-Hajri, S., and Traverse, A., 1996, New evidence for land plants from the lower Middle Ordovician of Saudi Arabia: *Geology*, v. 24, p. 55-58.
- Strother, P.K., Wood, G., Taylor, W., and Beck, J., 2004, Middle Cambrian cryptospores and the origin of land plants: *Memoirs of the Association of Australasian Palaeontologists*, v. 29, p. 99-113.
- Taunton, A.E., Welch, S.A., and Banfield, J.F., 2000a, Geomicrobiological controls on light rare earth element, Y and Ba distributions during granite weathering and soil formation: *Journal of Alloys and Compounds*, v. 303-304, p. 30-36.
- , 2000b, Microbial controls on phosphate and lanthanide distributions during granite weathering and soil formation: *Chemical Geology*, v. 169, p. 371-382.
- van Breemen, N., Lundstrom, U.S., and Jongmans, T., 2000, Do plants drive podzolization via rock-eating mycorrhizal fungi?: *Geoderma*, v. 94, p. 163-171.

- Watanabe, Y., Stewart, B.W., and Ohmoto, H., 2004, Organic- and carbonate-rich soil formation *Geochimica et Cosmochimica Acta*, v. 68, p. 2129-2151.
- Welch, S.A., Taunton, A.E., and Banfield, J.F., 2002, Effect of Microorganisms and Microbial Metabolites on Apatite Dissolution: *Geomicrobiology journal*, v. 19, p. 343-367.
- Wellman, C.H., Osterloff, P.L., and Mohiuddin, U., 2003, Fragments of the earliest land plants: *Nature*, v. 425, p. 282-285.

Tables and Figures

Table 4-1:

<i>Site</i>	<i>Division</i>	<i>Average Organic C Content (wt%)</i>	<i>Average $\delta^{13}C$ (‰)</i>
Harris	Sandstone	0.02 ± 0.01	-25.3 ± 0.4
	Paleosaprolite	0.03 ± 0.01	-25.8 ± 0.3
	Granite	0.03 ± 0.01	-25.9
Elk Point	Sandstone	0.05 ± 0.03	-52.7 ± 2.2
	Paleosol	0.06 ± 0.02	-25.3 ± 2.2
	Paleosaprolite	0.02 ± 0.02	-30.2 ± 6.6
	Metagabbro	0.02 ± 0.02	-26.2 ± 12.6
Camp Quest	Sandstone	0.04 ± 0.02	-25.5 ± 0.5
	Paleosaprolite	0.03 ± 0.02	-24.2 ± 1.7
	Granitic Gneiss	0.03 ± 0.01	-25.1 ± 0.4
Sharp	Sandstone	0.02 ± 0.01	-23.6 ± 0.4
	Paleosol	0.05 ± 0.01	-23.0 ± 0.5
	Paleosaprolite	0.04 ± 0.01	-23.8 ± 0.4
	Basalt	0.02	-24.3
Hummell	Sandstone	0.04 ± 0.03	-24.2 ± 0.1
	Paleosol	0.05 ± 0.02	-23.7 ± 0.1
	Paleosaprolite	0.05 ± 0.01	-24.8 ± 0.6
Nelson	Sandstone	0.03	-23.8
	Paleosaprolite	0.23	-29.0
	Basalt	0.04 ± 0.01	
Western Sites (excluding Elk Point)	Sandstone		-25.4 ± 0.4
	Weathering		-24.8 ± 1.6
Eastern Sites	Sandstone		-23.9 ± 0.4
	Weathering		-24.1 ± 1.4

Table 4-2:

<i>Depth (m)</i>	<i>Pyrite (wt%)</i>	<i>Apatite (wt%)</i>	<i>Dolomite (wt%)</i>	<i>Calcite (wt%)</i>	<i>Hematite (wt%)</i>	<i>Hem-P (wt%)</i>	<i>Illite (wt%)</i>	<i>Quartz (wt%)</i>	<i>Ti-Ox (wt%)</i>
273.84	2.83	0.30	0.19	0.00	17.76	0.00	58.82	25.11	2.76
274.02	0.00	0.34	0.11	0.00	14.50	0.00	61.09	26.35	3.20
274.32	0.00	3.28	1.20	0.00	17.10	0.00	55.40	22.60	2.88
274.62	0.00	4.42	1.23	0.00	15.90	0.00	55.02	24.75	3.08
274.93	0.00	4.85	0.00	0.00	13.90	0.00	52.37	25.35	3.47
275.23	0.00	3.87	0.43	0.00	16.30	0.00	52.75	26.41	2.94
275.54	0.00	3.83	1.27	0.00	13.20	0.00	55.78	27.56	2.82
275.84	0.00	2.87	2.21	0.00	15.80	0.00	49.71	30.56	2.19
276.15	0.00	2.87	0.92	0.00	14.80	0.00	51.99	27.90	2.71
276.45	0.00	3.40	8.94	0.00	12.00	0.00	50.47	26.07	3.33
276.70	0.00	2.53	27.45	0.00	11.90	0.00	38.71	21.53	2.49
276.76	0.00	3.05	6.86	0.00	9.83	0.00	51.23	29.69	3.55
277.06	0.00	3.28	13.10	0.00	10.90	0.00	48.95	25.45	3.23
277.52	0.00	4.79	5.80	0.00	10.90	0.00	55.40	24.80	3.84
277.83	0.00	3.46	19.26	0.00	10.30	0.00	43.64	22.56	3.49
278.02	0.00	2.64	24.83	0.00	9.74	0.00	35.14	25.08	2.72
278.28	0.00	2.21	14.12	0.00	9.01	0.00	43.26	33.01	3.04

273.87 m – 276.70 m : Elk Point paleosol

276.76 m – 278.28 m : Elk Point paleosaprolite

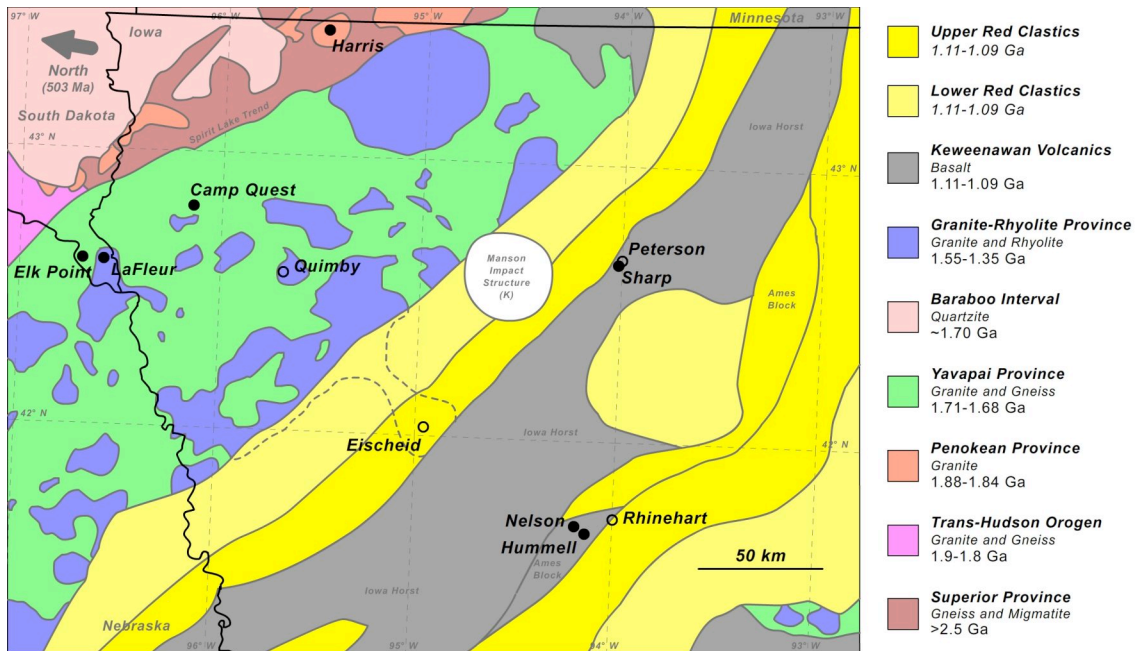


Figure 4-1: Detailed bedrock map of the study region, showing the variety of terranes upon which paleoweathering features developed (solid circles). Open circles indicate additional cores that were used to constrain the age of the overlying Middle Cambrian Mt. Simon Sandstone and differentiate older "Red Clastics" from the Mt. Simon Sandstone. Modified from Anderson (2006).

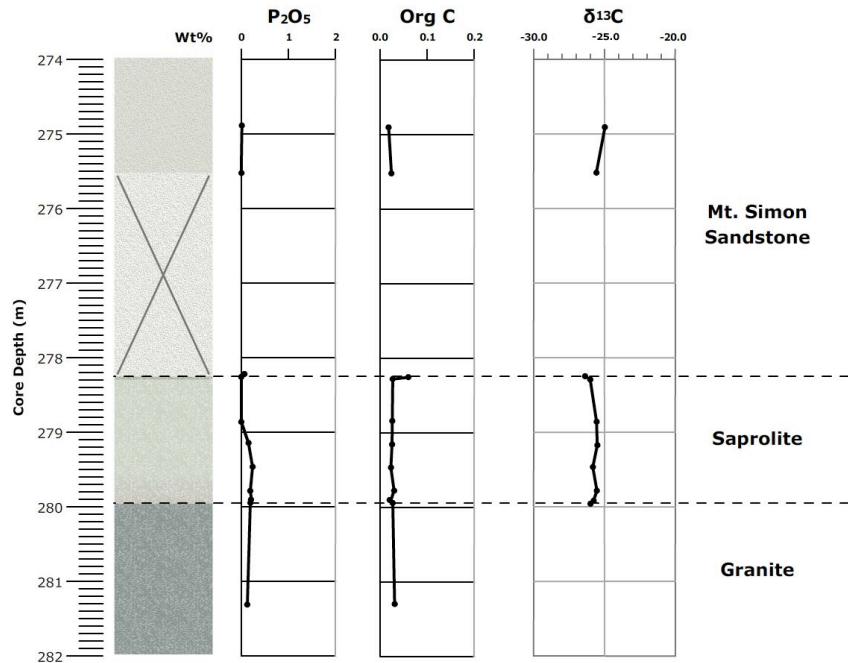


Figure 4-2a: Phosphorus, organic carbon, and carbon isotope profiles through the Harris core.

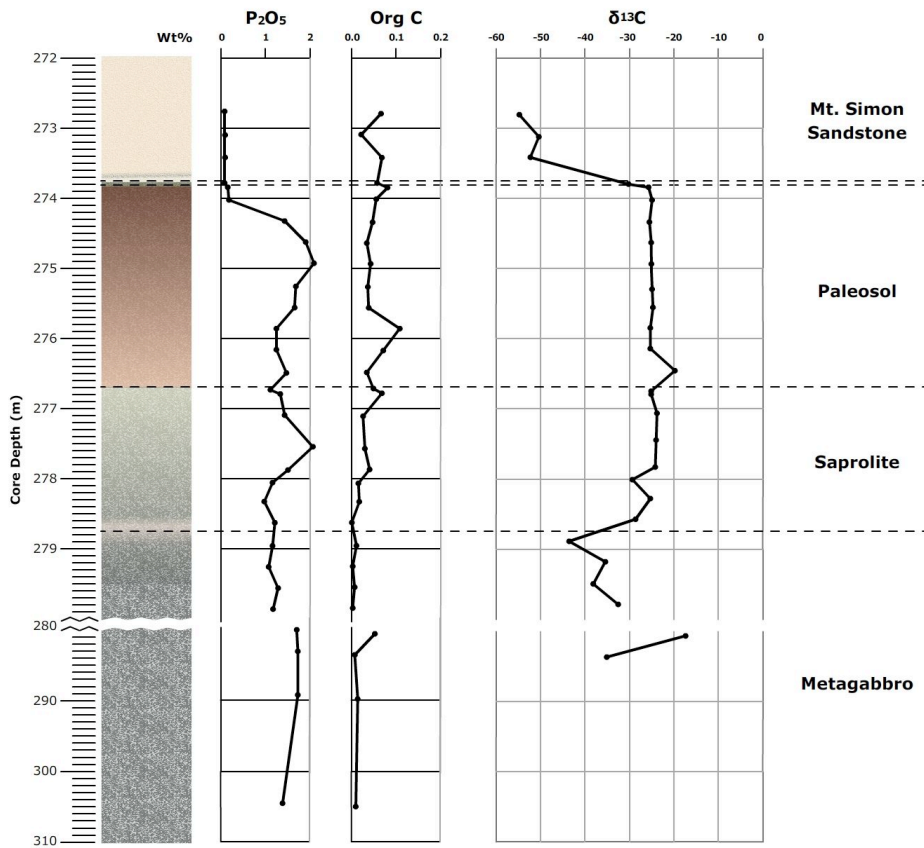


Figure 4-2b: Phosphorus, organic carbon, and carbon isotope profiles through the Elk Point core.

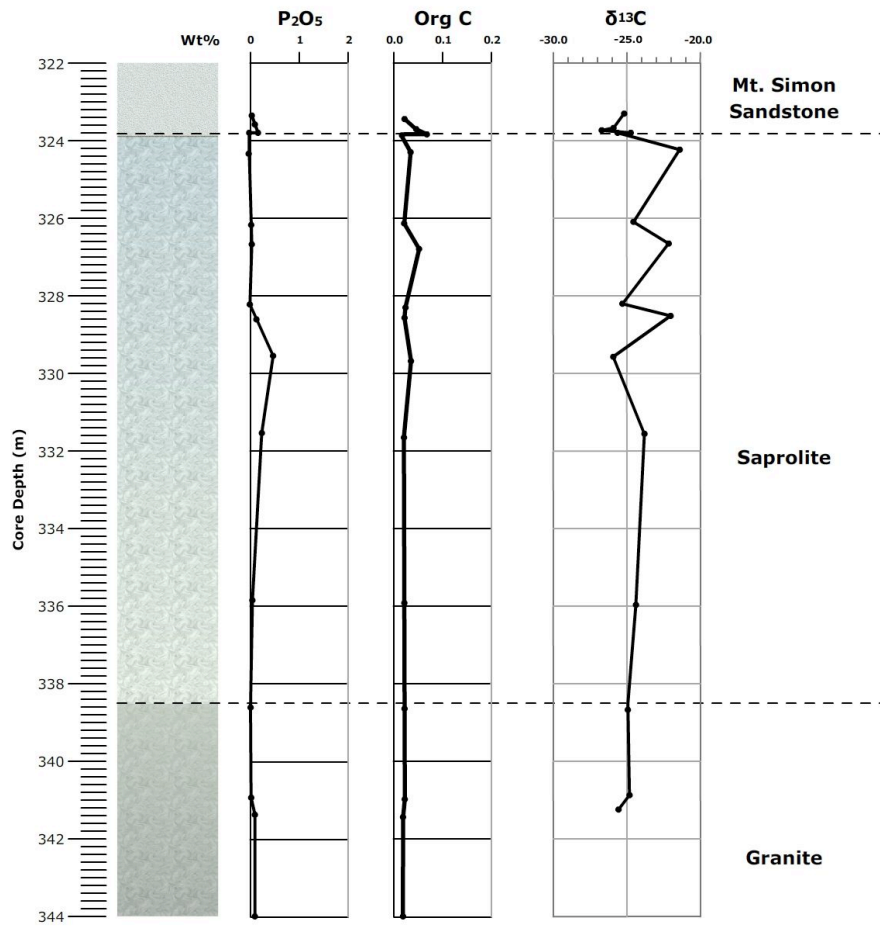


Figure 4-2c: Phosphorus, organic carbon, and carbon isotope profiles through the Camp Quest core.

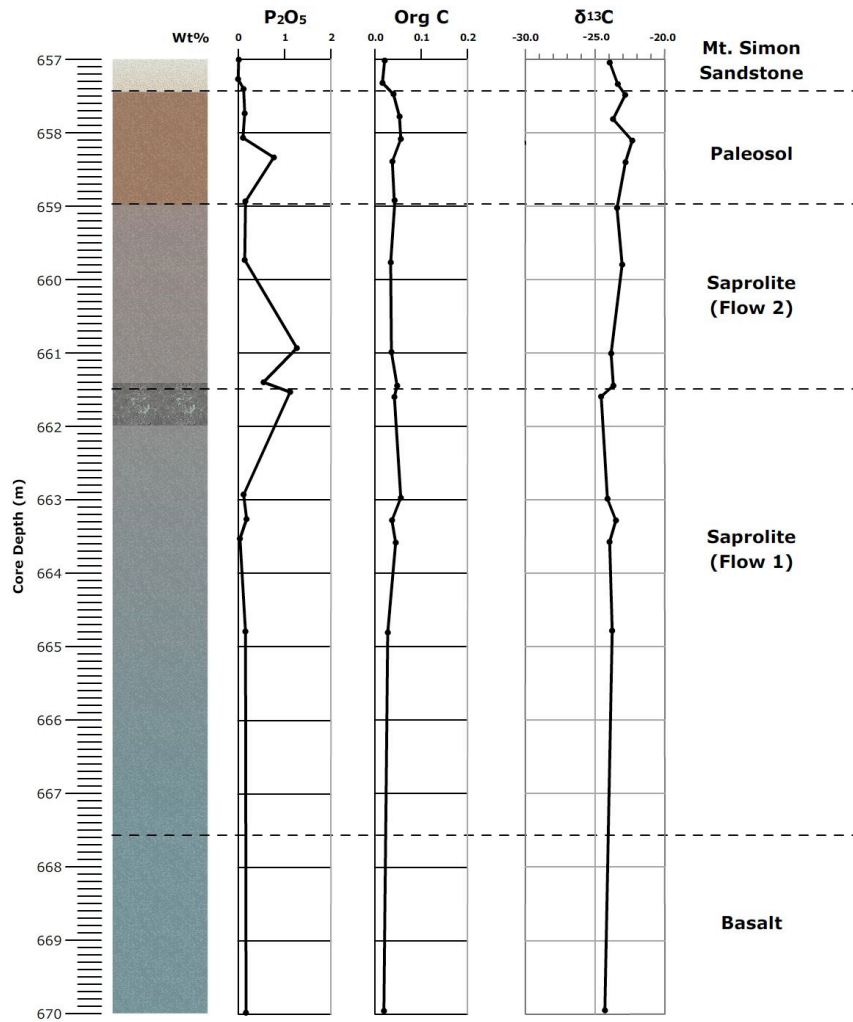


Figure 4-2d: Phosphorus, organic carbon, and carbon isotope profiles through the Sharp core.

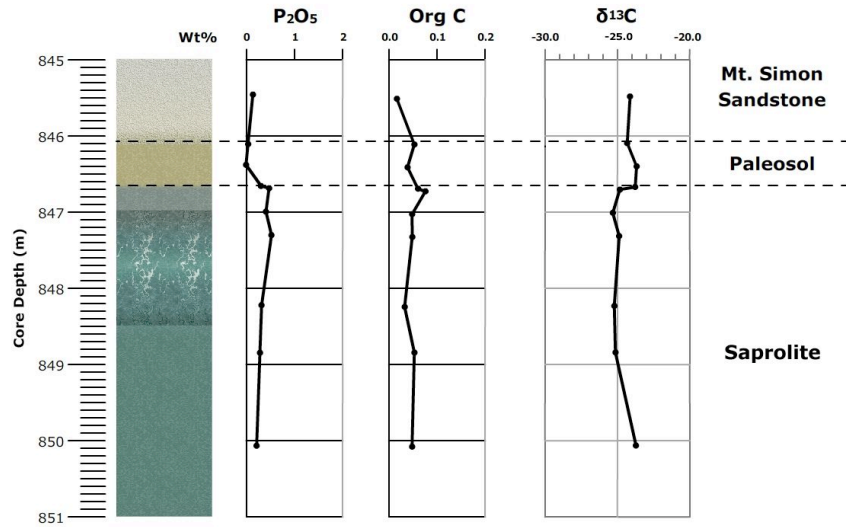


Figure 4-2e: Phosphorus, organic carbon, and carbon isotope profiles through the Hummell core.

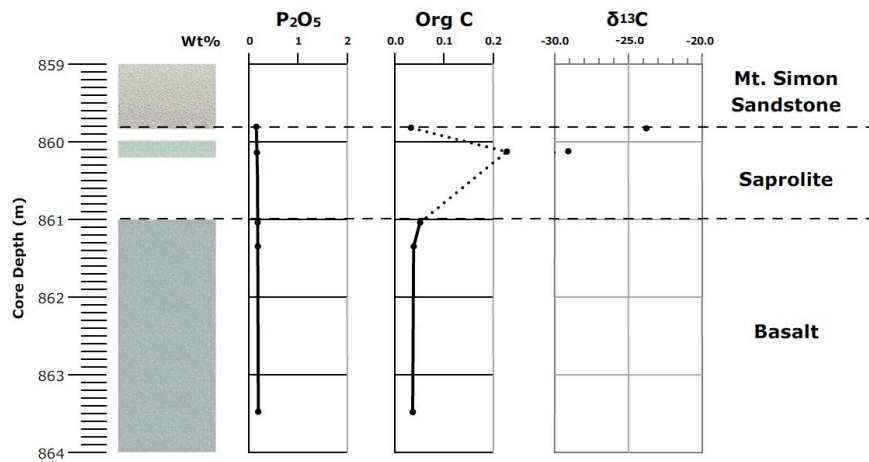


Figure 4-2f: Phosphorus, organic carbon, and carbon isotope profiles through the Nelson core.

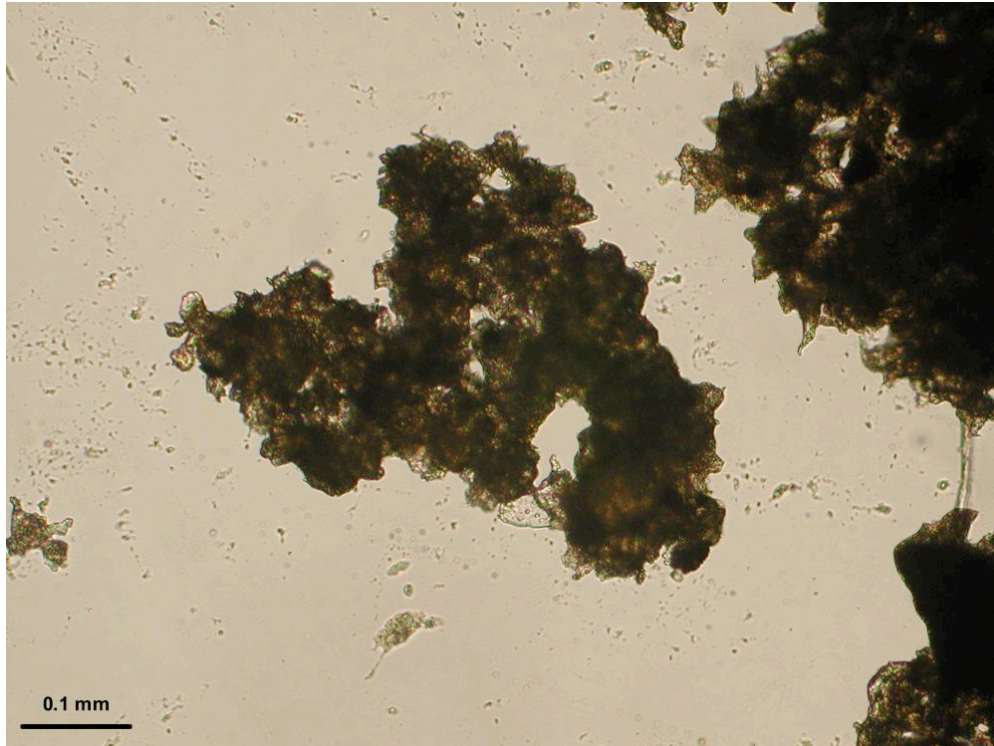


Figure 4-3a: Extracted amorphous organic matter from the sandstone overlying the Elk Point paleosol (core depth: 273.1 m)

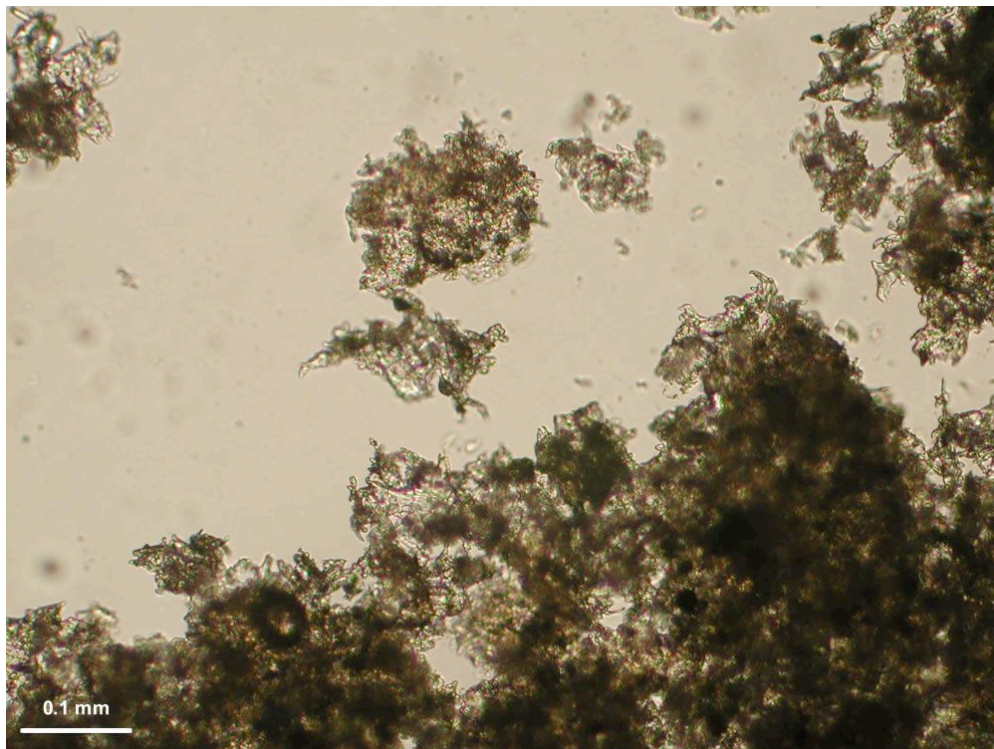


Figure 4-3b: Extracted amorphous organic matter from the surface horizon of the Elk Point paleosol (core depth: 274.0 m)

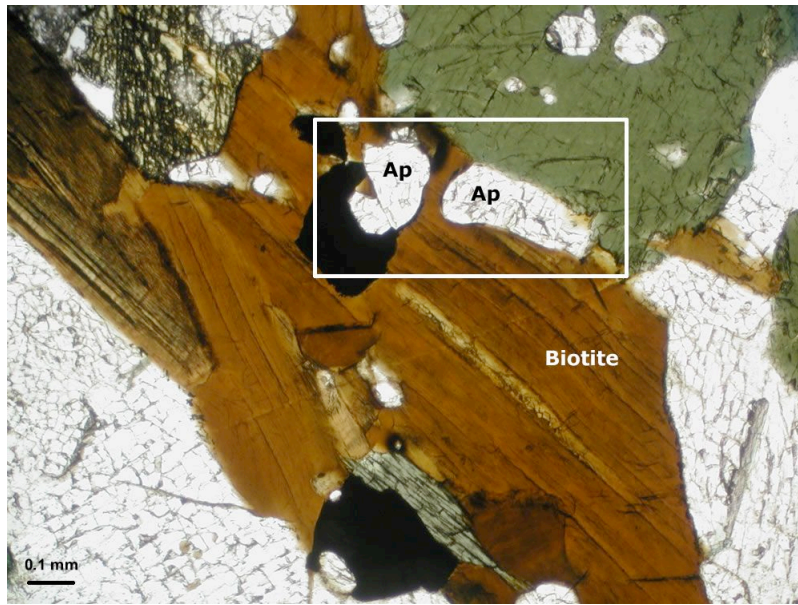


Figure 4-4a: Apatite grains associated with biotite in the unweathered metagabbro in the Elk Point core (core depth: 289.6 m)

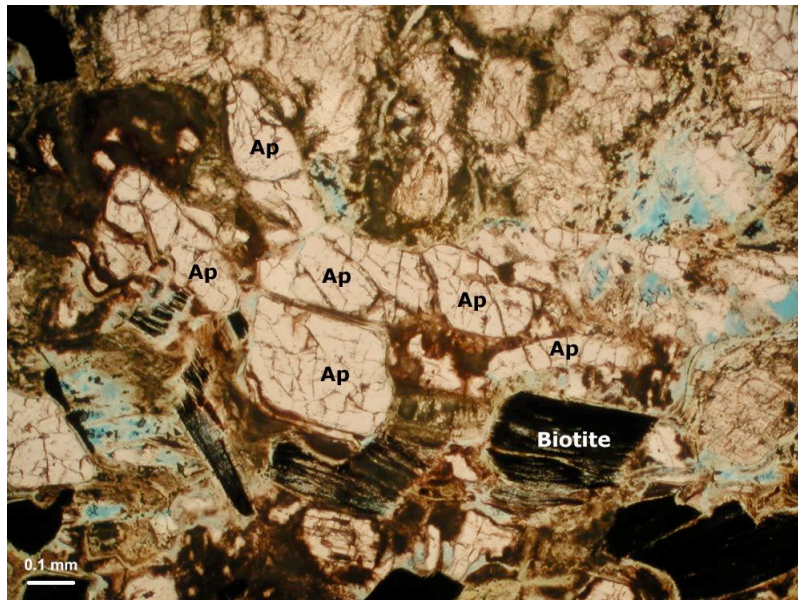


Figure 4-4b: Within the Elk Point paleosaprolite, biotite has undergone considerable chemical alteration, while apatite grains, although fractured, remain mostly intact (core depth: 277.1 m)

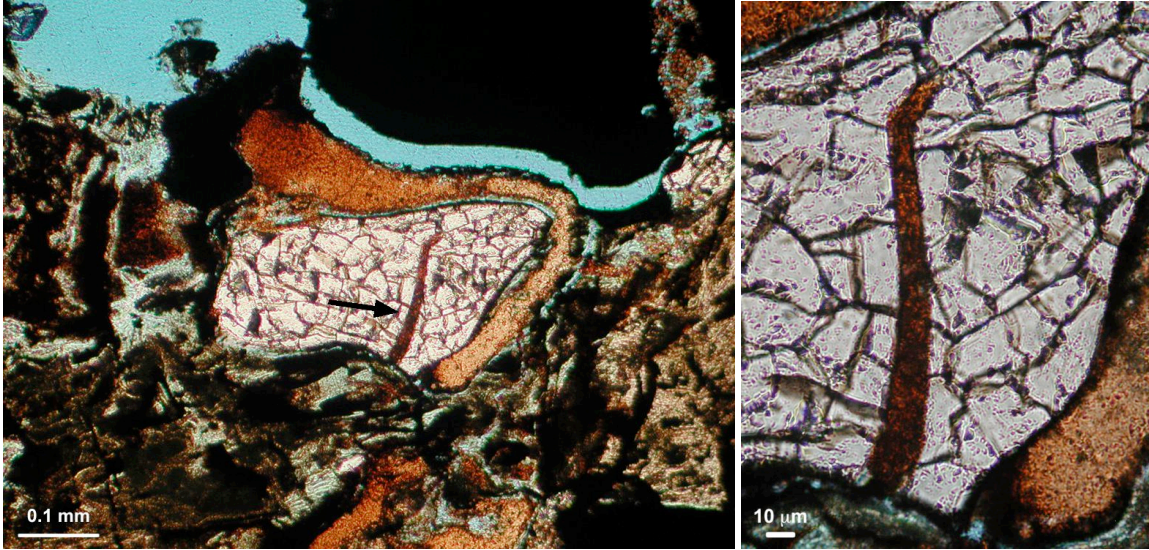


Figure 4-4c: Possible tunnel structure filled with kerogen (likely formed by an endolith) in an apatite grain 140 cm below paleosol surface (Elk Point core depth: 275.2 m)

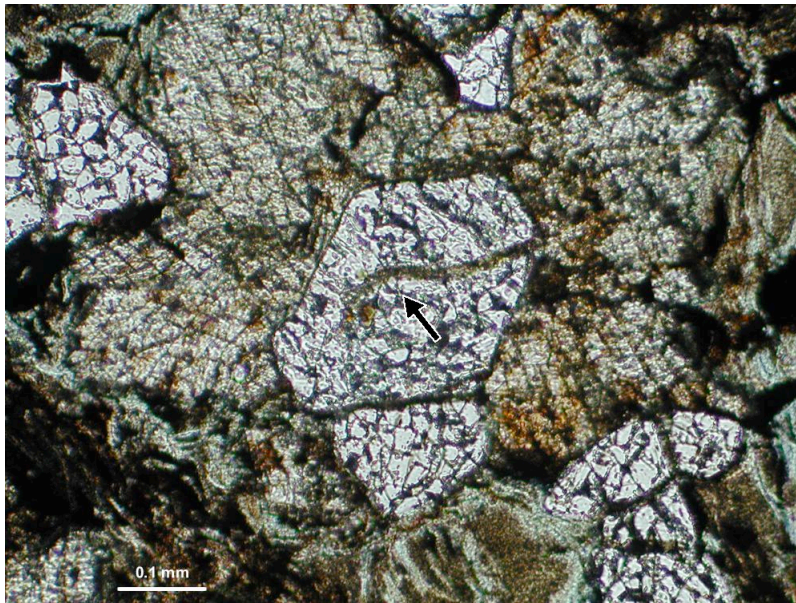


Figure 4-4d: Possible tunnel structure in an apatite grain 50 cm below paleosol surface (Elk Point core depth: 274.3 m)

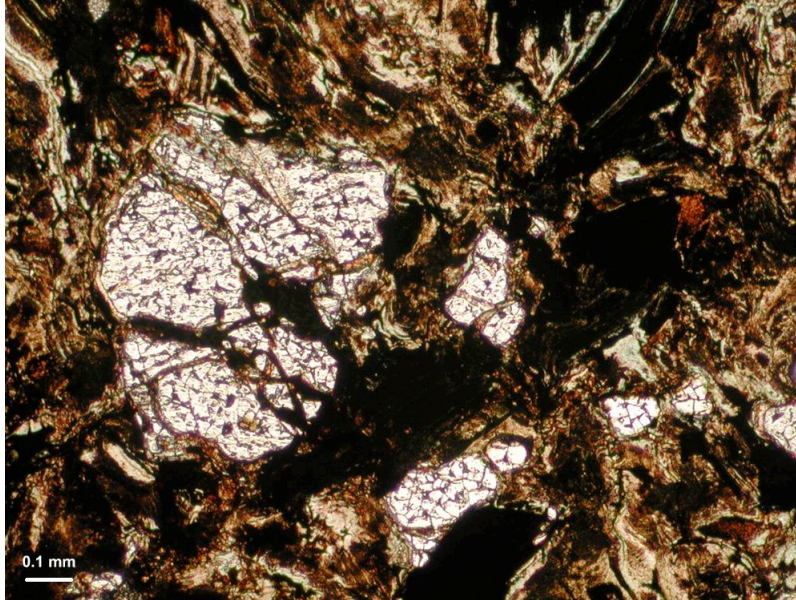


Figure 4-4e: A heavily degraded apatite grain 50 cm below the top of paleosol showing signs of dissolution, fracturing, and possible tunneling (infilled with hematite) and alteration rinds (Elk Point core depth: 274.3 m)

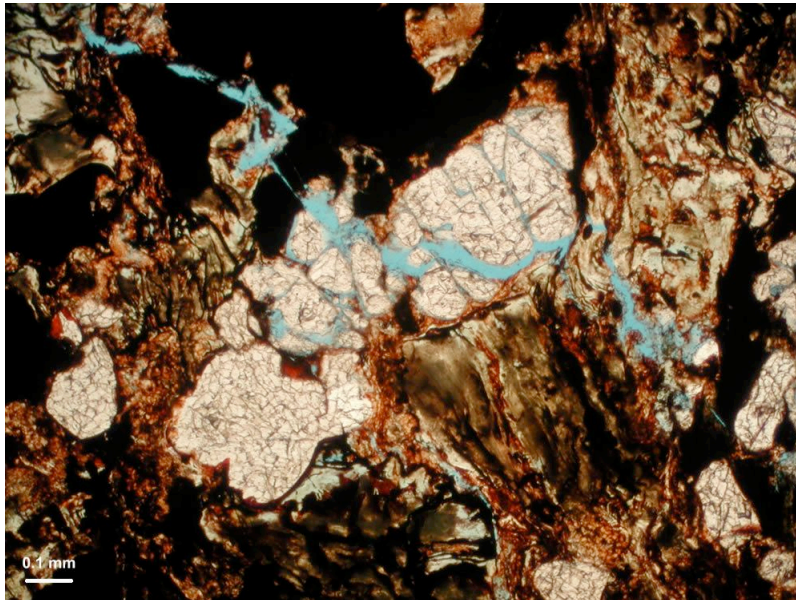


Figure 4-4f: Heavily fractured apatite grain in the zone of apatite dissolution (Elk Point core depth: 274.2 m)

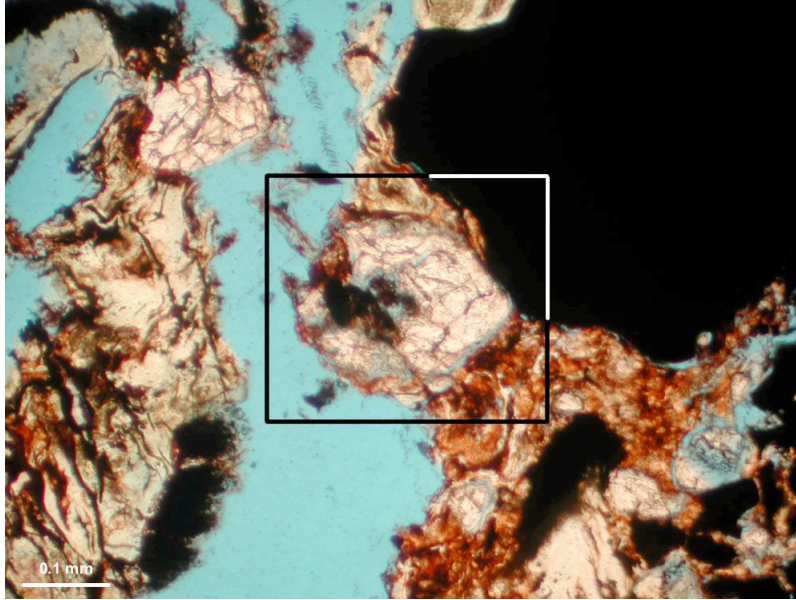


Figure 4-4g: Dissolving apatite grain in the zone of apatite dissolution (Elk Point core depth: 274.2 m)

CHAPTER 5

Concluding Remarks

5.1 Current Work

Terrestrial landscape and ecosystems during the Cambrian and early Ordovician are the subject of frequent speculation due to both a very poor fossil record and a general lack of intensive investigations (Labandeira, 2005). This thesis aimed to address that deficiency by investigating a geographically extensive and geologically heterogeneous weathering surface to better understand the abiotic and biological factors that contributed to the development of weathered profiles in the absence of widespread terrestrial vegetation. The paleoweathered profiles in this study developed close to the equator during the Middle Cambrian in a climate that was most likely subtropical, which contributed to the development of profiles that would most likely be classified as Alfisols and Ultisols in today's world. Western sites (Elk Point, Camp Quest, and LaFleur) developed in a slightly drier climate than the eastern sites (Sharp, Hummell, and Nelson), with one example of weathering in an aquic moisture regime (Harris). Differences in basement material (granite vs mafic) and minor variability in topography contributed to variable drainage conditions that further differentiated weathering at the various sites. As a result of this heterogeneity, no one site proved to be representative of the entire study region, as some showed persistent water saturation while other nearby sites showed drier subsurface conditions. As a result, caution must be used when interpreting paleoweathering data to avoid mistaking local conditions for global ones.

A thorough geochemical analysis of the Middle Cambrian paleoweathered horizons revealed several geochemical trends, particularly among Si, Al, and P, that could not be explained by chemical weathering alone. Chief among these was the peculiar depletion of P from surface horizons, particularly at Elk Point. Organic carbon contents throughout the study area, although low, are consistent with those of younger paleosols and are greater than organic carbon contents of Proterozoic paleosols. Carbon isotope composition of this organic matter is consistent with a photosynthetic origin. Because

organic carbon contents throughout the study area were low, extraction of organic matter for microscopic characterization was extremely difficult and did not yield useful information aside from indicating that sandstone and paleosol organic matter at the Elk Point site differ from each other both visually and in consistency. Apatite dissolution at Elk Point is complete down to 30 cm and may be indicative of organic acid attack by a possibly rhizosphere. Apatite is remarkably persistent in the Elk Point core, indicating that a majority of the paleosol developed in alkaline conditions. Acidic surface conditions affecting only apatite solubility that were not a result of biological activity is an unsatisfactory explanation, particularly because no secondary phosphates are present. Once apatite at Elk Point was solubilized, P was removed from soil solution, most likely by a surface biota. Argillan formation in the zone of apatite dissolution can potentially be explained by increasing Ca concentrations in soil solution, a behavior that is characteristic of modern-day mycorrhizal fungi. Tunnel features present in apatite are inconclusive, although there are some preliminary indications that they are biological in origin. An earlier origin for the rhizosphere, which may have been dominated by fungi, is consistent with biological clock studies that suggest an earlier origin. The presence of a more deeply weathering terrestrial ecosystem prior to the mid-Ordovician, as is suggested by the 30-cm of complete apatite dissolution at Elk Point, may have had important consequences for biogeochemical cycles in the Cambrian, such as increased nutrient flow to the ocean and increased uptake of atmospheric carbon dioxide.

5.2 Future Work

A thorough understanding of abiotic and biological weathering allows for a more complete understanding of the central Laurentian landscape during the Middle Cambrian. However, much work remains to be done. This study investigated six cores, but there are many more available for study. Better investigation of Cambrian cores throughout Laurentia would help elucidate a period of time that has not been well-studied and confirm trends that were detected in the Iowa region during the course of this study. Better investigation of K-metasomatism throughout the Midcontinent region would be

beneficial for future researchers who are investigating alteration on the Precambrian basement.

The best approach for future studies would be a much more intensive investigation of biosignatures in Cambrian paleoweathered zones. The most important biosignature to investigate would be apatite dissolution and P mobilization, as some studies indicate that P mobilization may have intensified during the Proterozoic and Cambrian (Driese et al., 2007; Horodyskyj et al., 2008). Better characterization of P mobilization from Proterozoic and Phanerozoic soils would be very beneficial for testing this idea. It would be especially important to test if this pattern is widespread or if it is recorded in only certain portions of the world.

The purported tunnel features found in apatite at Elk Point are the most intriguing discovery yielded by this study. At least one of the tunnel features is biogenic (Bill Schopf, personal communication), although the inhabitant of this tunnel is enigmatic. Further characterization of this tunnel and others found at Elk Point would be an obvious future research direction. The rare presence of tunnel features in two-dimensional thin sections indicate that they are likely more numerous in three-dimensions. Characterization of the number, frequency, and morphology of tunnel features would be beneficial, but would require a large number of thin sections from the same horizon, which was beyond the scope of this project. In addition, characterization of the organic matter present in some of the tunnel features would be beneficial in determining what organism formed them. Preliminary Raman spectroscopy results indicate that a fungal origin is not likely. However, this does not preclude a fungal presence elsewhere in the profile. Better characterization of kerogen in the paleosols would be a good starting place to determine what organisms contributed to organic matter content of paleosols. Since fungi and very early bryophytes are hypothesized to have been present in the study region, based on molecular clock phylogenies, cryptospore evidence, and apatite dissolution and P mobilization patterns, biosignatures specific to these organisms would be a useful starting point. Chitin is the most promising biosignature, as it is generated by fungi and is difficult to degrade. Detection of chitin may be possible through GC-MS or

through antibody studies (Jake Bailey, personal communication). New drill cores from the Midcontinent region in the coming years (Kelli McCormick, personal communication) may help shed further light on terrestrial biology during the Cambrian.

A combination of a variety of proxy techniques, including ones utilized in this study (apatite dissolution, carbon isotopes, organic carbon contents) and new ones (antibody chitin detection, Raman spectroscopy), can allow for the determination of likely terrestrial biota in the absence of fossils. The confirmation of mycorrhizal fungi (perhaps associated with early bryophytes) during the Middle Cambrian would verify predictions made by molecular clocks and may provide new calibration points for future studies. These research methods are applicable to earlier Cambrian and Precambrian weathered surfaces and may help to further elucidate changes in terrestrial biota during this enigmatic period of time in terrestrial ecosystem history. In addition, the use of biosignatures, including most notably phosphorus mobilization, has important applications for the search for life on Mars and elsewhere in the universe.

5.3 References

- Driese, S.G., Medaris, L.G., Ren, M., Runkel, A.C., and Langford, R.P., 2007, Differentiating Pedogenesis from Diagenesis in Early Terrestrial Paleoweathering Surfaces Formed on Granitic Composition Parent Materials: *Journal of Geology*, v. 115, p. 387-406.
- Horodyskyj, L.B., White, T.S., and Kump, L.R., 2008, Biosignatures in Middle Cambrian Paleosols: *Eos Trans. AGU, Fall Meeting Supplemental*, v. 89, p. Abstract P54A-03.
- Labandeira, C.C., 2005, Invasion of the continents: cyanobacterial crusts to tree-inhabiting arthropods: *TRENDS in Ecology and Evolution*, v. 20, p. 253-262.

Lev Horodyskyj

Curriculum Vitae

441 Deike Building, Pennsylvania State University, University Park, PA 16802

E-Mail: LevH@psu.edu, lhorodys@geosc.psu.edu

Education

PhD, Geosciences and Astrobiology, Pennsylvania State University. May 2009

BA, Earth and Planetary Sciences, Johns Hopkins University. May 2003

Academic Interests

Astrobiology, Earth system history, Early Paleozoic terrestrial ecosystems, paleosols, soil formation and surface alteration, soil/paleosol geochemistry, soil/paleosol biosignatures (carbon isotopes, phosphorus mobilization, iodine), applications of soil/paleosol science to Mars and Titan.

Abstracts

Horodyskyj, L. B., White, T. S., Kump, L. R., 2008; Biosignatures in Middle Cambrian Paleosols; *Eos Trans. AGU*, 89(53), Fall Meeting Supplemental, Abstract P54A-03

Budney, C., Burke, C., Cartwright, M., Gadre, R., Horodyskyj, L., Klesh, A., Milam, K., Moskovitz, N., Oiler, J., Ostrowski, D., Pagano, M., Smith, R., Springmann, A., Taniguchi, S., Townsend-Small, A., U-Yen, K., Vance, S., Wang, J., Westlake, J., Zacny, K., 2008; SHOTPUT: A mission proposal to study composition and origins of small bodies in the outer solar system through fly-by and impactor science; *Eos Trans*, 89(53), Fall Meeting Supplemental, Abstract P51C-1426

Horodyskyj, L., White, T., Kump, L., 2008; 24-21-O; "Soil Formation in the Prevegetated World"; *Astrobiology* 8(2), p. 408

Horodyskyj, L. B., White, T. S., and Kump, L. R., 2006; "Search for Early Terrestrial Life: Tantalizing Hints from a Terminal Proterozoic Paleosol"; *Abstracts with Programs* 38(7), p. 494

Teaching Experience

Pennsylvania State University

Co-Instructor, Spring 2008 (Geosc 21, Earth and Life)

Teaching Assistant, Spring 2005 (Geosc 21, Earth and Life)

Teaching Assistant, Spring 2004 (Geosc 21, Earth and Life)

Teaching Assistant, Fall 2003 (Geosc 301, Environmental Geology)

Other

Guest Speaker, Pennsylvania State University, *Shake, Rattle, and Rocks* (January 2007, 2008)

Co-instructor, Pennsylvania State University, *Summer Experience in Earth and Mineral Sciences (SEEMS) Program* (Summer 2005)

Guest Speaker, Padua Franciscan High School (2001-2003)

Awards

ConocoPhillips Graduate Fellowship (2007); Geosciences TA Award, 3rd place (2004)

Professional Organizations

Penn State Astrobiology Research Center (2003-present)

Geological Society of America (2006-present)

American Geophysical Union (2008-present)